Smart Headband for Jaw Rehabilitation Following Reconstruction

by

Pradipika Natamai Vasudevan

A thesis submitted in partial fulfillment of the requirements for the degree of

Master of Science

In

MATERIALS ENGINEERING

Department of Chemical and Materials Engineering
University of Alberta

Abstract

Head and neck cancer is a devastating disease resulting in difficulties in mastication (chewing) and deglutition (swallowing) even after treatment. Jaw reconstruction together with oral prostheses can restore anatomical structures. Without embedded sensory function in the prosthesis, however, patients will still suffer from a loss of sensation of force and texture during mastication. As a result, the patients often exert excessive pressure and difficulties in swallowing that leads to further injuries and complications. Various technologies for biofeedback have been explored over the previous years; they show that tactile stimulation can be an effective sensory substitute. Here, the overall objective of the project is to realize a sensory system that consists of a jaw prosthesis with an embedded array of pressure sensors and a smart garment with an array of piezoelectric actuators for providing biofeedback signals regarding chewing. The specific objective of the current thesis is to develop the smart garment.

The piezoelectric actuators were selected based on our hypothesis that they can deliver precise feedback about the food texture compared to other types of actuators such as linear resonant actuators (a.k.a., coin vibration motors). Using the laser Doppler vibrometer (LDV) as the characterization tool, we confirmed that the piezoelectric actuators delivered the texture signals with high fidelity. The LDV measurements were performed by passing a sinusoidal signal in the range of 100-300 Hz (the optimal frequency range at which low amplitude vibrations become perceivable) as well as texture signals. The results from the LDV showed that these piezoelectric discs are able to vibrate in accordance with the input signals provided to them. In addition, it was observed that they are able to deliver different types of signals with different input intensities superimposed onto the background vibration in the sinusoidal waveform. These results were used

for designing perception tests for assessing the psychophysics of human participants (*i.e.*, establishing the relationship between the tactile stimuli and the level of perception of the subject).

A smart headband structure was designed with three piezoelectric disks to deliver the food texture signals and a pressure sensor to control the headband tightness. The structure is robust, washable after removing the Velcroed actuators and sensor, and is able to provide the right amount of pressure for stimulation. Food texture signal tests were conducted on the author and her three supervisors using the smart headband. The results showed that the textures were correctly identified above chance. The perception tests were also able to provide important information about the just noticeable difference and spatial differentiation. The sensitivity of the skin towards the actuator was also studied. Overall, our smart headband design can be useful in providing feedback as well as comfort to patients having experienced jaw reconstruction.

Keywords: jaw reconstruction patients, piezoelectric actuators, smart textiles, rehabilitation, biofeedback, mastication

Preface

This thesis is organized into six chapters. Chapter 1 consists of the introduction. Chapter 2 is the literature review. Chapter 3 describes the method of selecting the actuator and studying it using a scanning laser Doppler vibrometer. Rosmi Abraham helped with training on the scanning laser Doppler vibrometer and analysis of the results. Chapter 4 presents the requirements for the biofeedback garment, and the design and fabrication of the smart headband. Chapter 5 involves the design of the perception study and its conduction on the author and her three supervisors. Andrew Chao performed experiments for breaking food textures with a load cell which were used in Chapter 5. Chapter 6 is the conclusion and future work.

Acknowledgement

It is a genuine pleasure to express my deep sense of thanks and gratitude to my supervisors Dr Hyun-Joong Chung, Dr Patricia Dolez and Dr Daniel Aalto for all the guidance and support throughout my program at the University of Alberta. They have always provided me with advice that has helped me to grow and evolve into the person I am today. It has been an honor to work with them and learn from them. They have been the best role models to me when it comes to research and working towards my goals.

I would like to thank Rosmi Abraham for her guidance and support during the laser Doppler vibrometer studies. She helped me with a lot of brainstorming sessions and analysis of the results. I am thankful to Mr Walter Boddez for sharing his knowledge during the initial phases of my study. I would also like to extend my gratitude to my lab members who have been my family in Canada. Diana, Laura, Dinara, Lelin, Wendy, Shide, Chungyeon and Ankit I owe you all a big one.

I would like to acknowledge the constant support from my parents for believing in me. My friends Matthew, Wantei, Madhu and Gopika have always been the most encouraging. I wouldn't have achieved this without all of you.

Pradipika Natamai Vasudevan

August 2021

Table of Contents

List of figures

List of tables

Chapter 1- Introduction

1.1 Head and neck cancer rehabilitation

Rehabilitation refers to the process of enabling people in restoring normal life activities in order to achieve and maintain their optimal quality of life [1]. This takes place in various stages in forms of preventive rehabilitation therapy, restorative rehabilitation therapy, supportive rehabilitation therapy and palliative rehabilitation therapy [2]. Restorative rehabilitation therapy aims at restoring maximum function for patients with residual physical impairment and disability.

The population of long-term cancer survivors is increasing every day [3]. Advancements in treatment are responsible for higher survival rates and life expectancies for cancer survivors. However, more often than not these treatments have negative impacts on physical and psychological health of patients. In a US comprehensive cancer center's study studying 14 major types of cancer, 29 to 43 percent patients were seen to experience psychological distress [4]. These patients are also seen to experience other chronic conditions (42%) and functional disabilities (58%). Therefore, cancer management is seen as a long-term process and the need for rehabilitation interventions for cancer survivors is growing [3]. The goals of rehabilitation in cancer are to maximize physiological function while addressing psychological concerns. Many cancer related impairments can be treated through timely and appropriate rehabilitation measures.

For rehabilitation purposes, cancer can be divided into five different stages namely diagnosis, treatment, surveillance, recurrence, temporization and advanced disease [5]. Head and neck cancer patients often have intensive rehabilitation needs following surgical neck dissection and/or external radiation treatment. This rehabilitation is provided in the early diagnosis and treatment stages. Once the primary cancer treatment is completed, patients usually need to be

acquainted with altered anatomy. In the case of head and neck cancer patients, alteration in physiology could mean removal of parts of the jaw and insertion of oral implants.

Patients with cancer in the oral cavity, pharynx (the throat) or larynx (the voice box) are usually treated with one or a combination of radiotherapy, chemotherapy, and surgery [6]. These treatments usually lead to long term effects in terms of chewing, swallowing, impaired speech as well deformities of the face that require medical attention. The loss of soft and hard tissue leads to difficulties in mastication. Swallow dysfunction is observed after surgery and swallowing disorders may occur in the oral preparatory and pharyngeal stages of swallow. Tongue resection leads to inability to trigger a pharyngeal swallow (involuntary action of swallowing produced by the muscles in the throat), difficulties in clearing the bolus from the pharynx, and severe choking.

Although tumor stage and advanced age are factors that negatively influence treatment, typically these patients require functional rehabilitation for up to five years after initial diagnosis [7]. Dental implants have been used in the rehabilitation of these patients. They provide stability and support for the prosthesis, which in turn limits the pressure exerted on soft tissues affected by surgery and radiation therapy. Dental implant rehabilitation in oral cancer patients requires a multi-disciplinary approach. The stability and support provided by dental implants reduces reliance on the patient's oral coordination, which is important for patients who struggle to adapt to an oral prosthesis resection. It helps in facilitating speech and chewing.

Rehabilitation has been a major part of cancer treatment and post treatment care for survivors [8]. A number of rehabilitation devices have been developed thanks to the efforts of multi-disciplinary teams combing knowledge of wearable technology, medicine, and engineering. Wearables have formed a key part in rehabilitating patients with ease at the comfort of homes. These allow for remote tracking of progress and ability to perform tasks with greater ease. Smart

or e textiles have played a role in the development of these devices keeping in mind the fact that most patients do not want to be seen in the public with larger devices. These textiles are able to provide feedback signals while being discreet. The next section talks about them in greater detail.

1.2 Smart textiles

Textiles provide an attractive medium for integration of electronics because of the fact that they are such a fundamental component of our everyday lives. Smart textiles exhibit the ability to integrate new sensing and actuation functionalities into normally inaccessible surfaces and present a new way of revolutionizing textiles [9]. Smart textiles, e-textiles or intelligent textiles are able to sense, respond, and adapt to environmental stimuli such as light, motion etc.

Smart textiles are textiles that exhibit a sensing, actuating, or responsive function provided with smart materials and/or embedded electronics [10]. They can be fabricated using textile fibers that have additional functions, attaching of-the-shelf electronic components such as sensors, actuators, integrated circuits, and power sources, and combining commercial and textile functionalities [11]. The development of these textiles is an inter-disciplinary effort by electrical engineers, textile experts, biophysicists, etc. The idea of smart textiles appeared in Japan in 1989 with a silk thread with a shape memory effect. This discovery led to further research in intelligent polymers which were subsequently integrated into textiles. Smart textiles can be described as textiles that have the ability to sense stimuli from the environment, react to them, and/or adapt to changes by integrating various functionalities in the textile structure. There are different kinds of stimuli a smart textile can react to: electrical, mechanical, chemical, thermal, etc. Smart textiles can be grouped based on the level of intelligence they exhibit [12]:

1) Passive smart textiles are only able to sense the environment (also known as sensors);

2) Active smart textiles are able to sense a stimulus from the environment and produce a reaction pertaining to the stimulus (also known as actuators);
3) The third category consists of textiles that are able to adapt to a change in the environment, for instance a membrane whose porosity varies with the temperature.

They can also be classified into three distinct categories based on architecture and design [13]. The first category is formed using traditional textiles as substrates and attaching sensors, output devices and printed circuit boards to provide the electronic functions. Commercial electronic components are secured on the fabric, for instance by stitching or embroidery, and connected by wires in order to produce e-textiles with a particular function.

The second category comprises smart textiles in which the active components are added during the fabric manufacturing stage. It uses methods like embroidery, weaving, and knitting in order to achieve hybrid structures [13]. In these structures, the fabric is an essential component of the textile device and circuitry. For example, the Georgia Tech wearable motherboard (GTWM) was developed in 1966 and was made from integrating optical fibers for data transmission during the textile fabrication process and then attaching sensors to the fabric structure [14]. The design of smart textiles was initially approached from a traditional electronic system design perspective, but more and more functions have been incorporated within the textile itself. Researchers are now able to merge traditional textile fabrication methods (like knitting and weaving) with methods for making electronic circuits such as printed circuit board design.

The third category involves incorporating the functionalities at the fiber or yarn level [13]. Fiber electronics, which is also called fibertronics, has led to attempts to create devices and logic circuits with higher order electronic functions, which helps in implementing more advanced smart

textiles [15]. Research efforts in this area include building technology and systems from fiber upwards instead of the top-down method used in the other two categories.

Conductive yarns have been developed and incorporated into textile structures using traditional techniques like knitting, weaving, embroidery, and stitching [13]. Conductive yarns are particularly interesting for the purpose of textile integration since they can replace the traditional wires used in electrical circuits [16]. They are flexible and more comfortable to the skin. However, they face the problem of high resistance. Conductive wires like copper wires on the other hand are able to provide the required low resistance but are limited in terms of processability for textile integration. Often, a tradeoff needs to be made between resistance and processability while choosing between the two options.

Weaving, knitting, and embroidery have received a lot of attention when it comes to manufacturing smart textiles [17]. These are advantageous because of their ability to produce large surface areas in a short amount of time. Weaving is a process that interlaces two perpendicular sets of yarns in the "warp" or "weft" direction. During the process of weaving, some of the warp yarns are moved up and the others are moved down, and weft yarns are inserted in the openings thus created. Knitting is another technique used in smart textiles that allows the integration of electronic components [18]. Knitting can be done in weft (interlacing loops in the horizontal direction) and warp (interlacing loops in the vertical direction) configurations. General advantages of fabrics fabricated using knitting and weaving are low weight and breathable [13]. Woven fabrics are stronger than knitted fabrics whereas knitted fabrics have higher elasticity and elongation and good conformability in mechanically active environments. These techniques are also used to make 3D fabric structures. For instance, the Georgia Tech wearable motherboard used a novel 3D weaving process to produce the garment [14].

Smart textiles have been used both as output and input devices [19]. As output devices, they are able to provide information to the outside world about signals received by the textile system. Displays are the most common type of output devices used in textiles. Optical output using LEDs and optical fibers can be used in combination with conductive yarns for displays. Vibro-active displays are those that provide insight about localized tactile stimulus to the skin by using vibrations. This is done by using electro-motors that can be combined with the textile structure. This has been used in commercial applications such as "emotion" generating jackets for gaming or mental health therapy by Phillips [20]. Artificial muscles are another example of textile output systems [13]. These are made using electro-active polymers that can be integrated with electronic circuits to control the shape of the textile surface and produce movements similar to muscles. Hence, smart textiles are valuable resources for multiple applications including rehabilitation.

1.3 Scope of the thesis

This thesis focuses on the development of a wearable garment that provides feedback to patients that have undergone surgery in the head and neck due to multiple reasons like cancer. In this work, we fabricated a garment with embedded piezoelectric actuators in order to provide biofeedback in the form of vibrotactile signals. First, we identified a method to provide this biofeedback and surveyed multiple of-the-shelf commercial actuators. They were studied using a laser Doppler vibrometer to assess their vibrational characteristics. The best performing actuators were then embedded in a garment design to produce a smart textile. The headband obtained was used to perform psychophysical tests on the author and her supervisors and analyze if the feedback is being provided efficiently.

Chapter 2 contains a literature review on sensory substitution, vibrotactile perception, and the application of smart textiles and piezoelectricity in biomedical engineering.

Chapter 3 to 5 describe my original contributions to the field.

Chapter 3 of the thesis covers piezoelectric actuators, their working principle, a survey of different commercially available actuators, and the study of the piezoelectric actuator using laser Doppler vibrometer.

Chapter 4 of the thesis talks about the development of the design for the biofeedback smart headband for jaw rehabilitation.

In Chapter 5, psychophysical methods of testing are discussed. It also describes the protocol used to test the smart headband on human participants and the results obtained on the author and her supervisors.

The conclusions and future work are discussed in Chapter 6.

Chapter 2- Literature review

2.1 Sensory substitution

Sensory feedback is feedback provided by the sensory system depending on what is stimulating them (touch, visual, audio, etc.) [21]. The stimulus is captured by the sensory receptors present in the body and it is then processed by the central nervous system. When these receptors or feedback systems are damaged or have been removed due to cancer or surgery, a surrogate system can be used. It will employ a different site and feedback system for providing the information regarding the stimulus. Sensory substitution is a method of changing characteristics of one sensory modality to suit another sensory modality. It is often used in rehabilitation following the removal of tumors which causes a loss of muscle and nerves surrounding the cancerous site.

The method of tactile sensory substitution is based on the concept of brain plasticity [21]. This concept was born from experiments that looked into the capacity of the brain to reorganize. It then led to results indicating that it can be used to help people who suffer from sensory loss. The concept of brain plasticity means that it is not necessary for the brain to receive signals from natural sensory systems in order to interpret them accurately. For example, vision is a process that involves the eyes capturing an image. However, the image does not travel beyond the retina. Instead, it is converted into electrical signals that are conducted by nerves to the brain which then forms the image. Therefore, working with these electrical signals directly via receptors to the brain-machine interface allows compensating for sensory loss.

The tongue can act as an electrotactile stimulation site for substitution of a display unit [22]. Bach-y-Rita et al developed a tongue display unit that consisted of an input sensor coupled with a two dimensional electrotactile array placed on the tongue. The tongue also is always moist and contains a good amount of saliva that serves as an electrical conductor, which is an advantage.

The tongue has another benefit of having sensory receptors very close to the surface when compared to most parts of the body including the fingers which allows for the application of a lower voltage and current. There have been variations to the tongue display unit including providing signals from a portable base unit.

Bach-y-rita et al studied the method of substituting sensation and providing stimuli to the tongue in order to substitute vision [23]. The electrodes providing electrical stimulation were arranged on a square grid with 0.1 inch spacing. They observed that when electrical stimuli are provided to the tongue, the results from the perception study are significantly better compared to when the electro tactile stimulation is provided to the fingertip. In addition, the tongue requires only 3% of the voltage and less current when compared to with the fingertip. These results confirm that the tongue is capable of conveying complex spatial patterns and is therefore an ideal site for somatosensory system excitation.

The Tongue Display Unit of Bach-y-Rita et al has also been used as a balance prosthesis in work done by Vuillerme et al [24]. Their device consists of a pair of force sensing shoe soles. These were used to determine the center of pressure applied by the individual to the ground. The difference in the center of pressure is sent as a discrete signal when the value exceeds a particular value. Feedback is then given to the user regarding the values. Vuillerme et al have also used the same device to display the joint angle position information during a study which tested joint angles between healthy subjects [25]. This display was made of a six by six electrotactile array which was placed on the tongue. The coding is done so that the display shows when the subject has a joint angle exceeding or receding a reference value. A signal is triggered when this happens and the tongue is stimulated in 12 of the 36 sites, either in the posterior or the anterior of the electrotactile array.

Bach-y-rita et al also looked into providing visual cues via stimulators in contact with the skin in different parts of the body like the back, abdomen, thigh, forehead and fingertip [26]. This method was successfully used in rehabilitation of blind patients; after appropriate training, they were able to experience images in space using tactile stimuli. They were also able to recognize faces and make accurate judgements on the speed and direction of a rolling ball with more than 95% accuracy.

Benjamin et al studied a method to provide information about rhythms in music to deaf people [27]. They used visual and vibrotactile cues sent with wireless sensor display pairs in the form of a smartwatch like device. The device was strapped onto the hand of the participants and questions regarding discrimination, rhythm reproduction and expressiveness were asked. The researchers observed that the participants preferred vibrotactile feedback to visual feedback for reasons of privacy. However, the usage of the device did improve the understanding of the participants during the music lessons.

Other examples include the ability of a one-dimensional vibrotactile display to provide information regarding the angle of movement of the elbow, to the skin [28]. Also, Saunders et al developed an auditory feedback system to improve speech clarity to deaf children via the use of electrodes [29]. Each electrode was able to provide information intensity and frequency of a signal present in the audio spectrum of humans. Tactile stimulation can also be used for providing spatial visual information to mimic the function of the retina [30]. Bach-y-rita et al studied the ability of a vibrotactile display skin to provide visual information and found that the subjects were able to identify horizontal, vertical, and diagonal lines. Subjects that had more experience were also able

to differentiate between faces. Bliss et al developed an optical to tactile converter that was able to convert the outline of printed letters to vibrotactile signals on the person's fingertip [31].

For patients with leprosy, daily tasks are harder to perform due to the loss of touch sensation in their fingers and hands that leads to injuries during simple tasks like grasping objects. Collins et al came up with a tactile feedback system with strain gauges that were attached to a special glove [32]. This glove was able to measure forces on each fingertip and each of the five sensors controlled the electrotactile stimulation. Subjects were able to differentiate between rough and smooth surfaces, and hard and soft objects, and were able to recognize corners and edges. In another study, Sparks et al used a two-dimensional display system with 288 electrodes to provide auditory information to the skin on the abdomen [33].

Therefore, sensory substitution is a very effective method for different kinds of applications. It can be used in the human computer interface by which users can interact with digital information. It has been used in virtual reality to feel and see things in an environment separate from their own. It is most often used in rehabilitation to provide individuals with a different method for sensing, with large benefit s to their quality of life. In this study, we have used the method of substituting some of the sensory receptors involved in chewing to provide vibrational signals on the forehead of the user. The method of vibrotactile perception is explained in the next section.

2.2 Vibrotactile perception

The experience of touch can give rise to a number of different sensory (discrimination and sensitivity) and emotional (pleasant, painful, etc.) cues [34]. Tactile sensitivity varies across different parts of the body. The fingertips and parts of the face are more sensitive when compared

to the upper arm or other body parts. Vibrotactile stimulation is a well-known sensory substitution for a variety of rehabilitation applications like display and for providing feedback signals to the skin as alarms. Human mechanoreceptors present in the skin respond to tactile perception through mechanical stimulation that is obtained by direct contact with external stimuli in the environment. The process of vibrotactile perception is a complicated one [35]. There are five main types of mechanoreceptors in the skin. These have been classified into two major categories: the fast adapting (FA) and slow adapting (SA) mechanoreceptors. These are again divided into two subcategories namely FA I and II and SA I and II.

The FA mechanoreceptors are sensitive towards the motion of the skin whereas the SA ones are responsive towards the motion of the stimulus and the amount of resulting deformation of the skin. Type I receptors are smaller in terms of the receptive field whereas the type II receptors have larger fields. The FA I units respond to vibrations in the lower frequency range, typically 5-50 Hz. FA II are sensitive towards vibration and mechanical stimuli of higher frequencies, typically above 40-50 Hz. The SA I mechanoreceptors contribute towards vibrotactile perception. For signals with higher amplitudes, all/most of the receptors play a role in the perception.

One type of FA II mechanoreceptors called the Pacinian corpuscles, is responsible for the detection of higher frequency signals usually exceeding 30 Hz with a peak sensitivity of 100-300 Hz [36]. These are located in the deeper layers of the skin and are surrounded by liquid. They are used for finding very tiny differences in texture, roughness, and coefficient of friction. Pacinian corpuscles have been seen to be activated when rapid vibration occurs at higher frequencies close to the high sensitivity frequency range (which is ranged between 100-300 Hz) as seen in Figure 2.1 [37]. An increase in contact area is also beneficial for activating these cells at that frequency

range. The Pacinian corpuscle mechanoreceptors typically respond to sinusoidal signals that are presented in the stimuli.

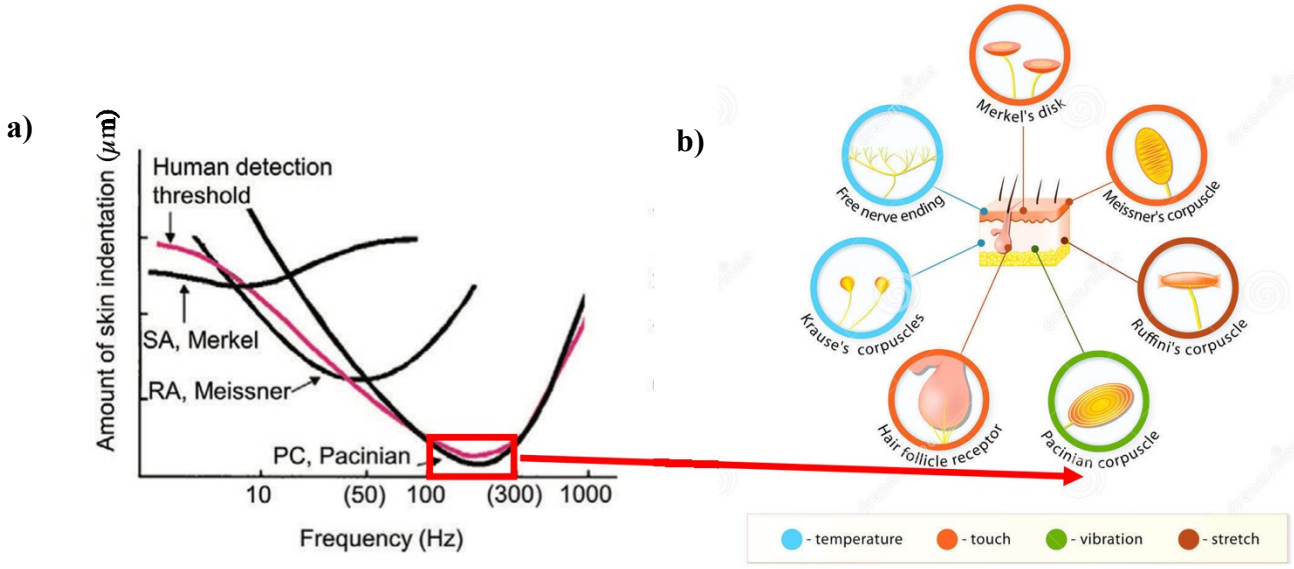

Figure 2.1: a) Relationship between amount of skin indentation and stimulated frequency [37] b) Types of mechanoreceptors [38].

Tactile sensory substitution has been used in the Braille script where the characters are raised from the surface. This is because of their heightened tactile perception. Sadato et al performed a study with Braille and braille like dots used as stimuli to the fingers of the participants [39]. For this experiment, they had subjects performing one non-discrimination task based on sweeping and three discrimination tasks based on angle, width, and character. Positron emission tomography was done in order to study what part of the brain is activated during these tasks. It was observed that for blind subjects, the primary visual cortex which is responsible for sight is capable of reorganizing to accept non-visual tactile information. Braille reading further improves the plasticity of the process of tactile reading and perception.

Barghout et al studied a method of using vibrotactile stimulation for immersive experiences [40]. This method consisted of vibrotactile actuators that are sequentially attached on the arm.

These actuators are of the linear resonating type, which contain a DC motor and are used in cell phones. They were embedded into an arm band and controlled using a microcontroller. The psychophysical experiments for the evaluation of the spatial location of a stationary stimulus and for a moving stimulus were conducted for 12 subjects. The accuracy of detection was found to be 75% for the elbow and 60% at the wrist for the stationary stimulus and 65% and 55% respectively for the moving stimulus. The results were consistent with the two point discrimination test's threshold of 38 mm to 40 mm [41]. Studies have shown that feedback related to texture like that of clouds, water and can also be provided by smart textiles [42].

Cipriani et al studied a vibrotactile sensory substitution device that can be used for multifingered prosthetics [43]. Their work consists of testing a flexible vibrotactile system that is made of vibratory stimuli that can be used in the form of prostheses. It also contains sensors that work in conjunction with each other to provide feedback. Their device can control amplitude and frequency and is made of low-cost components. They performed psychophysical tests to study the discrimination of different amplitudes, of frequency-amplitude amongst signals, and of sites and patterns. The first experiment showed that participants were able to discriminate among three different amplitudes with more than 75% accuracy. All the participants were able to discriminate between the reference signal and the comparing signal during the frequency experiment with an accuracy greater than 70%.

During the site discrimination test, the subjects were also able to differentiate between three different vibratory elements with greater than 90% accuracy [43]. The most encouraging results were obtained in the pattern recognition experiment. The participants were successfully able to evaluate between 6 different patterns with 78% accuracy. They also mentioned that for an artificial sense of touch, three important parameters need to be considered. First, feedback needs to be

provided about contact which instantly triggers a signal about the occurrence of an event; second, the second parameter is a tactile map of where the stimuli is being delivered for what type of signal; and third, they need the information about forces applied by the prosthesis.

Vibrotactile flow is similar to optical flow (pattern of motion of objects as perceived by human brain) but within the haptic domain [44]. It is defined as the space-time variation of vibrotactile stimulation. Cancar et al developed a device consisting of multiple vibrotactile actuators in order to present haptic flow through variations in the area of stimulation and intensity of vibration. The vibrotactile actuators that were used of coin type. Participants were asked if they were able to feel the difference in the frequency of vibration of the actuators in a step wise manner. All the participants confirmed that they were able to differentiate between frequencies in the 10 to 100% of the duty cycle whereas in the 0-10% range, they did not feel the change. This is because in that range, not enough energy was given to drive the actuators.

To check if the information regarding optical flow can be provided by the device an experiment involving twelve participants was conducted [44]. During this experiment, a large and lightweight ball was attached to a wire and the participants were trained for 10 minutes during which the ball was thrown towards them. They were first asked to use their sense of sight and then were blindfolded. The perception of flow using the vibrotactile device was done as follows: when the ball is approaching the participant, the area of skin stimulation decreases. The opposite occurs when it's moving away from the participant. The time to come in contact with the object was calculated for visual and tactile conditions. The visual and tactile results were compared and the differences between both were shown as insignificant. The researchers thus concluded that the optical flow information can be provided using vibrotactile stimulation.

There are many variables controlling vibrotactile perception like the frequency of vibration, intensity of vibration, duration of stimulus, etc. Cohen et al studied vibrotactile adaptation as measured by the change in actuation threshold [45]. They found that stimuli at supra-threshold intensities lead to an increase in the threshold value whereas near-threshold intensities don't cause the same to occur. Wedell et al observed that when the skin was stimulated with a signal of 256 Hz, the recovery time was lower when compared to stimulations of higher frequencies [46]. Von Bekesy et al studied the effect of intensity (energy carried by sound waves) with respect to pitch (frequency of the sound wave) [47]. They found that the perceived intensity decreased due to the adaptation of the skin, while the pitch increased. However, the decrease in perceived intensity through time is not a clear indication of loss of sensitivity.

Verillo et al experimented the difference in perception amongst females and males [48]. They found that there is no significant difference in the perception of vibrational thresholds. Goff et al however found a higher sensitivity in case of females [49]. There is also a difference in sensitivity depending on the location of the part of the body, owing to the density of the receptors. Skin temperature also plays a role in sensitivity towards vibrotactile stimuli. Green et al and Verrillo et al studied the influence of temperature on perception [50]. They found a small variation of 2-3 dB between 28° and 32° C. As the temperature decreases, the sensitivity decreases. At a higher temperature of 40° C, no change in sensitivity was observed. Differences in contact area of the stimulus to the skin can also be a factor for an increase or decrease in sensitivity. An increase in contact area leads to a decrease in the threshold. However, at frequencies lower than 50 Hz the area does not seem to play a role in the perception.

2.3 Role of smart textiles in healthcare and rehabilitation medicine

Smart textiles have been used in healthcare since the 1998's to monitor physiological conditions [51]. For instance, they can be used to monitor the electrical activity of the heart in order to alert people about any irregularities such as a post myocardial infarction or a stroke [52]. The electrocardiogram (ECG) is typically measured using pre-gelled electrodes attached to the skin [53]–[55]. Gelled electrodes provide a high signal quality. However, they are not comfortable, need to be replaced at regular intervals because the gel dries out, and may generate skin irritation. They are generally limited to hospital settings. As a more comfortable alternative, electrodes in smart textiles are usually made of conductive threads that are directly knitted or woven as part of the fabric. Metallic conductive coatings applied on conventional fabrics is another technique that can be used to created textile electrodes. Because of the conformability of fabrics and the ability to have electrodes as part of a tight-fitting garment, textile electrodes lead to good signal quality without requiring the use of a gel. These gel-free electrodes are less irritating, in particular thanks to the porosity of the fabric, and allow an extended use compatible with the need of continuous monitoring of vital signs for patients and older adults.

Monitoring vital signs using smart textiles has been in used in hospitals where the data is collected and sent to servers, and alerts are sent to healthcare professionals if a potential issue is detected [56]. The MyHeart collaborative research project looked into a sensing garment for health surveillance that is based on a conductive woven structure embedding textile sensors [57]. The garment was developed by the company Sefar Inc. It is able to record body temperature, ECG, blood pressure, respiration activity, and electromyography (EMG). The product has been commercialized to allow early diagnosis of various conditions and prevent major cardiovascular diseases. Smart textiles with vital sign monitoring capabilities also offer ground breaking

perspectives for older adults, providing them the opportunity to age in the comfort of their homes while being constantly monitored by their medical team [58].

Sleep patterns are also recorded for patients who have been diagnosed with sleep disorders [59]. Currently, the standard for diagnosis is based on a combination of electrocardiography, electroencephalography, and electromyography [60], [61]. However, these measurements usually have to be carried out in clinical settings, which prevents tracking sleep on a day-to-day basis. For that purpose, smart shirts have been developed with the ability to assess ECG. The signal recorded by ECG sensors in the shirt are then compared with signals on a database. Researchers were able to detect sleep apnea events with an accuracy as high as 86% [61]. Adnane et al. have also studied the efficiency of a cardiorespiratory monitoring belt containing textile electrodes for ECG recording and thin films of polyvinylidene fluoride (PVDF) for respiratory signal monitoring [59]. The authors were able to show the ability of the system to detect apnea/hypopnea events using a ratio of low and high frequency components present in the respiratory signal.

Textile electrodes can also be used to measure bioimpedances related to body composition and volume. For instance, researchers have proposed a system using textile electrodes whereas each electrode is connected by a conductive yarn to a metallic snap fastener [62]. These electrodes were sewn to elastic bands which could then be worn on the wrist or the ankle. The author and supervisors were able to record multiple frequency (5 to 50 kHz) impedance signals during different activities like walking, cycling, and running. In a nine participant study, they qualitatively tracked changes in the body water levels. Marquez et al. estimated eight body composition parameters in three male subjects using textile electrodes that were composed of a silver-plated knitted fabric and were highly conductive and stretchable [63]. The fabric was layered with a thin foam and another knit fabric in order to improve surface contact. The researchers compared the

results provided by the textile electrode-measured impedances with traditional metal electrode measurements and did not find any statistically significant difference.

Vuorela et al. created 225 mm^2 square shaped textile electrodes from conductive silver yarns using embroidery [64]. Using a tetrapolar configuration, they quantitatively compared bioimpedance-based estimates of the thoracic volume to that given by the measurements obtained from a pneumotachograph. The measurements showed a maximum difference of 50 mL in volume, which was considered a disadvantage. This can however be rectified by placing the electrode in such a way that the heart is not in the measurement zone.

There are different applications of smart textiles for sensing posture, especially after a surgery or injury. Recognizing movement and posture in real time is important for doctors and physiotherapists to determine progress and quality of movement. Mattmann et al. studied the use of an elastomer sensor thread that was integrated with a commercial garment [65]. They used it to classify 27 different body postures. Once the database was created, the garment was tested with human subjects, and it was able to distinguish 27 postures with 84% accuracy. However, there was some confusion when it came to similar postures, which led to incorrect responses. Tormene et al. explored the use of conductive elastomers printed on a corset to measure specific trunk movements [66]. They observed that the textile was able to differentiate between small and large angle trunk flexion movements. Lorussi et al. proposed a distributed sensing system based on the direct deposition of strain sensors onto fabrics [67]. These sensors are of the piezo-resistive kind. They are manufactured by coating elastic fabrics with conducting polymers. These were positioned on gloves and sleeves and were able to measure shoulder and elbow angles during different postures with a 92% accuracy. Tognetti et al. designed a double layer knitted piezoresistive sensor that was able to measure resistance changes during bending [68]. It was integrated into a glove and used

for calibrating an optical tracking system. It is to be noted that this double layer knitted piezoresistive sensor could not characterize extension motions.

Smart textiles are also used in compression therapies following surgery and cancer [69]. Accumulation of fluids in the lymphatic system leads to the swelling of limbs and, when not treated, can have serious consequences. These conditions can be treated and managed using compression garments. Compression garments are normally manufactured in standard sizes and not customized according to the user. There have been attempts to scan the individual's limbs and then make garments suitable for the person. This is especially advantageous for patients who have severe ulcers due to age, injury or infection. These garments are also casually used by athletes for improving circulation of blood that helps in weight loss and strengthening of muscles. Going one step further, smart stockings have been developed to expand and contract to mimic the calf muscle contraction and improve blood circulation.

If e-textiles have been extensively used for their sensing capabilities, some of the most interesting avenues of their applications is in their potential to assist or perform biophysical activities [70]. Electrical stimulation of muscles and nerves using smart textiles is an area that has been researched for use in therapy and functional orthosis. Farina et al. developed a method for interfacing myoelectric prosthesis with neuromuscular stimulation. They fabricated a sleeve with stainless steel yarn electrodes sewn in a matrix pattern over the flexor and extensor muscles of the wrist and elbow. The study involved nine participants where signals were given by the sleeve to aid in the contraction which helps in movement of the hand. The analysis showed that the movements could be discriminated with 90% accuracy. Yang et al. have developed a screen-printed flexible and breathable fabric electrode array [71]. This array is in direct contact with the skin and does not need an electrolyte to stimulate the muscles. This makes the device easy to use,

comfortable and more durable. By stimulating the muscles, the researchers were able to recreate three different hand gestures accurately and comfortably with less than 7% error across all joints for each of the three postures. This technology, which allows measurements and stimulation of muscles using printed and embroidered electrodes, thus avoiding the use of a conductive gel, wires, pads, etc. is becoming more popular.

Electrical stimulation by smart textiles has also been used for pain relief [72]. These accessories include transcutaneous electrical nerve stimulation and electro-muscle stimulation machines. A garment in the shape of a belt has been developed by the company Cefar [73], [74]. It helps in pain relief at the lower back and the abdomen using electrostimulation. The stimulator is located inside a pocket in the belt which is worn around the targeted region. The electrodes are incorporated into the neoprene structure of the belt.

Orthopedic braces including supports for ankles, knees and back are used for the rehabilitation of patients with neurological diagnosis of post traumatic head injury or cerebral palsy [57]. The smart garment is for both children and adults, it provides assistance for better arm and hand function by addressing posture related issues. It's also used for individuals who need assistance regarding their trunk and pelvic stability. In addition, the device can be used for educational purpose to bring awareness about the entire body depending on the individual wearer's functions and objectives. The device helps the wearer perform daily activities in alternate and better positions giving muscles a greater biomechanical advantage. Smart textiles used in prosthetics may take advantage of the principle of electrical stimulation [75]. Korzeniewska et al. studied a method to stimulate the fingertips of stroke patients. It is done using two-dimensional pulse currents with a long interval time between pulses. The garment is shaped in the form of a glove that is worn by stroke patients. It contains two independent circuits: one stimulates the

median nerve and the other stimulates the ulnar nerve. The electrodes are placed in the tip and the middle phalanges of the fingers. This device was tested on a stroke patient. They were able to perform daily tasks like writing, flipping cards, etc. more rapidly and over extended periods.

Hence, smart textiles have great potential in rehabilitation applications in terms of sensing, actuating, and providing feedback. This technology is also able to provide more personal feedback in real time. It opens a lot of avenues to rehabilitation medicine. In our project, we have devised a smart textile design to help in jaw rehabilitation. The smart headband structure will be able to provide tactile feedback to the patients via actuators. The actuators will be in constant contact with the skin and vibrate depending on the signals provided to them by a sensor located as part of the jaw prosthesis.

2.4 Piezoelectric sensors and actuators in rehabilitation

Piezoelectric actuators are frequently used in various active mechanical systems [76]. They are made from different piezoelectric materials, however the ones made from piezoceramics are the most frequently used. These materials are used for various applications like accelerometers, sensors, flow meters, level detectors, and hydrophones as well as force and displacement sensors. The inverse of the piezoelectric effect is used in actuators and in generating sonic and ultrasonic signals. Piezoelectric actuators work on the principle of conversion of electrical energy into mechanical deformation.

Piezoelectric sensors and actuators have been utilized in the field of biomechanics, clinical medicine, sports devices, ergonomics and the evaluation of biomechanical loads [77]. They are also used in leisure applications of the device, for example sending vibrotactile feedback to a user in a smartwatch or phone. They were used very early on for measuring vibration (ergonomics),

impacts (such as heel strike), as uniaxial accelerometers etc. They have also been used in pressure sensors between different body parts and support surfaces.

A notable example is in the use of exoskeletons for rehabilitation [77]. These act mechanically with a body segment to restore lost function. The exoskeletons are used to stabilize gait function in cases of muscles weakness after neurological disorders. Piezoceramic sensors have been used in these exoskeletons for obtaining kinematic information as a force transducer for the measurement of plantar pressure. Piezoelectric actuators have also been used in exoskeletons for the activation of upper limb prosthetic devices.

As piezoelectric actuators are employed as tactile stimulator in the current thesis, piezoelectric materials are reviewed in terms of operating mechanism, key materials, fabrications, and their applications in bioelectronics.

2.4.1. Operating Mechanism of Piezoelectricity

Piezoelectricity is described as the phenomena that generates electrical charges occurs when pressure is applied to a crystal [78]. The effect was first discovered by Pierre and Jacques Curie in 1880 during their studies on natural crystals like quartz, tourmaline, Rochester salt etc. [79]. When the crystal is subject to pressure, the electric dipoles in the crystal get aligned so that the crystal develops positive and negatives charges on the opposite faces, resulting in the production of an electric field [80]. This is more commonly also referred to as the direct piezoelectric effect. This has been shown in Figure 2.2. However, the opposite effect is called the indirect effect as shown in Figure 2.3. Here, the concept of ‘poling’ is explained in the later part of the section. The applications for both the direct and indirect effects vary since one result in the production of electric field and the other results in the production of mechanical deformation. For the direct

effect, the application involves generation of ultrasonic waves and pressure sensors. The indirect effect is used in actuators.

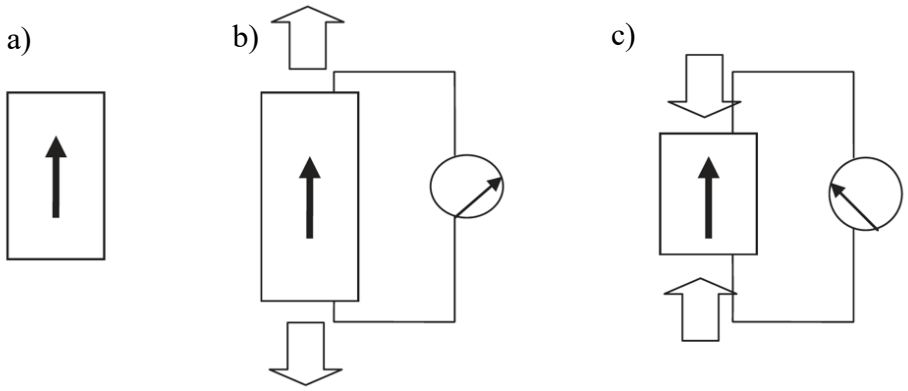

Figure 2.2: a) Polled piezoelectric material b) When pressure is applied in the form of tension the material develops a voltage across its ends in the same polarity as the voltage c) When pressure is applied in the form of compression, the material develops a voltage across the ends in the opposite polarity to that of the voltage [80].

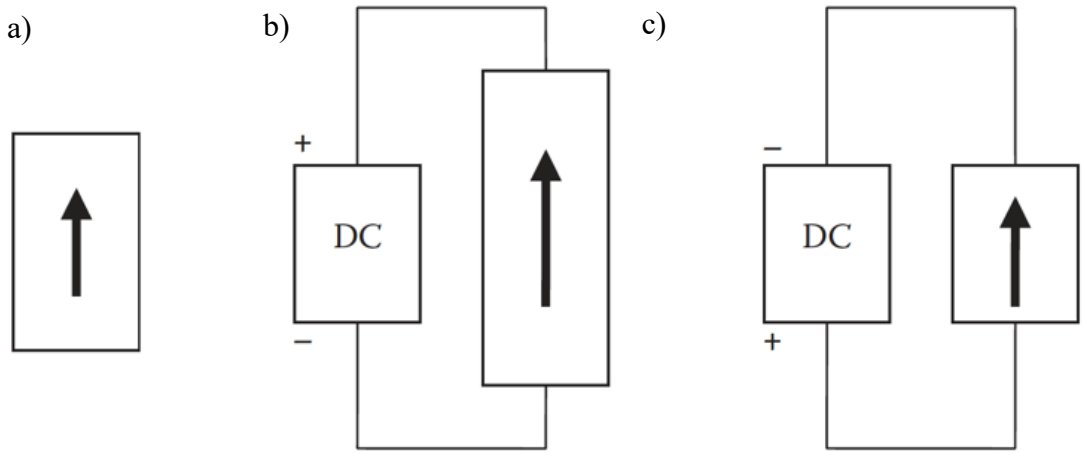

Figure 2.3: a) Poled piezoelectric effect b) when a DC field is applied with the same polarity as the poling field, the material extends c) when the field is applied in the opposite direction a compressive force acts on the material [80].

The appearance of these surface charges leads to a voltage difference between the opposite faces of the crystal which can be measured as seen in Figure 2.4 [81]. Ceramic materials that exhibit piezoelectricity when they do not have a symmetricity in their crystalline structure. For example, in a unit cell of NaCl, the center of symmetry is in the center of the unit cell because if a vector is drawn from this point to any charge and then draw the reverse vector, the same type of charge is found. Therefore, when mechanical stress is applied to the crystal, the negative charges coincide with the positive charge in the center and the net polarization is zero.

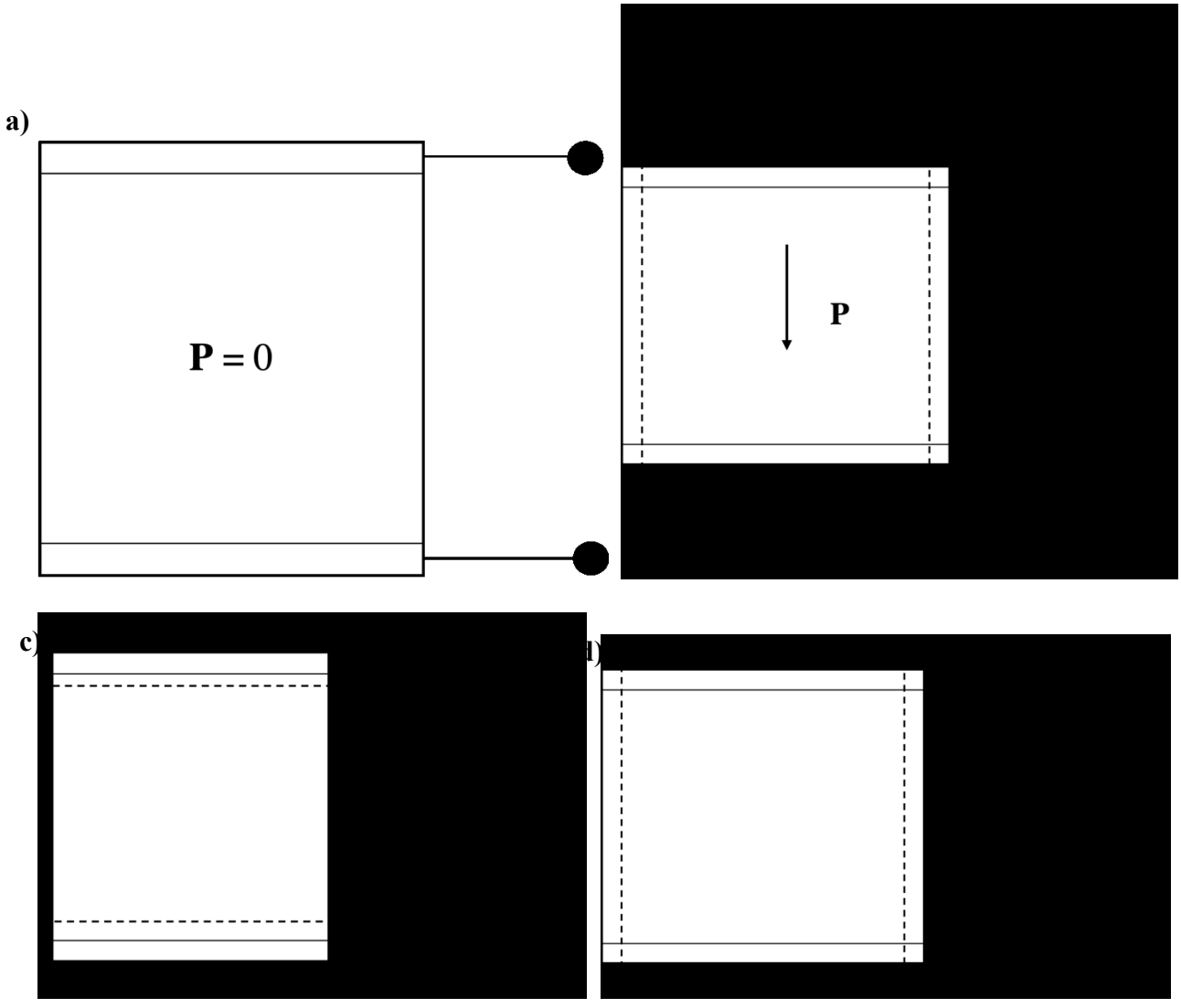

Figure 2.4: The piezoelectric effect: a) A piezoelectric crystal with no applied stress b) A piezoelectric crystal that when applied compressive forces leads to surface charges and polarization c) An applied field causes the crystal to be strained d) The strain changes with the applied field and the crystal is extended [81].

However, in the hexagonal unit cell shown in Figure 2.5 does not have a center of symmetry [81]. If a vector is drawn from the point O to any charge and then reverse the vector, an opposite charge will be found. Therefore, the unit cell is noncentrosymmetric. When mechanical stress is applied, the positive charge at A and the negative charge at B both become displaced inwards to A' and B' respectively. The center of masses therefore shifts, and a net polarization is created. The direction of the induced polarization depends on the direction of the applied stress. When the same unit cell is stressed along the x direction, the induced dipole moment is zero along the x direction but there is displacement of the centers of mass in the direction. The stress leads to displacement of the atoms in the outward direction to position A'' and B''. Applied stress in one direction can give rise to induced polarization in different directions. If T_j is the applied mechanical stress along some *j* direction and P_i is the induced polarization along some *i* direction, then the two are linearly related by:

$$P_i = d_{ij} T_j \qquad \ldots(i)$$

where d_{ij} are the piezoelectric coefficients. Therefore, if mechanical stress is applied in either the x or the z direction and polarization is produced in the y direction, the coefficient is defined as d_{31}. However, if the stress is applied in the y direction and the polarization is formed in the y direction the coefficient is defined as d_{33}.

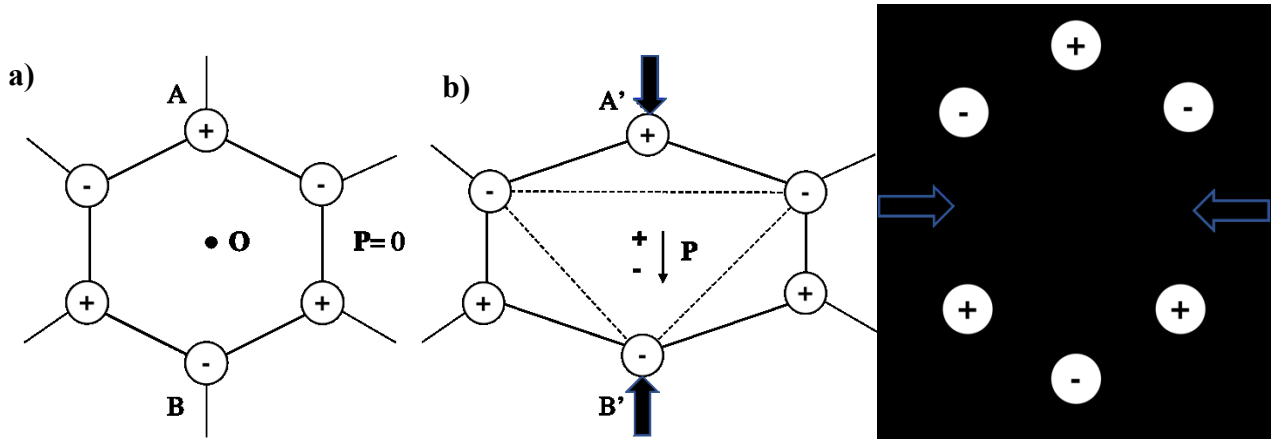

Figure 2.5: a) A hexagonal unit with no center of symmetry b) Under an applied force in the y direction c) Under an applied force in the x direction [81].

There are crystals that are permanently polarized even in the absence of an applied field [81]. These kinds of crystals have a permanent polarization due to the separation of positive and negative charges in the crystal. These are called ferroelectric crystals. The difference between a piezoelectric and a ferroelectric crystal is the presence of a residual electric field when the applied stress is removed. $BaTiO_3$ is an example of a ferroelectric crystal. Above the critical temperature, called the Curie temperature (T_c) the ferroelectric property of the crystal is lost. For $BaTiO_3$, the T_c is 130º C. Below the Curie temperature, spontaneous polarization occurs. The development of permanent dipoles above the Curie temperature is due to long range interactions between the ions outside the simple cell seen in Figure 2.6. Since above 130º C, there is no spontaneous polarization the temperature, a temporary field is applied in order to induce spontaneous polarization P along the field direction. This process is called poling. During poling, the electric dipoles of the crystal align in the direction of the electric field.

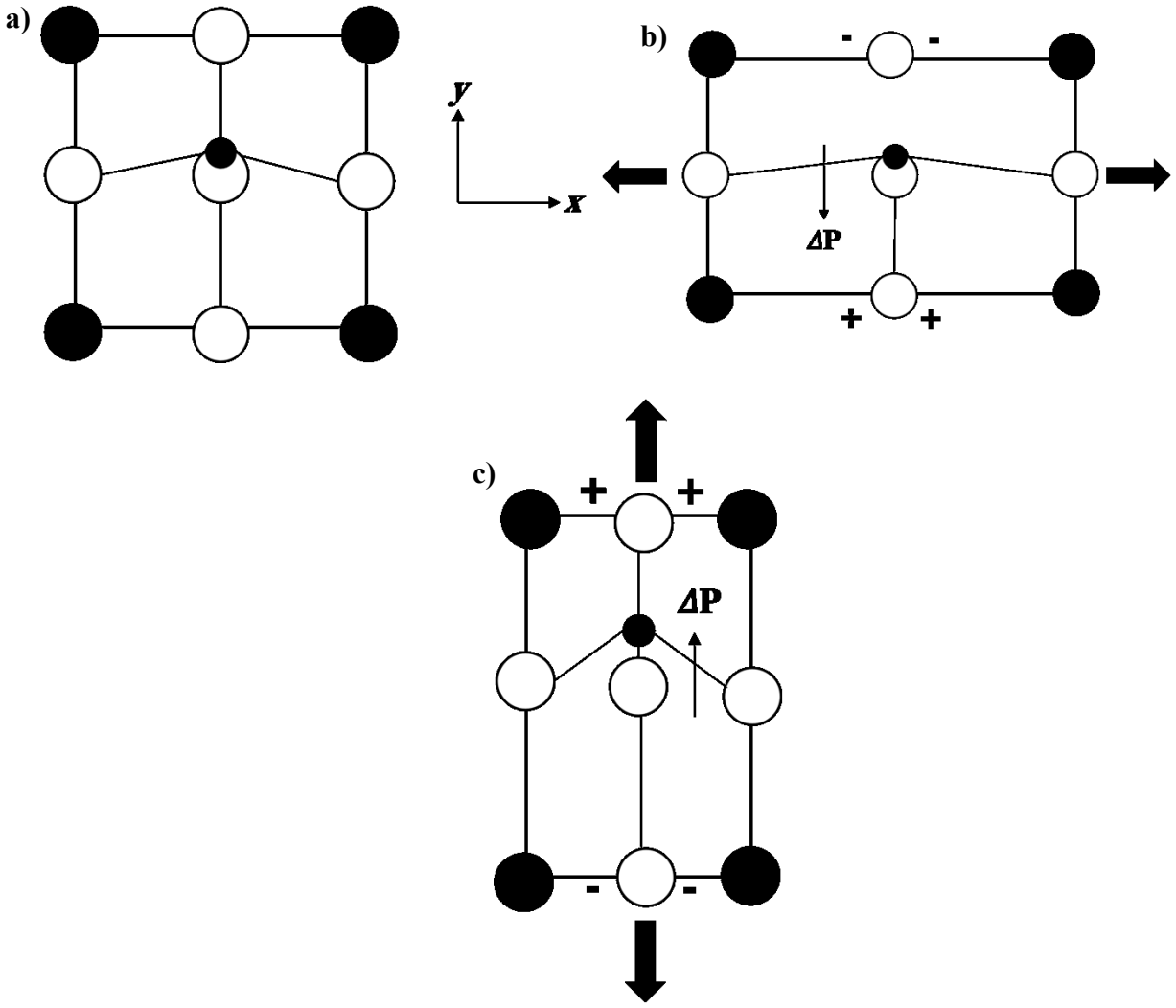

Figure 2.6: $BaTiO_3$ tetragonal structure below 130º C b) $BaTiO_3$ crystal under stress in the x direction c) $BaTiO_3$ under stress in the y direction [81].

2.4.2. Piezoelectric materials

Piezoelectric materials are a special type of dielectric material that possess transducer characteristics that convert mechanical strain of materials into electricity and vice versa [80]. Ferroelectric materials also exhibit piezoelectric properties and are extensively used in real-life applications more than non-ferroelectric materials. This is due to the fact that their transducer and actuator characteristics are better than the latter. Some piezoelectric materials that have been

commonly used include lead zirconate (PZT), aluminum nitride (AlN), zinc oxide (ZnO), barium titanate ($BaTiO_3$), lithium niobate ($LiNbO_3$) and quartz [82]. Organic piezoelectric materials like polyvinyl fluoride (PVDF) are ferroelectric materials which tend to show piezoelectric properties after poling treatments [83]. Devices made of piezoelectric polymers are usually less expensive because they do not require advanced microfabrication facilities like high temperature and/or vacuum processing that are needed for thin film fabrication [84]. However, organic piezoelectric materials are not able to provide piezoelectric output of comparable amounts to inorganic piezoelectric materials [85].

Quartz: Quartz is non-ferroelectric crystalline silicone dioxide. It is one of the most popular non-ferroelectric piezoelectric material being used [80]. An alternating current can be given to the quartz plate in order to make it vibrate. If the frequency of the AC signal coincides with the natural frequency of the quartz crystal, the crystal resonates at the frequency of the AC signal with maximal amplitude. This is often used in a feedback system (system that compares the output to the input and takes corrective action to match the output to the input) to get an extremely stable frequency output. Resonator made of quartz has good mechanical properties, high modulus, high Q factor, good reliability, and long lifetime.

Aluminum nitride (AlN): AlN is a tetrahedrally bonded semiconductor that has a N atom in a tetrahedral interstice with surrounding Al atoms [86]. There is no center of symmetry present in the interstice and this leads to a dipole moment when stress is applied on it. AlN is a popular piezoelectric material used in the fabrication of resonators, filters, sensors, optical devices, and surface acoustic wave devices (devices that make use of electromechanical waves that form on the surface of piezoelectric crystals like radio) [87]. It is an attractive material for the production of biosensors and other biodevices. The numerous advantageous properties of AlN include its

chemical stability, a wide bandgap and high acoustic velocity. The high acoustic velocity and electromechanical coupling ability makes AlN films great for gigahertz devices and sensor applications.

Lead zirconate titanate (PZT): One of the most popular piezoelectric materials that has been studied widely is the PZT [80]. PZT is a ferroelectric ceramic extensively used in transducer and actuator applications with its outstanding piezoelectric and mechanical properties. It can be fabricated into different shapes and sizes. The chemical formula of lead zirconate titanate is $PbZr(Ti)O_3$ [88]. It is formed when $PbZrO_3$ and $PbTiO_3$ are combined. The presence of large sized cations (Pb^{2+} ions), small sized cations (Zr^{4+}/Ti^{4+} ions) and oxygen atoms at the edges, faces and body center in the perovskite ABO_3 structure makes the PZT structure suitable for piezoelectric effect.

The crystal structure is non-centrosymmetric and has a net nonzero charge in each unit cell before stress is applied on it [89]. The process of polarization of PZT is alike that of AlN. Once stress is applied on the crystal, the titanium ion in the unit cell shifts its position and electrical polarity comes into play. The internal diploes of PZT can be reoriented by applying electric field to it so that there is remaining polarization even when there is no electric field [84]. PZT shows greater sensitivity to higher operating temperatures when compared to other metallic oxide based piezoelectric materials.

It has good mechanical properties, is chemically inert and relatively inexpensive to manufacture [90], [91]. It exhibits superior electromechanical properties due to its large piezoelectric charge constant which makes it attractive for the manufacturing of biodevices. PZT has also been studied for its biocompatibility for its application in *in vitro* and *in vivo* biosensors [92]. Researchers have been able to show that the biocompatibility of PZT can be improved

immensely by treating it with titanium which is a metal with high biocompatibility and is used in bone implants.

Zinc Oxide (ZnO): ZnO is an inorganic piezoelectric material and has special properties like excellent transparency, high electron mobility and biocompatibility [93]–[95]. ZnO has also been in flexible mechanical energy harvesting devices and as an active material for transient electronic and strain sensing devices [96]. However, high quality ZnO films with piezoelectricity often require very high processing temperatures for manufacturing [97].

Gallium Nitride (GaN): GaN is another piezoelectric material with properties of having of a energy bandgap of 3.4 eV, high electron mobility, excellent chemical stability as well as low electrical drift in ionic solutions, GaN does not have bio-functional influence on cellular environments which is important for biosensing applications [82].

2.4.3 Fabricating a piezoelectric actuator

For the application of actuators, piezoelectric materials are required to be shaped as a disc, cylinder or plate of varying dimensions; one specific example of cymbal-shaped actuator is shown in Section 3.1.2. For high-end piezoelectric actuators, such as PZT-based ones, powder sintering method is the most commonly used [80]. This can be done using a mold and pressing the powder using techniques like uniaxial and isostatic pressing at high temperatures. Tape casting technique is the method that is widely used to produce piezoelectric films. These are then used to produce different configurations of actuators. Cymbal actuators are produced by using piezoelectric films and metal endcaps that are bonded to each other at the circumference with epoxies [98]. The metal endcaps are made into the shape of cymbals by punching and pressing them using a punch die.

2.4.4 Examples of Biomedical Applications

Dagdeviren et al developed nanoribbons of PZT that help in *in vivo* measurements of soft tissue elasticity. The device was manufactured by a stacking process [99]. The actuator array consisted of a three layer electrode series: a bottom Pt/Ti electrode, a middle PZT layer and top Au/Cr electrode. An array of actuators is laminated on the skin and are then stimulated to generate tissue deformation that are then sensed by another array of PZT sensors to provide information about the mechanical properties of the skin. This was then applied on various soft tissues and organ systems in different animal models for validation. Nguyen et al made PZT nanoribbons for the measurement of mechanical changes that are generated in cells and tissues [100]. The PZT nanoribbon arrays were transferred onto a silicone elastomer and mechanical deformations of a cow lung that was explanted were studied. These nanoribbons are advantageous due to their minimal invasiveness and scalability for long term biosensing. Dagedeviren et al made flexible PZT based energy harvesters that are capable of energy storage coming from the natural movement of the heart, lung and diaphragm [101]. Hence, PZTs have been used as sensors and actuators in biomedicine.

ZnO nanoparticles (NPs) have been in used in many biomedical applications [102]. Li et al fabricated scaffolds made of PVDF doped with ZnO NPs using the electrospinning method [103]. These were tested for potential bone tissue engineering applications. The results showed an increase in the elasticity modulus and elongation at break. When the scaffolds were piezoelectrically excited there was an observed increase in the osteoblast density when compared to the control. Dermal patches composed of ZnO nanorods have the ability to send piezoelectric potential for wound healing [104]. ZnO is also used for anti-cancer applications since NPs made from piezoelectric materials can be loaded with therapeutic molecules for drug release

applications. Researchers have found that piezoelectric ZnO NPs help in simultaneous targeting and tracking of human breast cancer cells [105]. Excitation of these NPs leads to an optical signal which can be used for tracking of these cells.

Nanogenerators made of GaN can be used for harvesting biomedical energy [106]. Gallium nitride nanonrods are used as parts of biomedical devices due to their ability to deform and preserve performance under stress and strain. AlN piezoelectric biosensors are used for tracking multiple specific biological reactions which helps in providing information regarding reaction kinetics. These sensors are also used in the detection of protein interactions and antigen-antibody binding.

Chapter 3- Piezoelectric actuators

3.1 Introduction

In this chapter, we study the method of providing vibrotactile feedback. Piezoelectricity is discussed in detail because the working principle of the selected actuator is based on it. A survey of different actuators was conducted, and they were tested in order to understand which one will be able to provide feedback and also help in precise control. Once the actuator was chosen, we studied the vibrational characteristics of it in order to understand how different signals can be given to the skin. The actuator should be able to provide warning signals when the force applied on the jaw reaches levels that could lead to the breakage of the oral prosthesis, damage to their teeth and tongue. It should also be able to provide feedback on food texture signals in order to help patients distinguish between different foods that are being chewed by them. In order to study the ability of the actuator, it was characterized using a LDV. The working principle of a LDV and its applications is also discussed in more detail. The studies were designed in order to understand the behavior of the piezoelectric actuator and also help in designing the perception tests.

The tests conducted were displacement vs input intensity, displacement vs voltage, voltage vs input intensity and voltage vs frequency. The results of these experiments showed that when the input intensity and voltage are increased the output displacement produced by the actuator also increases. However, the frequency remains constant. This helped in understanding how to control the output displacement of the actuator. The actuator was then studied for its behavior when food texture signals were inputted in order to see if the input signal matches the output signals of the actuator. This was done in order to confirm the fact that we are able to provide food texture signals in the form of vibrotactile stimulation to the skin. We also compared the performance of linear resonating actuators (LRAs) for this application and concluded that they were not suitable because

of the inability to control their frequency of vibration. This chapter helped in understanding the vibrational characteristics of the piezoelectric actuator for stimulating the skin and in designing the perception tests in Chapter 5.

3.1.1 Piezoelectric actuators for biofeedback

Piezoelectric actuators can also be made into different configurations using a variety of fabrication techniques. Some of the commercially available piezoelectric actuators are monomorphs, bimorphs, stacks, co-fired, disk, and flexure elements. Their configuration varies depending on their application [80]. Piezoelectric stack or multilayer configurations are made by stacking the pieozoelectric disks or plates. Tube actuators are monolithic devices that displace laterally when a voltage is applied between the inner and outer electrodes. Disk actuators are those that are in the form of a planar disk and ring actuators are those with a center core making the actuator suitable for electrical, mechanical and optical applications. Piezoelectric actuators are used in telephones, stereo music systems and musical instruments [76]. In the medical field, they are used in endoscope lenses used for diagnosis.

A biofeedback system requires a sensor, actuator, user and a processing device. An actuator helps in providing controlled movement which is essential for precise feedback. Actuators are able to incite a particular response in correlation to the user's activity [107]. They are able to make use of human sense in order to generate movement. These senses mainly include the activity of the ear, skin and the eyes hence providing auditory, visual and haptic feedback.

An artificial tactile stimulation requires understanding how skin perceives vibrations [108]. There have been studies conducted on different materials that can be used for tactile perception [109].The way the brain classifies different kinds of materials is studied in tactile cognition [110].

These haptic feedback systems have been able to achieve very similar properties to that of the human skin. Haptic feedback systems require the use of an actuator that can be in contact with the body at all times to provide vibro-tactile feedback. Vibro-tactile actuators like linear electromagnetic actuators, rotary electromagnetic actuators and non-electromagnetic actuators have been used in the field of haptics for virtual reality applications [111], [112].

These commercially available vibrational actuators have a range of functionalities such as the amount of control that can be exercised by the user, the frequency of operation, the amplitude of vibration etc. These actuators also differ in terms of size, shape and price. Piezoelectric actuators transduce the input alternating current (AC) voltage signal into physical vibration, and thus deliver the signals to the skin in tactile manner. The piezoelectric actuators typically run at voltages higher than that of the other vibro-tactile actuators. However, they are able to provide precise mechanical deformation depending on the electrical input [113]. Most commercial piezoelectric actuators use piezoceramics as the active material [114]. These piezoceramic materials have quickly become popular due to their low cost, easy to integrate and execute into sensing and actuating applications, as well as active vibration control [115]. Ferroelectric ceramics with perovskite structures, such as lead zirconate titanate (PZT) are among the most popular choice [116].

3.1.2 Cymbal actuators

Cymbal actuator is a type of actuator configuration that is a piezoelectric disc sandwiched between two truncated conical metal endcaps, made of either titanium or brass [115]. The device configuration renders the advantage of high displacement when compared to other types of piezoelectric actuators. Dogan et al made a comparison of different actuator configurations of similar geometries [98]. In their study, the driving voltages were kept constant. The parameters

used for comparison were displacement produced, cost, fabrication techniques, generative force, position dependence on displacement, response time etc. The configurations compared were multilayer, bimorph, cymbal and moonie. The configurations of multilayer, bimorph and moonie are seen in Figure 3.1 and the design of cymbal actuator is seen in Figure 3.2. Cymbal actuators were seen to generate the highest force next to multilayer piezoelectric devices. This can be solved by using a multilayer disc as the driving element for the cymbal configuration in order to increase the force. Cymbal actuators were also seen to produce the highest displacement amongst all of the configurations compared. These are also advantageous for their easy fabrication technique and lower cost.

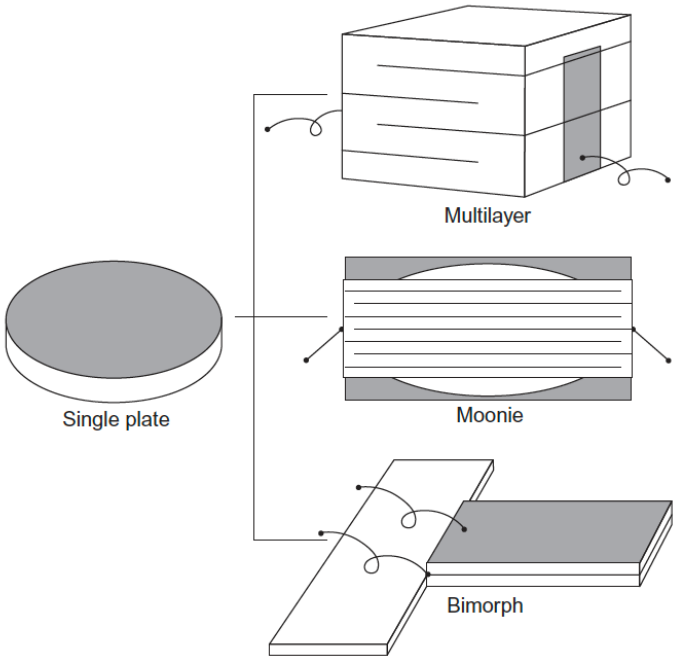

Figure 3.1: Different actuator configurations [117].

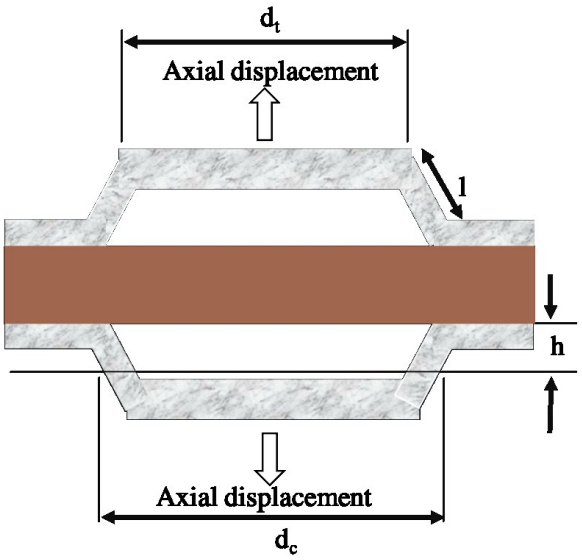

Figure 3.2:Cross-sectional view of piezoelectric actuator design

The cymbal actuators have been studied for applications like that for servo displacement transducer and pulse drive motor. The piezoelectric disc in a cymbal actuator serves as the driving element and the metal endcaps help in amplification of the displacement produced. This is done by converting the transverse shrinkage of the piezoelectric disc into longitudinal displacement. When electrical field parallel to the direction of the piezoelectric disc is applied, the radial motion of the disc is converted into flexural and rotational motions in the endcaps. This is supported by the stiffness of the material which helps in achieving a large displacement.

Cymbal actuators are derived from moonie actuators which have moon-shaped cavities between the metal endcaps and the piezoelectric ceramic [118]. The metal endcaps on the cymbal actuators have a truncated conical shape and act as mechanical transformers to convert the radial motion to displacement. The coefficients d_{31} and d_{33} of the piezoelectric ceramic help contribute to the axial displacement of the composite resulting in a high displacement. The cymbal design has been seen to show effective piezoelectric coefficients as large as 16,000 pC/N which accounts to

40 times more than the single plate piezoelectric ceramic, as shown in Figure 3.1. The displacements produced by cymbal actuators has also been recorded to be 40 μm, 40 times more than a single piezoelectric ceramic. Acceleration sensitivity was seen to be 50 times higher than that of a PZT disc. The fast response time of around 30 μs is advantageous for active vibration control applications like when providing feedback. They have been used in drug delivery systems (example insulin) due to its light, compact structure, and low resonance frequency in water. This configuration of actuator was chosen to its above stated advantages and the working was further studied.

3.1.4 Working principles of a cymbal actuator

For our application, a ferroelectric ceramic PZT layer sandwiched between two titanium cymbals was used (TDK PowerHap 0909H011V060, TDK Electronics, Japan). This operates between 0-60 V. The titanium cymbals help in amplifying the axial displacement of the PZT film for haptic feedback [37]. When the actuator is purely electrically driven, the displacement of the actuator can be given by:

$$d = 2\{[l^2 - \left[\frac{(d_c + d_{31}Ed_c - d_t)}{2}\right]^2]^2\}^{1/2} - h\} + d_{33}Et_p \qquad [115] \text{ …..(ii)}$$

where d_{33} corresponds to the piezoelectric constant, h is the height of the cymbals, d_c is the diameter of the cymbals, d_t is the diameter of the upper layer of the cymbals, E is the electric field being provided to the piezoelectric disc, t_p is the thickness of the piezoelectric PZT layer and l is the amount of incline from the top of the cymbals to the end where the cymbals are fixed. Here, d_{31} can be calculated by,

$$d_{31} = \frac{d_{33} - d_h}{2} \qquad [119] \text{ …..(iii)}$$

Here d_h is the hydrostatic coefficient which can be calculated by using a hydrostatic chamber. The parameters are illustrated in Figure 3.2.

It is important to observe that the electric field depends on the displacement in these actuators which become useful in precise control of the vibration control by AC and DC signals. The ability of these actuators to provide precise control, frequency, ease of integration with different softwares and drivers makes them a suitable device for this application. This was further studied using the LDV and the working of this is described in the next section.

3.1.5 Laser Doppler vibrometer

A laser Doppler vibrometer (LDV) detects the shift in Doppler frequency that occurs due to the movement of the surface of an object [120]. The frequency shift is directly proportional to the surface velocity (i.e., the rate of vibration at the surface of the object) and so its detection helps in easy non-contact measurement of vibration velocity. The detection process is not entirely straightforward because the frequency of the laser is usually 6 to 7 orders of magnitude more than the Doppler shifts, which are typically in the MHz range [121]. The light scattered from the object has to interfere with a mutually coherent reference beam in order to produce a beat in the collected light intensity at the difference in frequency between the target and reference beams. This setup does not give information about the direction since the demodulation can only detect the modulus of the shift in frequency. For solving this, a Bragg cell (shifts the frequency of the reference beam shown in Figure 3.3) is usually used in commercial instrumentation [122].

Scanning LDV (sLDV) enables mapping ability to LDV by automating the relocation of a single beam laser in order to capture and scan point by point across a surface [123]. The applications of sLDV initially were in the automotive and aerospace industry but has quickly

expanded [124]. The development of sLDV has led to a technique called the experimental modal analysis in which the measurement of the surface's vibration is characterized into parts: the temporal and spatial mode [125]. The temporal mode allows for gathering information by applying excitation forces and recording the response at a particular point. The spatial properties are however extracted by measurement at various different points. When individual transducers are used, the number of measurement points is limited to the cost and setup time which is not ideal, however the sLDV helps in solving this problem by balancing the recording of spatial and temporal modal properties.

sLDVs these days offer state-of-the-art automated, tri-axial vibration surveys on large, three-dimensional structures using sLDVs mounted on a robot arm or on microscopic structures with the help of a confocal microscope [126]. In a traditional sLDV, the laser beam is set at a particular measurement point for a particular time duration depending on the spectral resolution required. Measurement at multiple points can be sped up by the use of a continuous laser Doppler vibrometer, in which the laser beam scans continuously on a defined path at selected frequencies. There are many interesting applications of LDVs.

Davis and Kulcyzk et al used LDVs for their work on turbine blade. This was the very first application of LDV [127]. Since then, work has been done on loudspeakers and hearing followed by hard disk drive measurements and applications in engine torsional vibrations. LDV has hence proven to be an effective alternative to traditional contact vibrational measurements done by using transducers [120]. It has been used in many fields of mechanical, electrical and civil engineering and also in the medical field. It has been proven to be an effective diagnostic tool in detecting damages on structures using a non-contact method. Using 3D sLDV has led to measurements of

strain of complex structures and has been beneficial in locating defects. This has been conducted on composite materials in civil engineering.

In micro-electromechanical systems (MEMS), semiconductor fabrication technology is used to make systems by coupling mechanical and electrical properties [128]–[130]. These include small scale motors, fluid pumps and lab-on-a-chip technology. In some systems with dynamic parts which are driven at resonance LDV's advantages of three-dimensional measurements of picometer displacements and GHz frequencies are very useful. They have also been used in studying hearing mechanics [120]. The eardrum and three ossicles of the middle ear act as an acoustic impedance match between air and the fluid filled inner ear from which electrical impulses are sent to the brain [131]. The eardrum vibration is measured to be less than 1 mm at the threshold of hearing sensation. In clinical settings, studies have been done about ossicular prostheses and active middle ear implants[132], [133] . LDV measurements combined with finite element analysis has led to deeper understanding on how the bone connecting the eardrum to the inner ear transfers sound energy as efficiently as the three-ossicle system present in mammals. A schematic of the working principle of a LDV is shown in Figure 3.3.

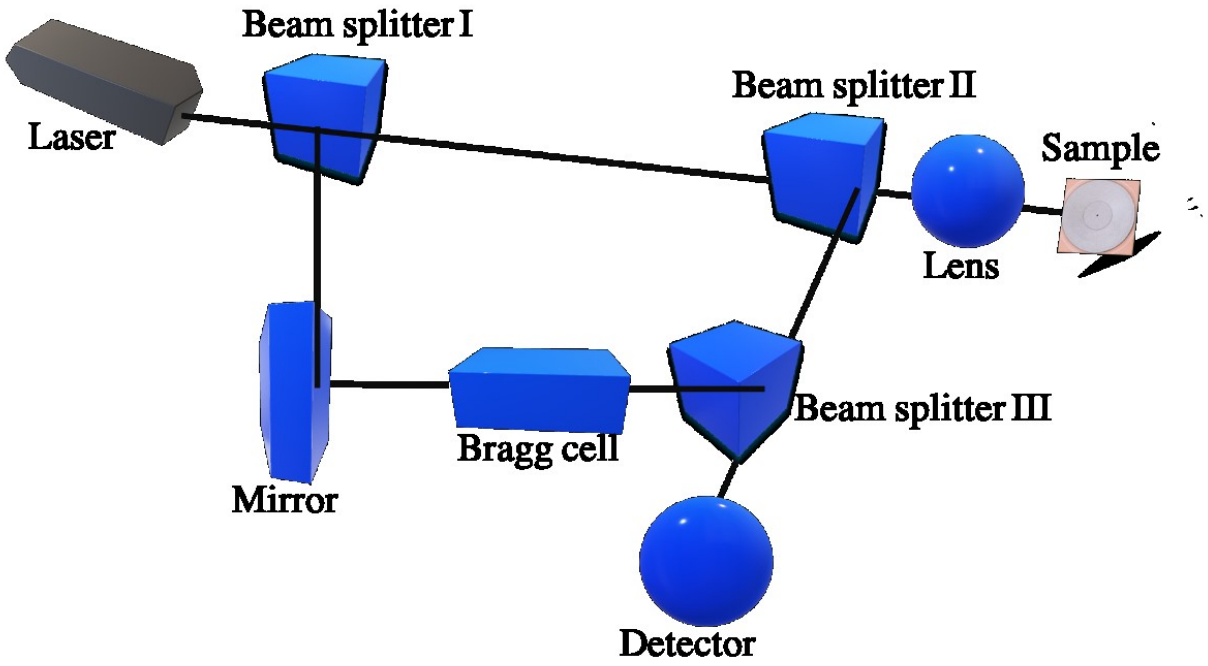

Figure 3.3: LDV working principle

LDVs have also been used to study loudspeaker phones, microphones, and ultrasound sensors [120]. They are also used for characterization of musical instruments like guitars and percussion instruments. The analysis includes examining vibrations on the structure with high spatial resolution and calculating the radiated sound pressure. LDVs are also capable of measuring the direct acoustic velocity of micro-particles in a fluid. Acoustic absorption coefficients measured from the end of a tube that is connected to a loudspeaker reflected from a test material is done by using sLDV. A sLDV was used in our study to measure and analyze the vibrational characteristics of the piezoelectric actuator. It was also used to scan the entire surface of the actuator in order to study differences in vibrational characteristics depending on distance.

3.2 Experimental section

3.2.1 Survey of commercially available piezoelectric actuators

Different commercially available piezoelectric actuators were surveyed for suitability. Factors considered for the best suitable candidate were: i) ability to actuate the skin with simple sinusoidal signal and complex texture signals, ii) thickness of the actuator, iii) design of the actuator, iv) displacement and acceleration that the actuator can provide, v) working voltage of the actuator and vi) ease of integration into a textile structure

Different vibro-tactile actuators were surveyed for the application of providing feedback. These actuators were based on different working principles like piezoelectricity, electromagnetism, and mechanical motors. Some of the actuators surveyed are listed in the Table below:

Table 1: Inventory of commercially available actuators

Model	Type	Dimensions	Voltage	Frequency
MEMS speaker (USound, Austria)	Piezo	6.7 x 4.7 x 1.56 mm	5 V	2-20 kHz
Linear resonating actuator (Jinlong Machinery & Electronics, Inc., China)	AC	5 mm	3 V	14000 rpm
Power haptic piezo disc (TDK Electronics, Japan)	Piezo	9 x 9 x 0.55 mm	0-60 & 0-120 V	At 60 V, 500 Hz
TDK haptic piezo actuator	Piezo	9 x 3.75 x 1.4 mm	0-60 V	Up to 500 Hz

(TDK Electronics, Japan)				

The actuators were studied and narrowed down based on the voltage, frequency range of operation, dimension and principle of operation. The actuators mentioned in Table 1 were tested for their feasibility, robustness, ability to integrate into textiles, vibrational characteristics. They were also tested to see how they can be controlled, and food signals can be delivered. The linear resonating actuators were studied extensively since they have been used for haptic applications. The MEMS speaker provided an auditory feedback compared to a tactile feedback. The haptic piezo actuators were studied in two shapes (circular and rectangular). These actuators when combined with the boreas technologies board consume lesser power when compared to LRAs. The TDK PowerHap 0909H011V060 was chosen for its compact design and ability to actuate the skin with a variety of signals of different amplitudes. They were also chosen after sensitivity experiments because of an increased surface area leading to increased stimulation of the skin.

3.2.2 Experiments with the piezoelectric actuators

The piezoelectric haptic actuators were tested for their application and ability to provide food texture signals. The rectangular shaped piezoelectric actuators (operated between 0-60 V) were able to stimulate the fingers, but the signals were weak for other parts of the body. As an attempt to improve the perception, an aluminum foil that encapsulate the piezoelectric disc was used to enlarge the effective area of contact. Signals with different waveforms, including sinusoidal vibration with or without superimposed food texture signals were delivered to explore the optimal condition for perception. Circular discs presented with a better perception and vibro-tactile sensation when compared to the rectangular shaped actuators.

Among the circular piezoelectric actuators, there were two options depending on the dimensions of the discs and the voltage of operation. The smaller circular discs are of dimension 9 mm* 9 mm *0.55 mm and operate at a voltage range of 0-60 V whereas the larger circular discs are of dimension 2.6 cm* 2.6 cm* 0.1 cm and operate at a voltage range of 0-120 V. The smaller discs were chosen because of their decreased voltage range of operation.

3.2.3 Characterization of the actuator

The piezoelectric actuator was studied for its application in haptics as well as its mechanical and vibrational characteristics. LDVs have been studied for their applications in the medical field to measuring vibrations [134]. The setup for the experiment is shown in Figure 3.4. A sLDV equipment (MSA-500; Polytec GmbH., Germany) was used for measuring the detailed acoustic output. The piezoelectric actuator was mount on a stand for the measuring displacement, frequency of vibration, to scan the real time displacement vs time and power spectrum of the piezo actuator.

The actuator was studied for its voltage vs input intensity, voltage vs frequency, displacement vs voltage characteristics. A schematic of the studies is shown in Figure 3.5. These measurements were made in the center of the piezoelectric actuator. The voltage was measured at the point where the piezo is connected to the board with the help of a digital source measure unit (SMU; Keithley 2402, U.S.A.). The piezoelectric discs are inputted with signals of different input intensities from the Audacity software. For these experiments, sinusoidal signals in the frequency range of 100-300 Hz were used, and measurements were made in triplets and the standard deviation was calculated. The change in displacement as we move away from the center of the actuator and the displacement vs input intensity characteristics at the periphery were also analyzed.

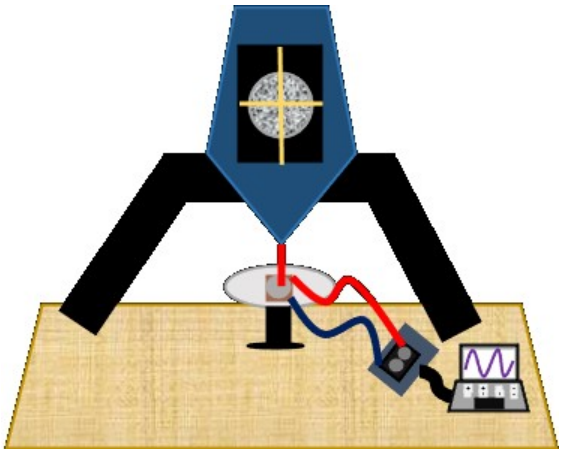

Figure 3.4: LDV setup

Further, the vibrational characteristics of the piezoelectric actuator when texture signals are used as input signals were also studied. All the four texture signals were used as input signals and the real time displacement vs amplitude, and the power spectrum of the signals were recorded to analyze and understand how the actuator is behaving when these signals are used as input signals.

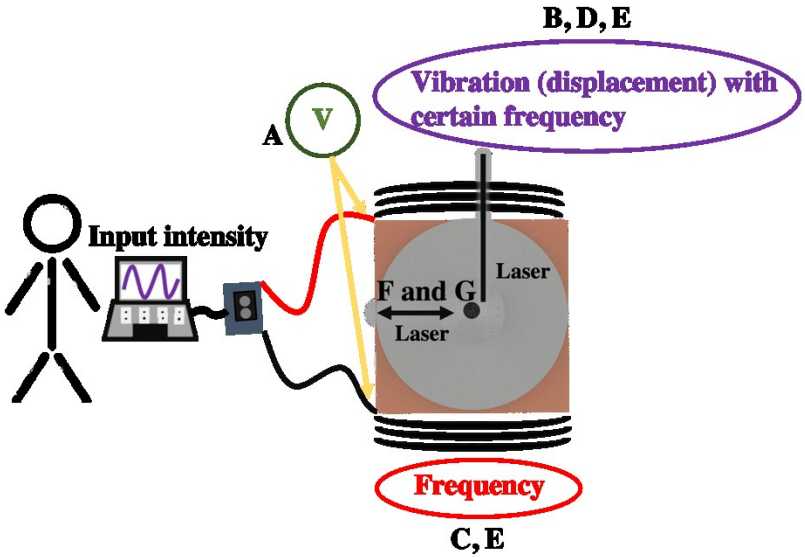

Figure 3.5: a) Voltage vs input intensity b) Displacement vs input intensity c) Voltage vs frequency d) Displacement vs voltage e) Food texture analysis f) Displacement vs input intensity across different points in the actuator g) Change in displacement according to distance.

3.2.4 Characterization of linear resonant actuators

Additionally, LDV experiments were also done with linear resonant actuators (LRAs). The LRAs were powered by a function generator (BK PRECISION 4047B; B&K Precision, U.S.A.). This was also used to provide DC signals to the coin cells. The LRAs were stimulated with DC signals ranging from 0.7 V up to 1.9 V in increments of 0.2 V. AC signals of 100-300 Hz sine waves was used in addition to the DC offset voltage. This was done to examine if the LRAs are able to effectively vibrate at a certain given frequency and if they can be used as a biofeedback system. The displacement vs time and power spectrum of the signals were collected and plotted.

3.3 Results and discussion

3.3.1 Voltage vs input intensity characteristics

The voltage vs input intensity characteristics was studied in order to understand the behavior of the piezoelectric discs under different input intensities. For the studies mentioned in this section, one actuator was used. The results are shown in Figure 3.6 (a). The piezoelectric discs were inputted with arbitrary values of input intensity ranging from 0.1 to 1 using the Audacity software (Open Source). The SMU was used to record the voltage measurements. This is important to study for the correlation between human perception and signals that are being provided to the human skin. It helps in understanding how the food texture signals need to be processed in terms of the input intensity and output displacement so they can be perceivable by the human skin. This also pertains to the biofeedback system and how much force is being exerted in the mouth of a human. If the force being exerted during chewing is very high, the displacement of vibration of the feedback signal needs to be high to indicate to the user that the force needs to be lowered in order to avoid injury.

The results for input intensity of the input signal and the displacement of the piezoelectric disc are shown in Figure 3.6 (b). These measurements were made using sinusoidal signals with 0.1 to 1 input intensity. The laser of the LDV was pointed near the center for recording the data. This study is important to understand the interconnection between the parameters of the input signal and the displacement being produced by the piezoelectric disc. The increase in displacement when the input intensity is increased is very encouraging because this can be correlated to the force exerted in the jaw to produce alarm signals to the subjects.

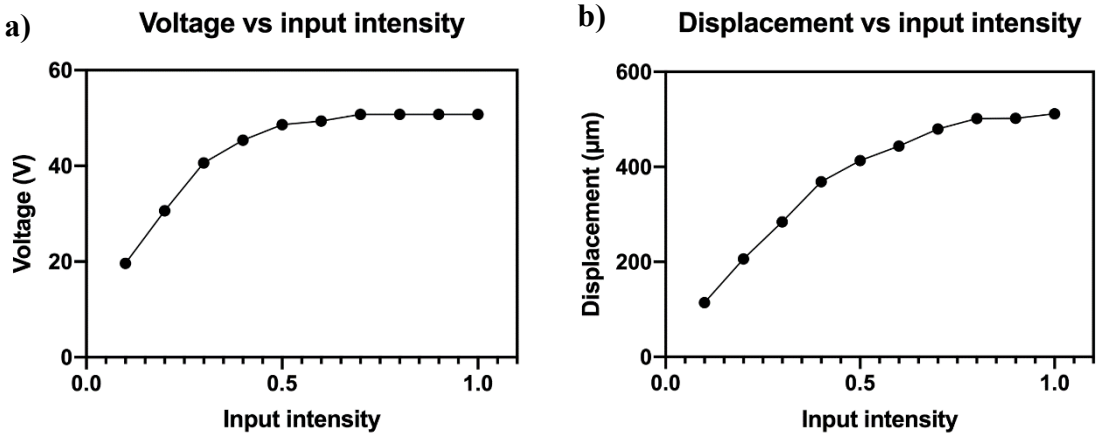

Figure 3.6: a) Voltage vs input intensity characteristics b) Displacement vs input intensity characteristics.

Understanding the correlation between frequency and voltage is also important since different food textures are broken down by different number of chewing cycles [135]. The voltage vs frequency characteristics is seen in Figure 3.7 (a). The frequency remains constant with increase in voltage. For biofeedback applications related to chewing this is beneficial because, the amplitude combined with the chewing frequency gives the information about texture. The input intensity is also correlated to an increase in the displacement when providing signals to the user. Therefore, an increase in displacement with an increase in frequency would lead to confusion.

From Figure 3.7 (b), it can be seen that as the voltage increases there is an increase in the displacement of vibration of the piezoelectric disc. This is due to the fact that the piezoelectric disc is a multi-layered piezoceramic system. Since, in a piezoceramic system the electric field depends on the axial displacement of the piezoelectric disc, the displacement increases as the voltage increases. This indicates that the intensity of the input signal corresponds to the input voltage to the piezoelectric disc. This is helpful in terms of understanding how to precisely control, process and deliver food signals in terms of amplitude.

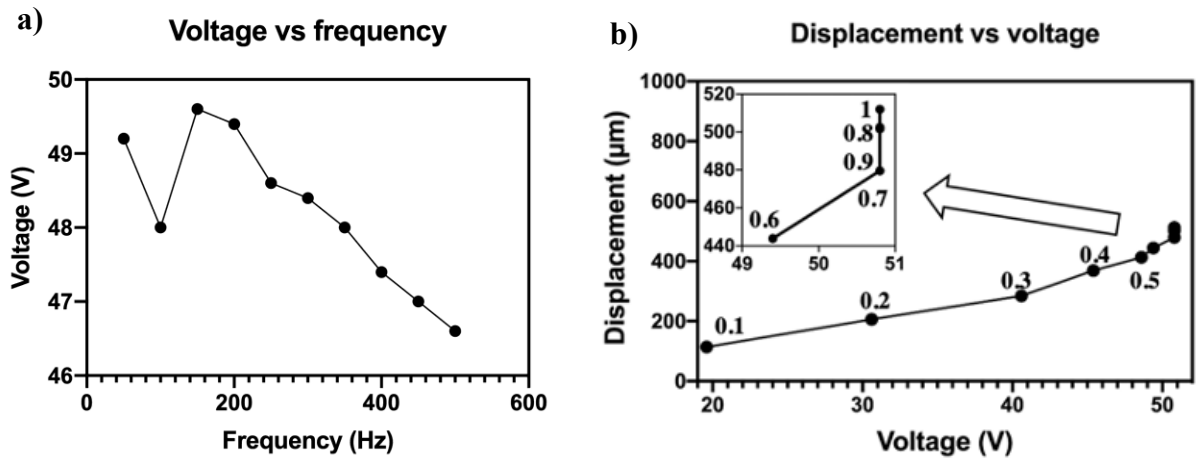

Figure 3.7: a) Voltage vs frequency characteristics b) Displacement vs voltage measurements

3.3.2 Food texture analysis

The piezoelectric actuator was also characterized for its ability to transmit food texture signals to the skin. The food texture signals that were presented to the author and supervisors in the perception test were used for this experiment. The LDV was used to see if the input food texture signal matches the vibrational characteristics of the piezoelectric disc. The results are seen in Figure 3.8. From the figure, it can be seen that we were able to precisely modulate the amplitude of food texture signals in a real time basis. This is important in understanding the role of the piezoelectric actuator as a biofeedback system for textures. The ability of the piezoelectric actuator

to provide different food texture signals to the skin is significant in this application. From the figure, we can see that it not only matches the input signals but is also able to provide different output displacements corresponding to the food texture. The ability of one piezoelectric actuator to provide this information has many advantages like usage of less surface area and lesser processing and delivery times as well. However, in the case of linear resonating actuators (LRAs), it has been seen that multiple actuators are needed for providing information related to texture [42].

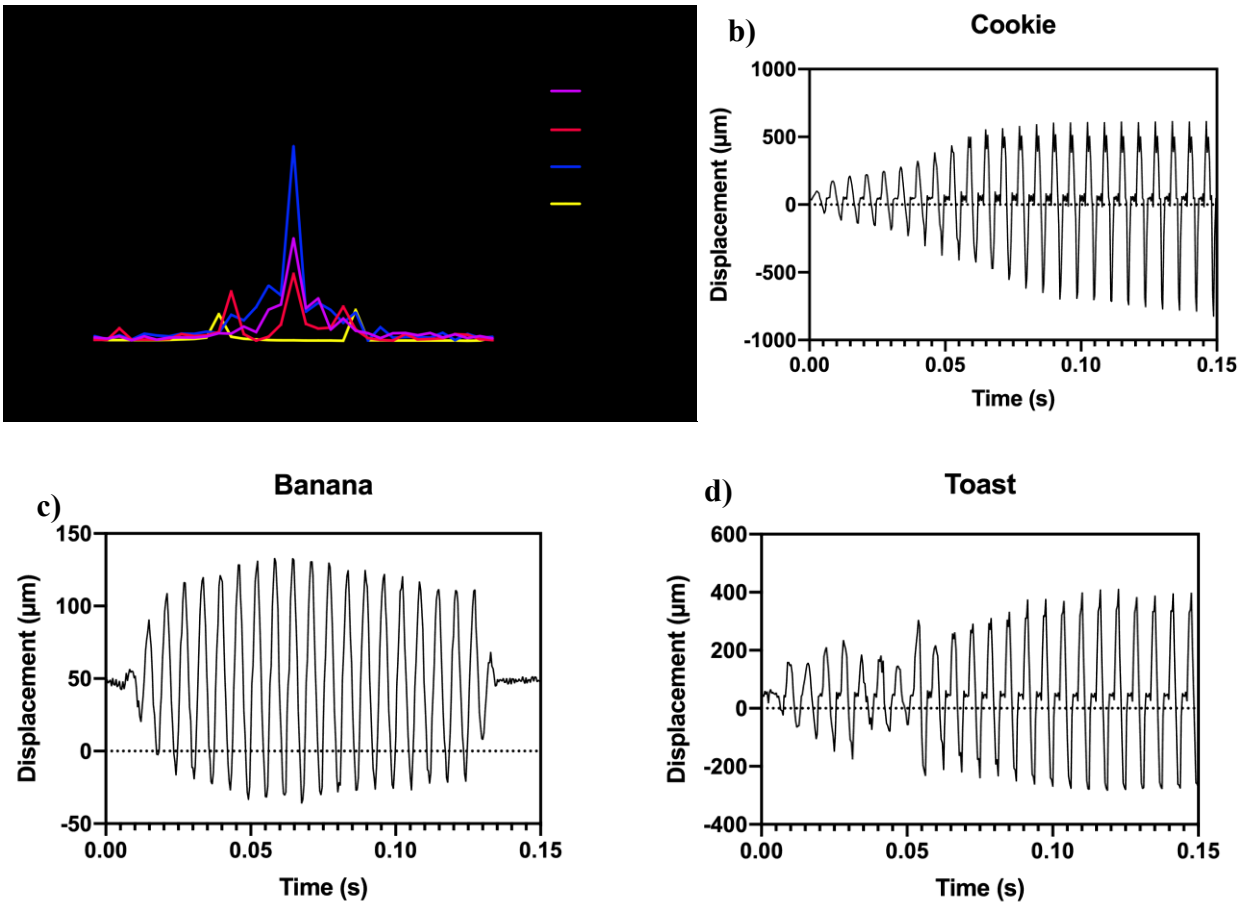

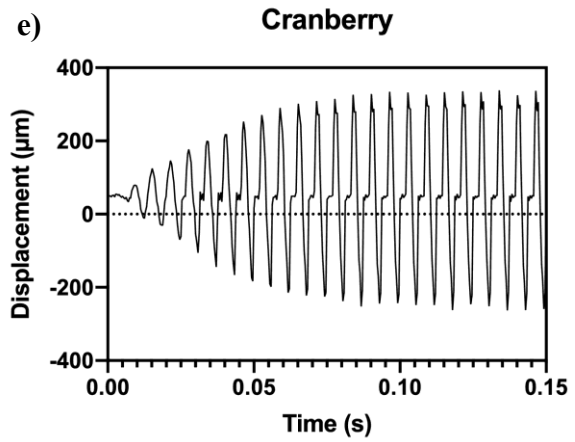

Figure 3.8: The displacement of the piezoelectric actuator as measured over time by LDV. a) Power spectra that shows the frequencies of vibration. The data from all the four textures over entire measured time are overlaid. Real time displacement data that convey chewing sensation obtained from b) Cookie, c) Banana, d) Toast, and e) Cranberry.

3.3.3 Displacement vs input intensity at different spatial points of the actuator

Since the displacement varies according to the location of the laser pointing on the piezoelectric disc, the displacement vs input intensity characteristics was interesting to compare for the center, a point in between and the edge. The results are plotted in Figure 3.9. For this study, three actuators were tested and the error bars are negligible. From Figure 3.9, we can see from the displacement vs input intensity characteristics of the center and the edge that the displacement at the center is approximately 13 times the displacement at the edge. The results also confirms that the displacement vs input intensity characteristics becomes stronger as we move from the edge towards the center. This is also due to the fact that center of the titanium cymbal has the most height when compared to the other parts. Since the displacement produced is related to the height of the cymbals from the PZT layer, it is evident that the farther the cymbal from the piezoelectric disc the higher the displacement [115]. The increase in displacement with the input intensity can

be justified by the fact that the displacement of vibration is directly related to the electric field which in turn is related to the input intensity. It can also be observed that the increase in displacement with input intensity is ubiquitous across the radius of the actuator.

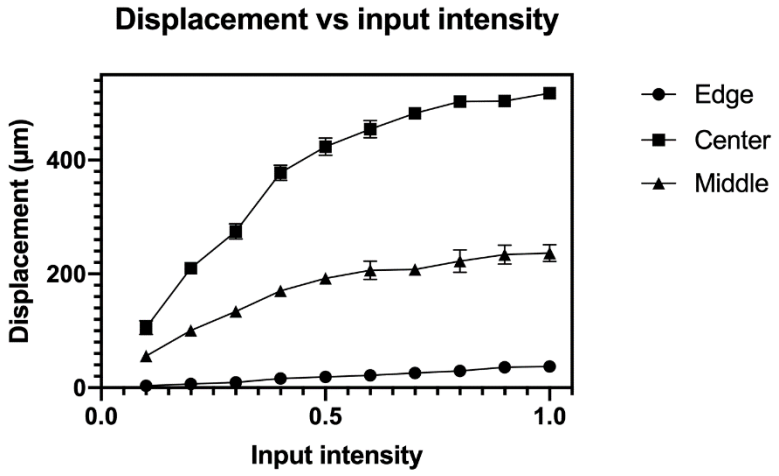

Figure 3.9: Displacement vs input intensity measurement for the edge, middle and center of the piezoelectric actuator.

3.3.4 Variation in the output displacement as a function of radial distance

Since the design of the actuator resembles that of a half hollow sphere with the edges clamped, understanding the displacement according to the distance is important. It also helps in understanding how the piezoelectric device behaves as a biofeedback system. A comparison was also done for 0.1 and 0.5 input intensities. For this study, three actuators were tested. Sinusoidal signals were used for this experiment and the distance between two measured points was approximately 307 µm. The total radius of the piezo disc was measured to be 4 mm, and hence 13 points were recorded and plotted. The results are shown in Figure 3.10. The error bars are negligible for the three actuators studied. From Figure 3.10, it can be seen that as the laser is pointed from the center to the edge, the displacement decreases. This is due to the fact that the

bending actuator is curved which leads to maximum thickness of the actuator at the center and in turn contributes to the higher displacement when compared to the edge [136].

The advantage of a higher displacement also comes from the fact that the metal cymbals that are used for amplifying the displacement are made of titanium, which has a very high Young's modulus of elasticity. Since the deflection of the metal cymbals is dependent on the Young's modulus, a higher displacement is produced which is important for the tactile feedback. It is also important to note that the displacement produced by the actuator rapidly decreases with increase in the thickness of the metal layer. The current piezoelectric disc has a thickness of 0.25 mm on each side of the disc which helps in the amplification of the displacement effectively.

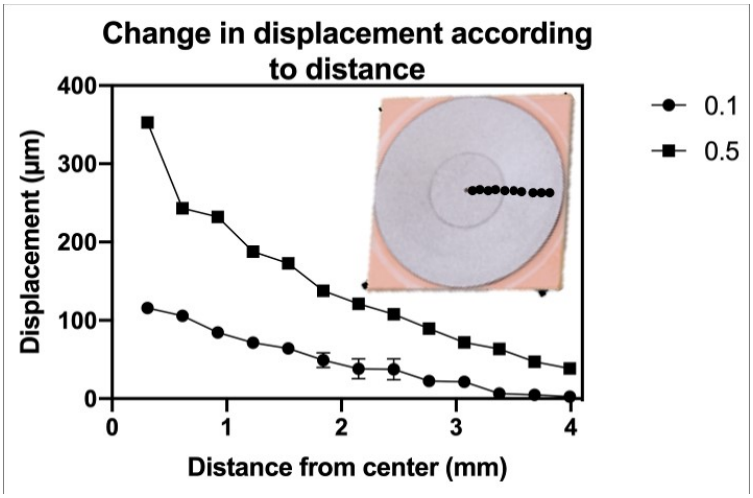

Figure 3.10: Change in displacement according to distance at 0.1 and. 0.5 input intensities.

3.3.5 Characterization of linear resonant actuators (LRAs)

The LRAs, also called as coin cell actuators, are studied for their efficiency to provide haptic feedback. These have been used for different haptic applications like virtual reality as well [137]. This is because of their ease of integration into textiles, low cost, compact size, ability to provide

high displacements at lower input voltages etc. This study was done to compare the performance differences between LRAs and piezoelectric actuators for providing tactile feedback related to chewing. It needs to be mentioned that the precision of tactile feedback is important in our application because the subtle texture of food must be delivered. The precision we require for the actuator is the ability to deliver the frequency and the amplitude of the actuator displacement precisely as driven by the input signal.

Our experiment was conducted to see if varying the voltage of the LRAs can produce varying displacements. It was also aimed to see if the LRAs vibrate at the frequency of the sinusoidal signals provided to them. The results are shown in Figure 3.11. The experiment was conducted from 0.7 (minimum voltage required to excite the LRA) up to 1.9 V. Sinusoidal signals of 100-300 Hz frequency was provided to the LRA. From the results, it can be seen that the dominant output frequency of vibration is not in the same order of magnitude as the input frequency. However, the displacement of the LRA does seem to increase as the input voltage increases. It needs to be stated that the LRA's vibration is much stronger than that of the piezoelectric disc. As a result of this, the laser of the LDV system could not be accurately positioned at one point during the measurement especially at voltages higher than 1.3 V; this is the limit of the instrumentation we use.

From this experiment, it becomes clear that the LRA is not able to control the actuation frequency with input signal. Instead, the frequency of vibration of the LRA changes with the input voltage. This can be attributed to the fact that the LRA has a particular resonant frequency [138]. When they are operated at their resonant frequency, their performance and displacement of vibration is the best and drastically decreases as we move away from the resonant frequency. Since, in the working principle of LRAs the voltage and displacement of vibration are two independent

parameters, it becomes harder to provide frequency related biofeedback to the skin. This makes from less suitable of a candidate for providing food texture related biofeedback signals even though they have been used in many commercially available products to provide different kinds of haptic feedback.

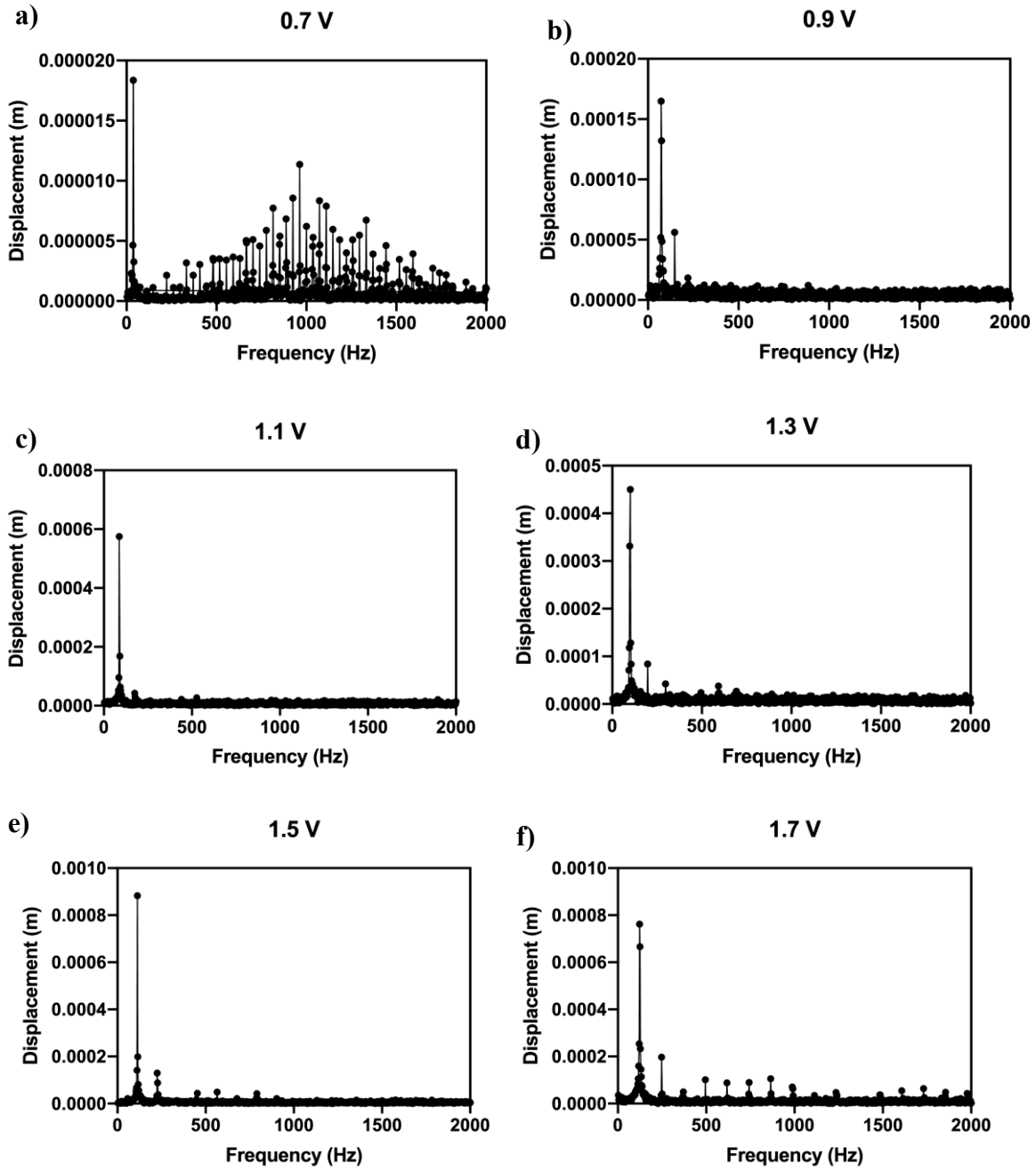

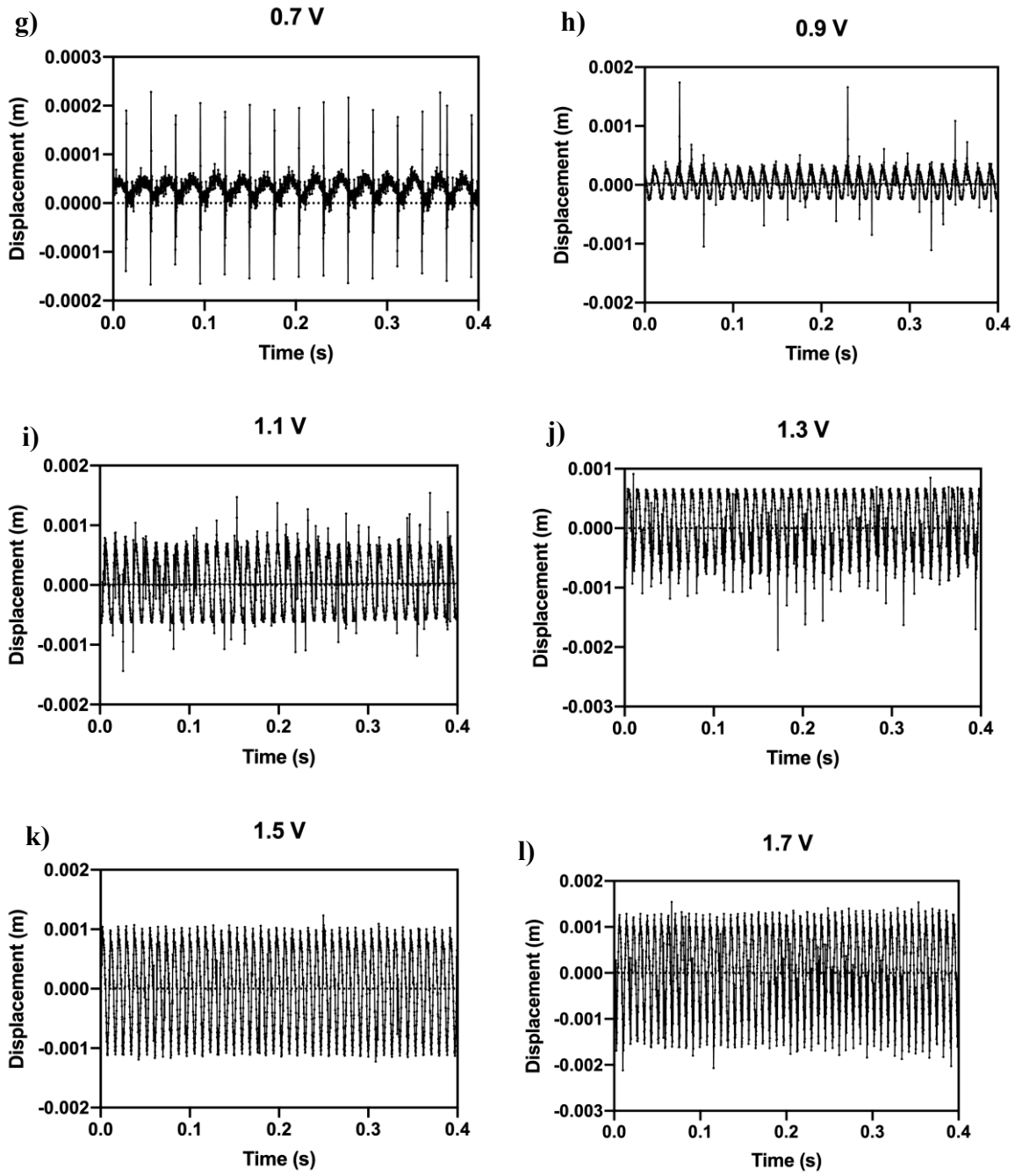

Figure 3.11: Frequency spectra of a) 0.7 V b) 0.9 c) 1.1 V d) 1.3 V e) 1.5 V f) 1.7 V and real time data for g) 0.7 V h) 0.9 i) 1.1 V j) 1.3 V k) 1.5 V l) 1.7 V.

3.4 Conclusion

Piezoelectric actuators, and in particular piezoceramic actuators have been studied for haptic feedback. Their ability to provide precise control is one of interest in the development of the smart garment. This was studied in the laser Doppler vibrometer experiments. The LDV was a very significant tool that was used in understanding how haptic feedback works. Characterizing the piezoelectric actuator with the help of a LDV was instrumental in learning about tactile feedback and the actuator's behavior from the author's point of view. These experiments gave a clear understanding of how the working of the piezoelectric actuator and helped us in controlling it and designing the perception tests. It also helped in understanding the motion of vibration throughout the actuator and its dependance to the time required to respond to a particular signal. The experiments also proved that the actuator is very suitable for the current application of haptic texture feedback.

The perception tests helped in validating the use of this actuator for mastication feedback. The actuator was able to provide feedback related to food texture accurately for most of the time. It was also able to provide different output displacements so it can be used for alarm signals and to also differentiate between food items that have different material properties like hardness. It was also able to provide spatial information which can be used for correlating to different events happening in different parts of the mouth. The tactile resolution really helps the patients in understanding and processing food into bolus for easier swallowing. All the perception tests also helped in confirming that the smart headband structure that was able to efficiently and effectively send signals to the skin and give feedback related to food signals.

Chapter 4- Smart textiles

4.1 Introduction

Smart textiles and wearable electronics have opened a new and significant realm in rehabilitation medicine [65]. Several methods used for the production of conventional textiles can be used in the production of smart textiles. For instance, a flatbed knitting machine can integrate conductive yarns with normal yarns like polyester [139]. In particular, the intarsia knitting technique is used to produce patches using different yarns, i.e. with different characteristics, e.g. restricting conductive yarns to a particular spot [140]. It has been largely used for the production of smart textiles [141]. In each of the areas, the knitting takes place with a separate yarn that is exclusively supplied by its own carrier [140]. At the points where the two different areas come in contact, the yarns supplied by the different carriers cross each other to bring physical integrity to the structure. Intarsia knitting is usually done using a V-bed flat knitting machine [142]. Intarsia knitting has been successfully used to create textile-based triboelectric nanogenerators with polyester yarns [143]. In addition to providing stretchability, washability and localization of the conductive yarns, the seamless connection of the different sections also helps making the garment comfortable and lightweight [144]. Intarsia knitting was also used to produce a surface EMG-based prosthetic hand with knitted sensors for myoelectric control [145]. The authors combined silver-coated conductive yarns with non-conductive polyester yarns. They used a circular knitting machine in which both ends of the conductive and non-conductive yarns were folded and connected to each other. The knitted fabric was double faced, with the external portion being non-conductive in order to insulate the current carrying yarns from the skin. The resulting sensor fabric was flexible, conductive, and washable, and can be of great help for amputees.

Embroidery also allows easily securing a yarn or a wire at the surface of a fabric [16]. It can produce textiles with varying pore patterns and elements to control the mechanical behavior [146]. One of the most demanding techniques based on embroidery is Tailored Fiber Placement which allows for orientation of a fiber on the structural material, helps preparing three-dimensional structures and offers flexibility in terms of making different shapes and sizes. Zeagler et al. have employed embroidery to manufacture e-textile interfaces, such as an embroidered jog wheel and a tilt sensor [147]. It has also been used for integrating snap fasteners in e-textiles [148].

In this study, we have developed a biofeedback system that is located on the forehead. The smart headband is equipped with three piezoelectric discs. It communicates with an oral prosthesis to deliver the signal corresponding to the food being chewed on as seen in Figure 4.1. The smart headband has been tested for its ability to deliver precise biofeedback signals in the form of a sensory substitute. It has also been tested for spatial differentiation to inform about events happening in different parts of the mouth during chewing. Finally, it was assessed for its efficiency at stimulating the skin with high frequency sinusoidal as well as food texture signals.

The piezoelectric discs are secured on the smart headband using velcro patches that are sewn to the headband fabric so that the structure is washable. The piezoelectric discs are connected to an interactive processing board via insulated conductive wires that are inserted into the headband. The processing board is connected to a computer. This construction makes the smart headband an effective, robust, and washable biofeedback system.

Figure 4.1: Biofeedback system

4.2 Experimental section

4.2.1 Materials

The materials used for the smart headband are:

- A fabric headband (Fly Away Tamer Headband II; lululemon athletica, Canada) made of a tubular sweat wicking, 4-way stretch knitted fabric composed of nylon and spandex fibers;
- TDK PowerHap piezoelectric actuators (TDK PowerHap 0909H011V060, TDK Electronics, Japan);
- Insulated multifilament copper wires (28 AWG);
- Quick-connect insulated tab-type connectors (3-520141-2, 2-520102-1, TE Connectivity AMP Connectors, Switzerland);
- A Boreas Technologies (BOS-1901, Boreas Technologies, Canada) board for each piezoelectric actuator.

A force sensitive resistor (Interlink 402 model) connected to an Arduino board via a 10kΩ resistor was used to control the force applied by the headband on the forehead.

Various types and gauges of conductive yarns (Shieldex 235/34 4-ply; Shieldex 117/17 2-ply; Shieldex 110/34 2-ply; Shieldex 235/34 2 ply; Sparkfun; Kitronix; Copper tinsel; and Silver coated nylon (see section 4.3.3 for more details)) were obtained to explore their ability to be used for data and power transmission between the control board and the piezoelectric actuators.

Finally, the use of silicones was explored to encapsulate the actuators so that they could resist washing. Experiments were conducted with different types of silicones (Ecoflex 00-30, Smooth On Inc., USA; Ecoflex 00-50, Smooth On Inc., USA; ShinEtsu 2230-45, ShinEtsu, USA; ShinEtsu 2230-55, ShinEtsu, USA; and Ecoflex gel, Smooth On Inc., USA) and a linear resonant actuator (W0825AB001G, Jinlong Machinery and Electronics, Inc., China).

4.2.2 Methods

For the experiments exploring the ability of silicone encapsulation to allow actuators resist washing, a layer of silicone was prepared in a plastic petri dish and cured for an hour at 25 ºC in an air oven. The actuator was then placed on top of the first silicone layer and silicone was poured over it to seal it from the environment, with making sure that the encapsulated area extended past the connection with the insulated wires. The assembly was set to cure for 24 hours in an air oven. The encapsulated actuator was then laundered using a front-loading washing machine (LG Electronics, South Korea, WM2377CS) and laundry detergent (Kirkland Signature, Free and Clear Ultra clean liquid laundry detergent, 15 mL) using the warm temperature setting and a normal cycle. After it has dried, the encapsulated actuator was tested for residual conductivity and the

ability to stimulate skin. A schematic of the different steps is shown in Figure 4.2. Five replicates were tested for each series of experiments.

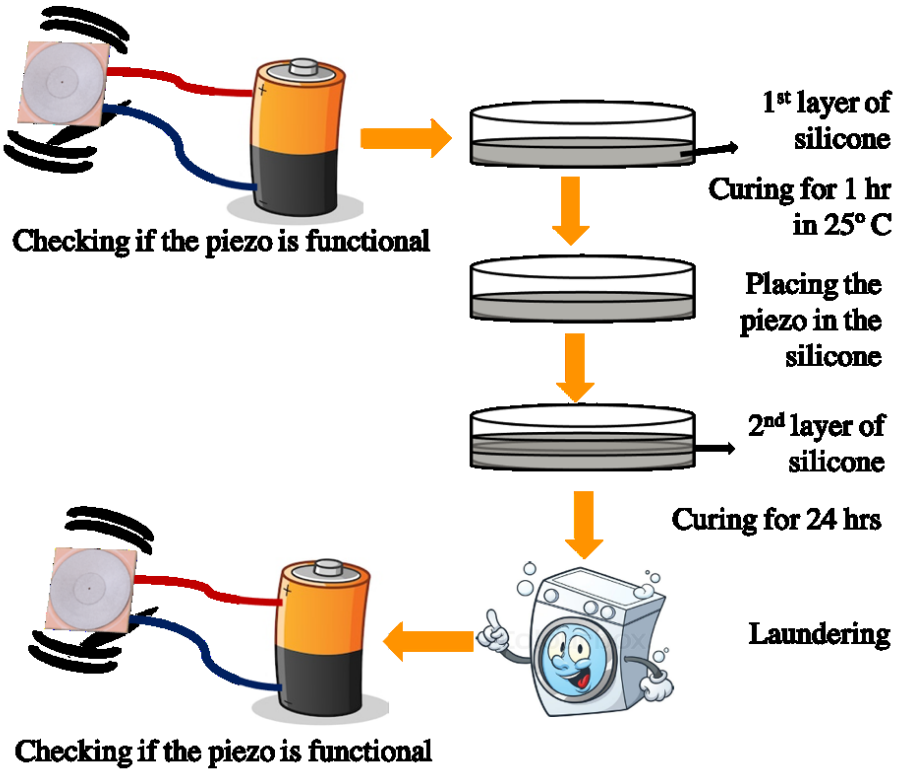

Figure 4.2: Laundering test for the encapsulated actuator

The microstructure of the conductive yarns was analyzed using a stereo microscope (Stemi 508, Carl Zeiss, Germany) at 2.6 x and 5 x magnifications. Their linear resistance was measured using a LCR meter (BK Precision 894, BK Precision Corporation, USA).

4.3 Results and discussion

4.3.1 Requirements for the biofeedback garment

The location for the placement of the piezoelectric actuators was determined based on a sensitivity test performed on different locations of the body as well as practical considerations (section 5.2.2).

This led to the identification of a knitted headband as the preferred host structure for the piezoelectric actuators. It provides the required amount of pressure to ensure a good contact between the piezoelectric actuators and the skin, it can be customized to include conductive tracks and other functional features, and it can efficiently conceal the active components, which helps avoiding the social stigma related to rehabilitation.

In addition to being comfortable for the user, the smart headband needs to have a design that ensures that the piezoelectric actuators are firmly attached and always at the same position on the forehead. The smart headband also needs to allow the power and data transmission between the piezo and the board. Finally, as for any piece of clothing, it needs to be washable [149].

4.3.2 Silicone encapsulation of actuators

Electronic components such as piezoelectric actuators can be damaged by exposure to water and other chemicals using during laundering. Encapsulation by silicones can seal the actuator from the outside environment and prevent liquid ingression and damage. Different types of silicones were studied for their efficacy at preventing water from entering the actuator and to make the connections waterproof during laundering. The silicones that were investigated for this purpose are listed in Table 2.

Table 2: Silicones tested and experimental observations

Silicones	**Comments**
Ecoflex 00-30	Low viscosity ensures easy mixing and de-airing. Cured rubber is very soft and will rebound to its original form without distortion. Certified skin-safe.
Ecoflex 00-50	Higher viscosity than 00-30. Certified skin-safe

ShinEtsu 2230-45	Low viscosity ensures easy mixing and de-airing. Cured rubber is very soft. However, it has a low tear strength.
ShinEtsu 2230-55	Difficult to degas in the vacuum pump. Cures before degassing is complete
Ecoflex gel	Clear when cured.

Table 2 also describes the observation that were made while attempting to use the different types of silicones to encapsulate a linear resonant actuator used for the test. The Ecoflex gel and Ecoflex 00-30 were found easy to cure and provided a satisfactory encapsulation of the actuator. They were used to prepare encapsulated actuators that were subjected to one laundering cycle. In total, eight tests were performed with the two silicones. The silicone encapsulation allowed the actuator to resist the laundering cycle. No damage to the silicone encapsulation was observed after the laundering cycle and the actuator successfully vibrated as expected when connecting it to the control board.

However, despite the success of this encapsulation process, we adopted a removable method because the smart garment needs to be able to survive several laundering cycles. There was a risk of the other electronic components like conductive wires being damaged during the washing cycles. Also, the risk of electrocution was something of concern and we were able to eliminate these disadvantages by using a removable design. Therefore, it was decided to opt for a strategy relying on the disconnection of the piezoelectric actuators and their removal from the headband when the headband had to be washed.

4.3.3 Conductive yarns for data and power transmission

Conductive yarns were explored to assess their potential use for data and power transmission between the piezoelectric actuators and the control board. Their large interest lies in their ability to be seamlessly integrated into textile structures to provide power and transmit data to electrical/electronic components [150]. The selection of a conductive yarn is made depending on the application and the amount of conductivity required. Some applications such as sensing and heating applications may have lower conductivity requirements when compared lighting applications where low resistance wires may be preferred. The linear resistance of conductive yarns generally ranges from 0.5 Ω/m to several kΩ/m, depending on the material used [17].

In addition, the structure of a yarn and its material decide the way it can be used during manufacturing of the smart fabric. Yarns can be made of a single filament or can consist of various thinner fibers that are twisted together to form a multifilament yarn [17]. Monofilament metal yarns tend to break easily during weaving and knitting whereas with multifilament yarns, they can more easily sustain the stress of the manufacturing process. Alternative to knitting and weaving, the use of embroidery allows avoiding these challenges. Also, it is important to note that the traditional way of cutting fabrics, which requires the application of heat, cannot be used for fabrics with conducting metal wires due to their high thermal conductivity [13].

Several commercial conductive yarns were identified and are listed in Table 3. Information available about their fiber content, yarn structure and linear density, and the resistance mentioned in the technical data sheet are also included in the table.

Table 3: Inventory of commercially available conductive yarns

#	**Description**	**Manufacturer**	**Part number**	**Resistance per unit length (from technical data sheet)**
1	Silver plated polyamide yarn, 235/34 4-ply, anti-tarnish coating	Shieldex, USA		<50 Ω /m
2	Silver plated polyamide yarn, 117/17 2-ply, anti-tarnish coating	Shieldex , USA		<3,000 Ω /m
3	Silver plated polyamide yarn, 110/34 2-ply, anti-tarnish coating	Shieldex , USA		< 500 Ω /m
4	Silver plated polyamide yarn, 235/34 2 ply, ant-tarnish coating	Shieldex, USA		<100 Ω /m
5	Silver plated polyamide yarn, 235/34 dtex 2 ply, anti-tarnish coating	Shieldex, USA	200121235343 B	< 100 Ω /m
6	Silver plated polyamide yarn, 235/34 dtex 4 ply, anti-tarnish coating	Shieldex, USA	20012123535H CB	< 50 Ω /m

7	Silver plated polyamide yarn, 235/36 dtex 2 ply, anti-tarnish coating	Shieldex, USA	200121235362 HCB	< 100 Ω /m ± 30 Ω /m
8	Silver plated polyamide yarn, 235/36 dtex 4 ply, anti-tarnish coating	Shieldex, USA	20012125364H CB	< 50 Ω /m
9	22% ultra fine inox steel filament wrapped around 78% raw linen core	Bart & Francis, Belgium	inoxlin gimp 4277	
10	Pure silver bonded to the surface of a non-conductive polymer such as nylon	Noble Biomaterials, USA	Circuitex	
11	Nanoplated silver, 875 dTex	Kitronik, UK	electro fashion conductive thread	40 Ω/m
12	316 L stainless steel yarn	Adafruit, USA		4.9 Ω/m
13	Stainless steel yarn	Sparkfun, USA		27 Ω/m
14	Copper tinsel	Karl Grimm Kupfer Blanc, Germany		

Figure 4.3 shows the optical microscopy image of the conductive yarns of the list below for which samples were obtained. The four Shieldex silver-coated conductive yarns (Figure 4.3 a-h) show a multifilament structure that appears appropriate to be used for knitting. The same comment can be

made for the Kitronik and Sparkfun stainless steel multifilament yarns (Figure 4.3 i-l). On the other hand, the copper tinsel yarn Figure 4.4 (a-b) is not suitable for knitting due to the fragility of the copper sheet wrapped around the nylon yarn, which might get torn apart during the knitting process.

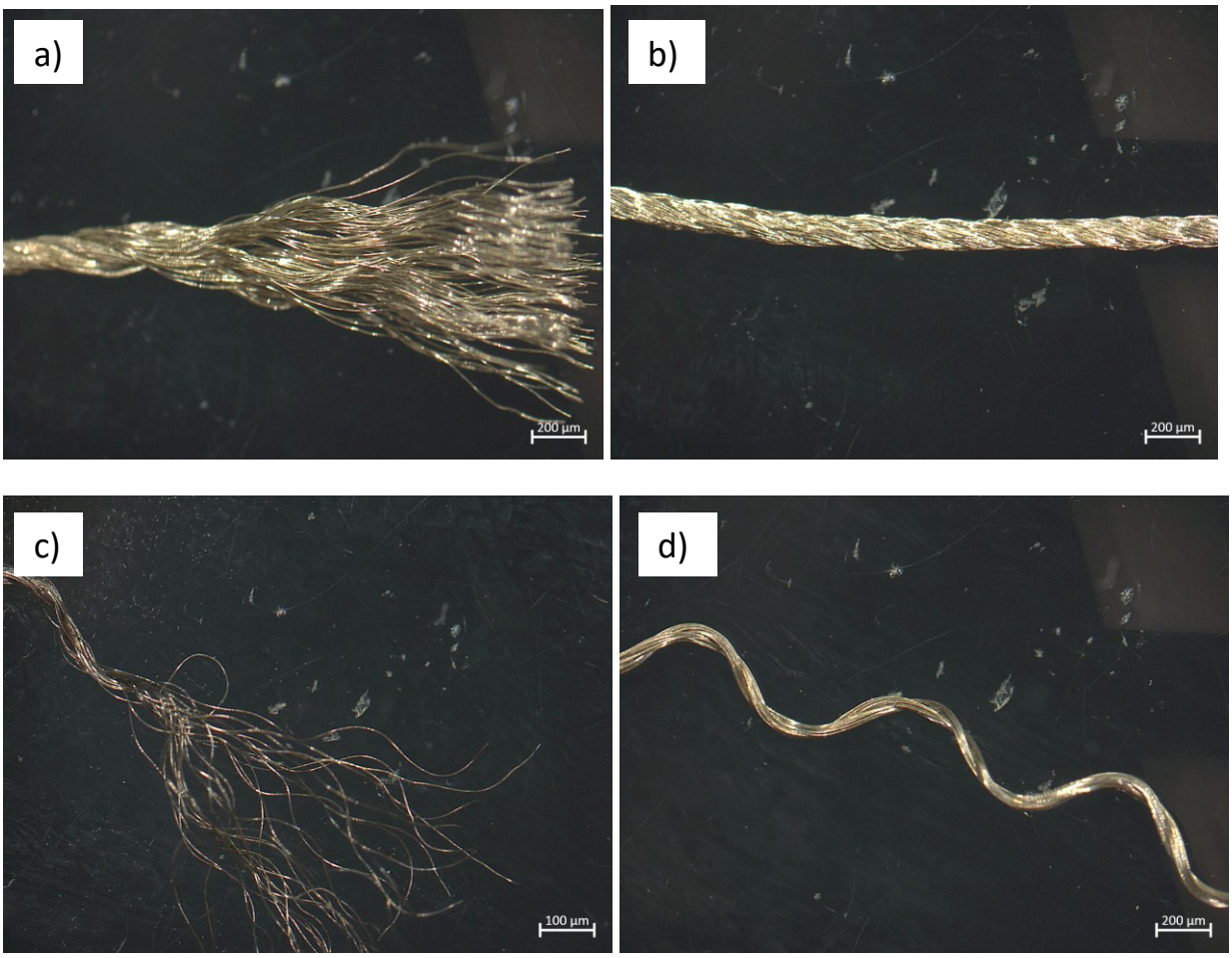

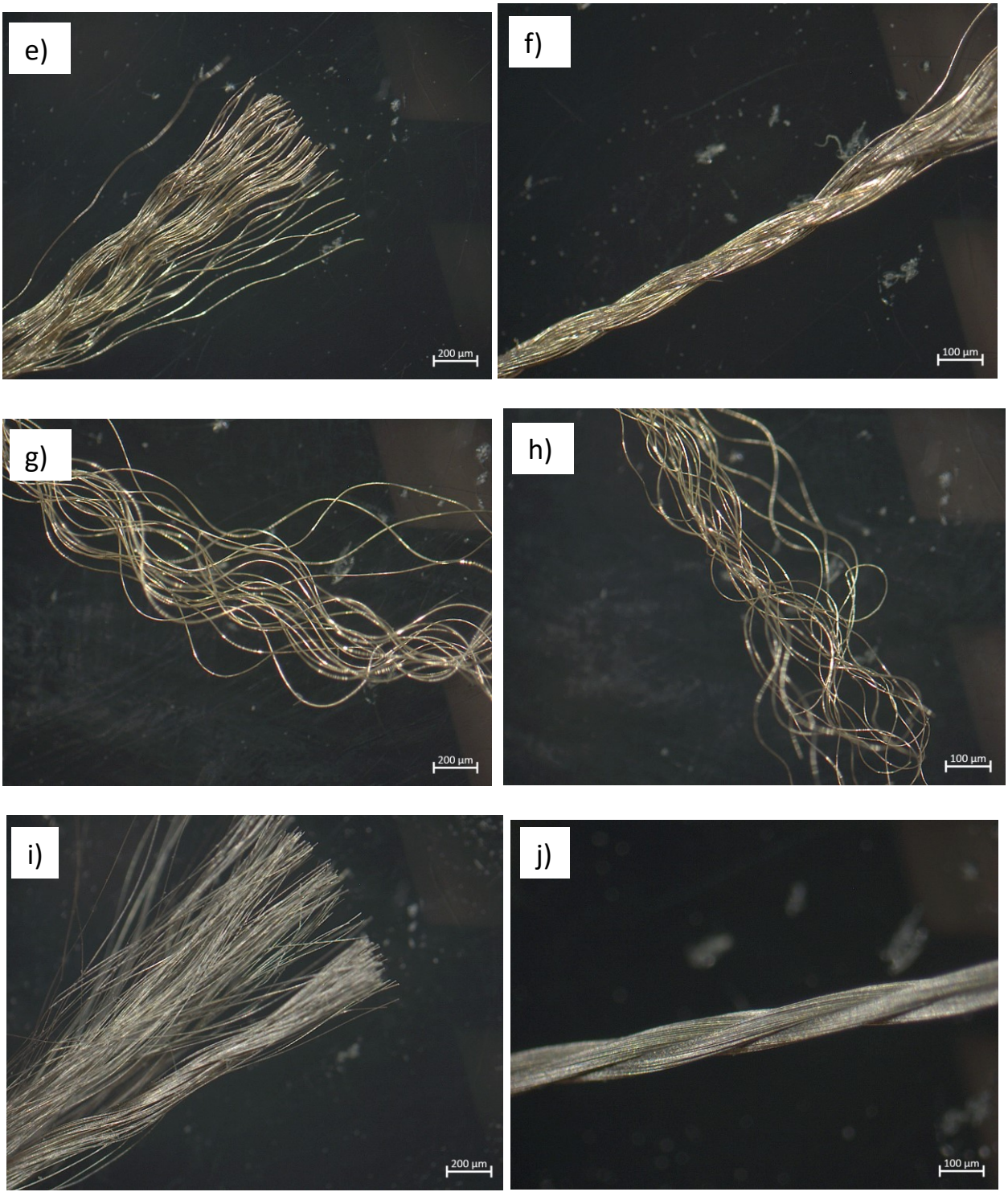
e)
200 µm
f)
100 µm
g)
200 µm
h)
100 µm
i)
200 µm
j)
100 µm

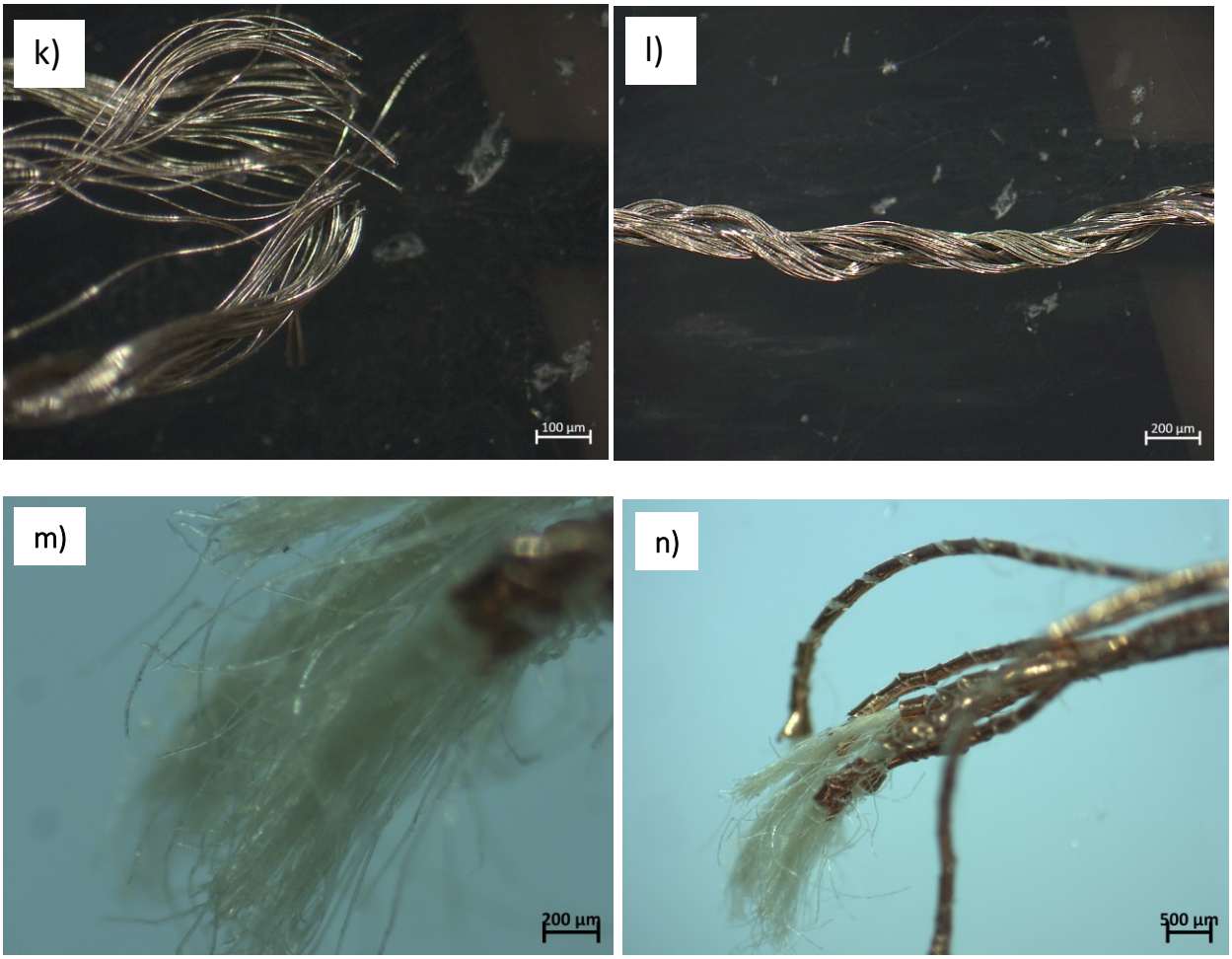

Figure 4.3: Optimal microscopy images (magnification in parenthesis): Yarn 1 (a: 5x; b: 1.6x); Yarn 2 (c: 5x; d: 1.6x); Yarn 3 (e: 5x; f: 1.6x); Yarn 4 (g: 5x; h: 1.6x); Yarn 7 (i: 5x; j: 1.6x); Yarn 9 (k: 5x; l: 1.6x); Yarn 10 (m: 5x; n: 1.6x).

Their linear resistance of the conductive yarns identified as potentially appropriate for knitting was measured and is listed in Table 4. The lowest resistance was measured for the Sparkfun stainless steel yarn, with 23 Ω/m. By comparison, a copper multifilament wire with a similar diameter has a linear resistance of 0.21 Ω/m. The requirement in terms of power to drive the piezoelectric actuators was computed and is equal to 18 W. In addition, the yarns will have to cover some

distance to reach the board, which will increase the resistance. None of the conductive yarns tested thus appeared to be appropriate to power the piezoelectric actuators.

Table 4: Linear resistance of conductive yarns

S.No	Conductive yarn	Linear resistance
1	Shieldex 235/34 4-ply	42 Ω/m
2	Shieldex 117/17 2-ply	129 Ω/m
3	Shieldex 110/34 2-ply	208 Ω/m
4	Shieldex 235/34 2 ply	110 Ω/m
7	Kitronix	57 Ω/m
9	Sparkfun	23 Ω/m

Soldering tests were also performed with the different yarns by attempting to connect each conductive yarn to a copper wire. Low temperature solder had to be used to avoid melting the polymer cores. The tinsel yarn (Figure 4.3 m-n) was observed to be easiest to solder due to the presence of the copper strip.

Based on the different observations performed on the conductive yarns, it was decided to opt for copper wires for the connections between the piezoelectric actuators and the control board so that the resistance is in line with the requirements of the circuit. These copper wires will be inserted into the lumen of the headband using small slits cut in the fabric.

4.2.8 Pressure sensors

To ensure a good quality of signal transmission between the piezoelectric actuators and the forehead skin while avoiding generating some discomfort in the patient, it is important to monitor

and control the tightness of the headband around the head. One strategy relies on the use of a pressure sensor located on the headband.

Pressure sensors work on different principles like piezoresistive, capacitive, piezoelectric, and triboelectric pressure sensors [151]. Piezoresistive and force sensitive resistors are particularly advantageous due to their high sensitivities when converting external pressures into discernable electrical signals [152]–[154]. Force sensitive resistors are devices in which the electrical resistance differs as a function of applied stress. They are used in accelerometry, monitoring of forces on the human body and pressure pads for security devices.

A force sensitive resistor (FSR) was selected for our application. The principle is that the resistance of a flexible printed interdigitating electrode changes when it pressed against a higher resistivity sensor pad (printed semi-conductor) as seen in Figure 4.5 [155]. The resistance of the sensor drops as the contact area between the electrode and printed semi-conductor increases. The decrease in resistance is due to a conductive path forming between printed semiconductor and the electrodes. The FSR model used (Interlink 402) combines a conductive silver trace and carbon elements below the silver. It is connected to a 10kΩ resistor and an Arduino board to measure the force [155]. The 10kΩ pull-down resistor is connected in series with the FSR to create a voltage divider circuit. The point between the pull-down resistor and the FSR is connected to the A0 input port of an Arduino. When no force is applied, the sensor acts like an infinite resistor or an open circuit. The harder one presses on the sensor, the lower the resistance is.

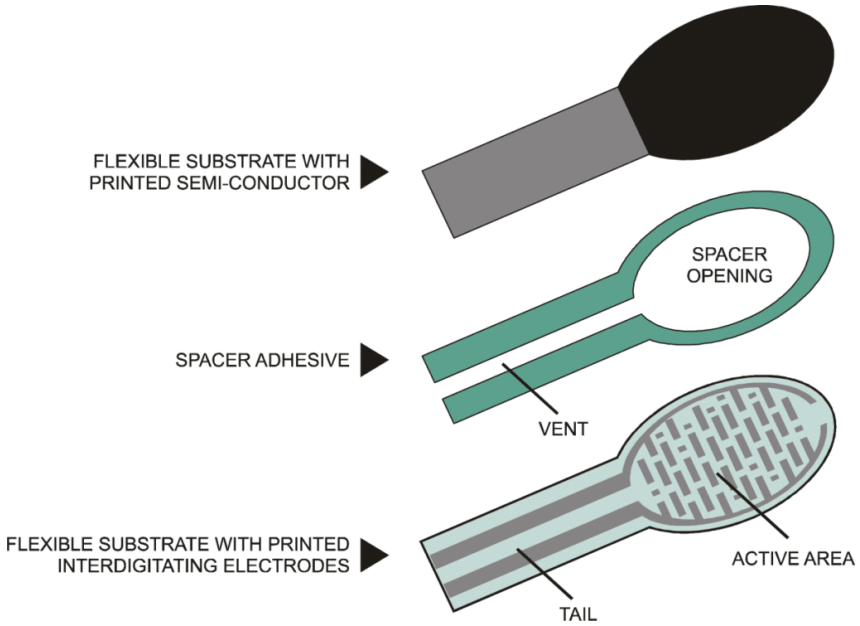

Figure 4.4: Construction of the FSR [155].

The sensor was calibrated using different weights in the relevant range of forces so that the force applied on the forehead is determined. The force applied by the headband that is appropriate for its use, i.e. leading to a good perception of the piezoelectric vibrations by the forehead skin while not being too tight, was measured using the sensor.

4.2.9 Final design of the smart headband

The final design of the smart headband is composed of five types of components (Fig. 4.6):

- A fabric headband made of a tubular sweat wicking, 4-way stretch knitted fabric;
- Three piezoelectric actuators;
- Insulated multifilament copper wires;
- Quick-connect insulated tab-type connectors;
- A Boreas Technologies board for each piezoelectric actuator.

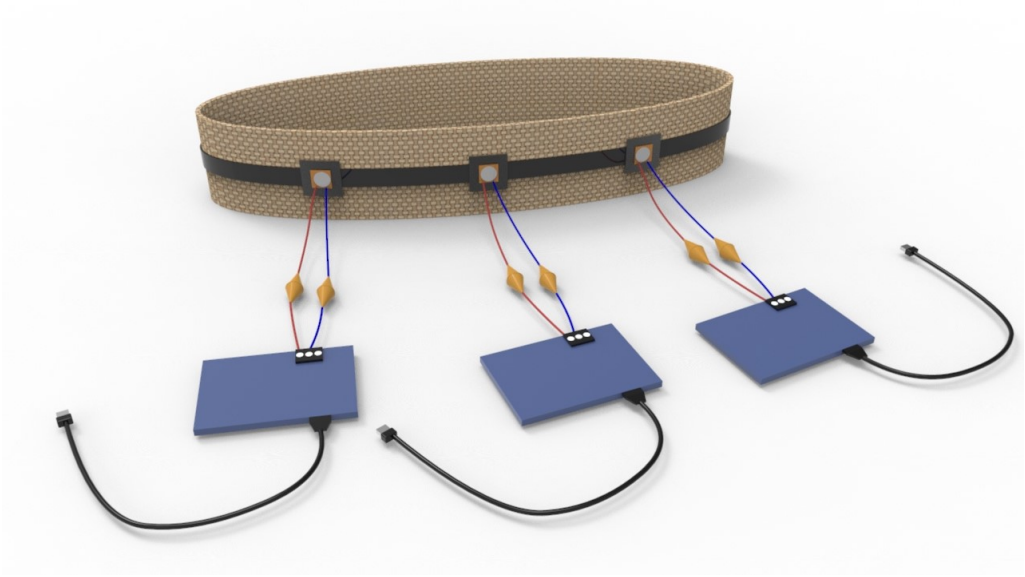

Figure 4.5: Smart headband

The knitted headband was selected so that the system is stretchable to provide comfort to the user while maintaining a small amount of pressure between the piezoelectric disks and the forehead to facilitate the perception of the vibrations on the skin. It has been modified to include an adjustable fixation at the back to fit different head sizes (Figure 4.7(c)). Its tubular construction allows using it as a gusset to hide the electrical wires connecting the piezoelectric disks and the control board. These wires are inserted through a small slit cut into the fabric (Figure 4.7 (a)).

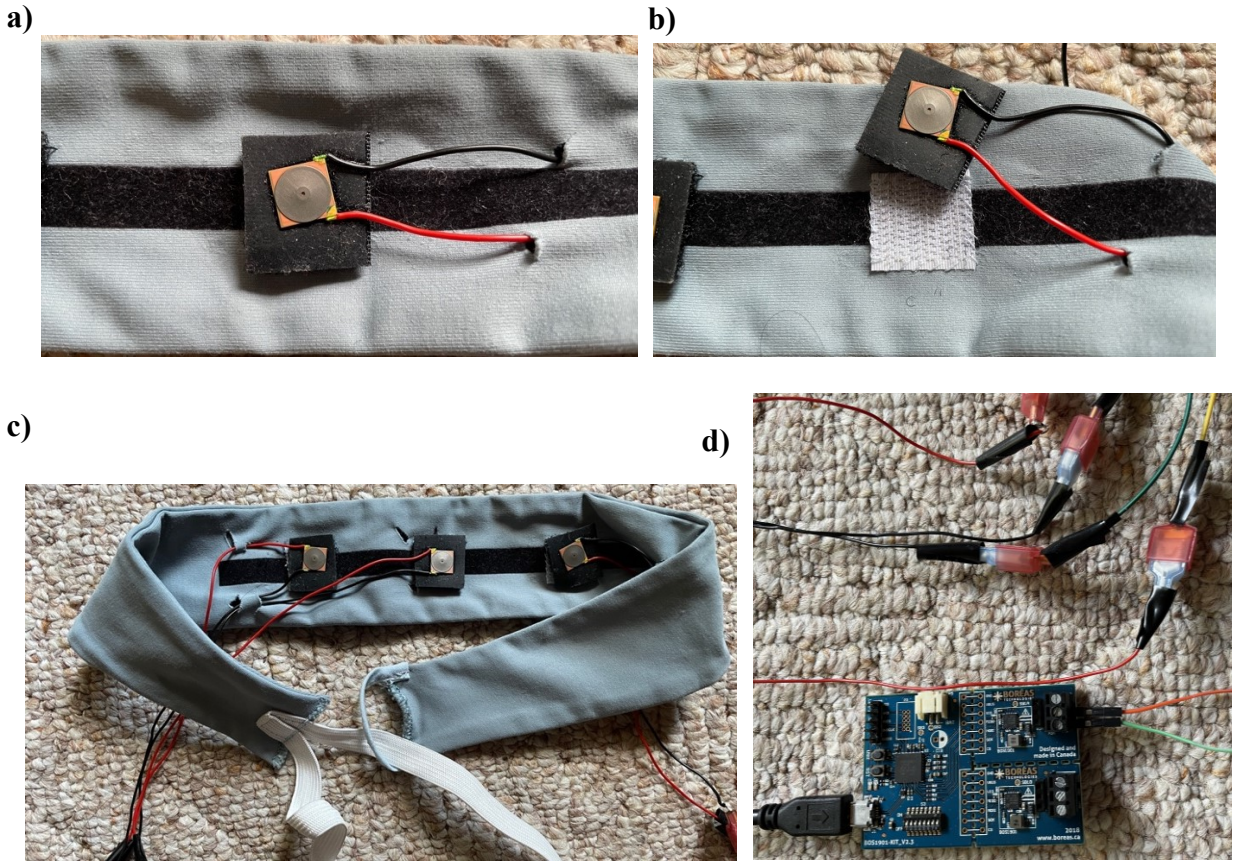

Figure 4.6: a) Tubular structure b) Velcro patches for attaching piezoelectric actuator c) Adjustable fixation d) Tab connectors design

Small square patches of the loop side of a hook-and-loop fastener strip of the same dimension as the piezoelectric disks were sewn on the headband using a nylon thread (Figure 4.7(b)). Pieces of the hook side of an adhesively-backed hook-and-loop fastener strip were fixed on the back of the piezoelectric actuators (Figure 4.7(b)).

The electrical wires are equipped with quick-connect insulated tab-type connectors to allow easily disconnecting the piezoelectric disks from the control board (Figure 4.7 (d)). This allows the system to be washable since the piezoelectric discs and the control board can be disassembled from the headband, and the headband washed when required.

The pressure sensor is used in order to measure the force exerted by the headband on the skin. This is placed in between the surfaces of the piezoelectric actuator and the skin to measure the force. The circuitry for this is shown in Figure 4.8.

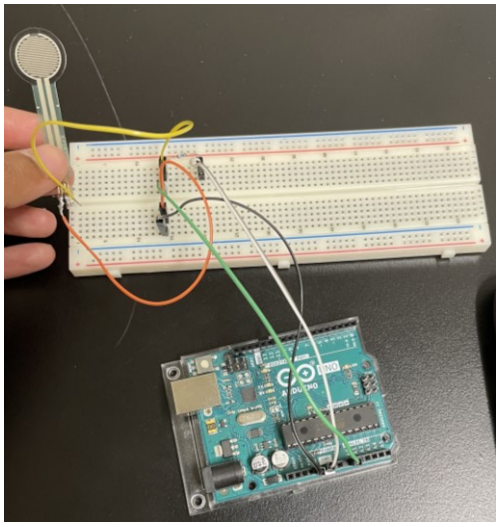

Figure 4.7: FSR circuitry

Finally, USB cables connect the control board to the computer. A microcontroller board from Boreas Technologies was used which helped in controlling the actuators using different programming platforms like MATLAB, Python etc. Figure 4.9 shows a picture of the entire setup.

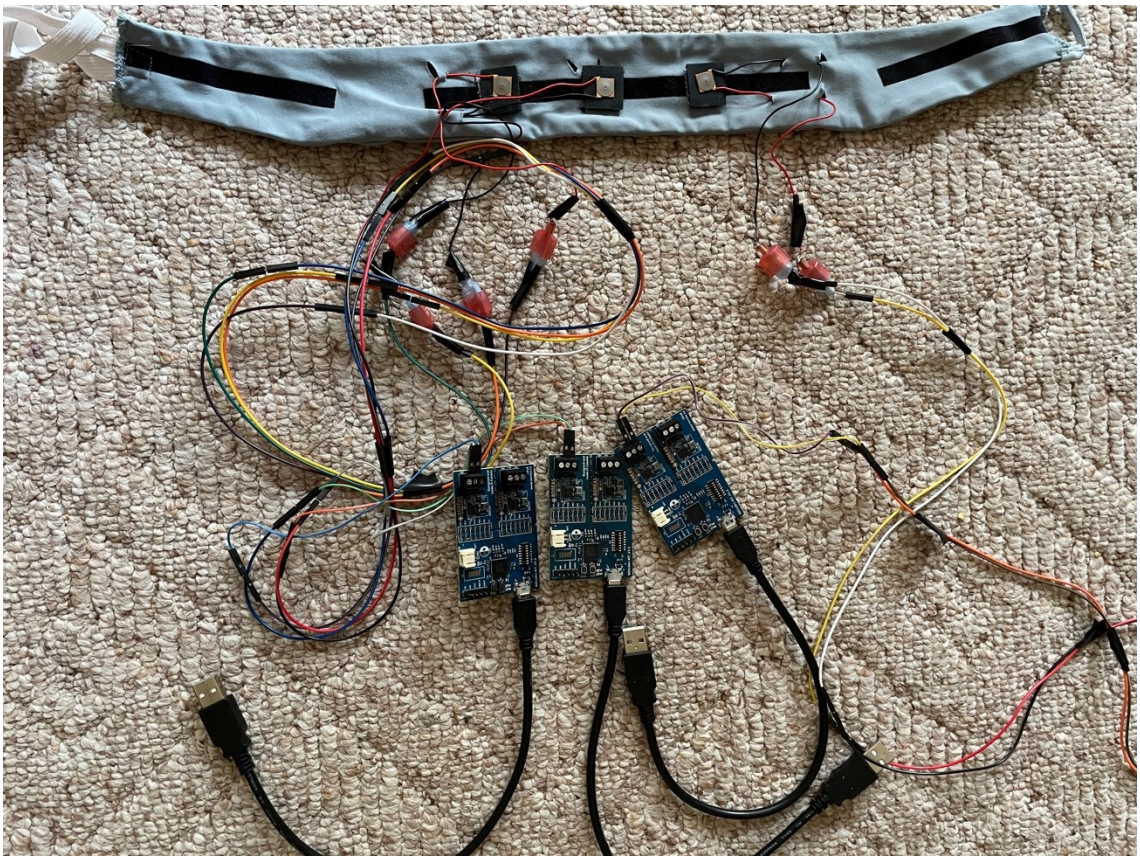

Figure 4.8: Smart headband final design

The choice of having multiple piezoelectric discs was made in order to provide spatial information. The three piezoelectric discs will communicate wirelessly with the sensors in the oral prosthesis present in the mouth of the patient to assist with chewing. The sensors will be able to provide signals depending on the events happening in the mouth during chewing. Each piezoelectric disc will be able to provide information depending on which sensor it is in constant communication with. Depending on the severity of the surgery and how much of the jaw needs reconstruction, the number of piezoelectric discs will be modified to suit the patient's needs.

4.4 Conclusion

Smart textiles have been instrumental in the development of many rehabilitation devices by integrating traditional textiles with active electrical components. These devices help in providing patients with timely feedback. Being integrated with textiles, they offer mobility to these patients among other major advantages. Therefore, patients can carry on day-to-day activities at ease. Smart textiles have also been advantageous in terms of providing comfort and flexibility; they can be produced into different shapes and sizes, have sweat absorbing properties, are washable, etc. In our work, we developed a smart headband with active piezoelectric actuators for providing biofeedback related to mastication.

The smart headband structure was built with washability in mind. This structure is robust, flexible and combines comfort with functionality. It is able to provide the right amount of pressure to stimulate the skin effectively. It also has the ability to provide connectivity to power the piezoelectric discs and the board. It can be washed after disconnection the removable parts, and the material of the headband is sweat wicking for the user's comfort. The smart headband is an important rehabilitation device that will improve the quality of lives of many head and neck cancer patients.

Chapter 5- Perception study

5.1 Introduction

5.1.1 Mastication

The process of breaking down food into smaller particles for further digestion is known as chewing or mastication [156]. Chewing is a complex voluntary movement that involves different muscles, nerves and bones in the mouth. From the moment food enters someone's mouth a series of events takes place that leads to swallowing [157]. The pattern of movement of the muscles in the jaw forms a tear shaped pattern [158]. The initial breakdown is usually by the incisors whereas most of the chewing takes place in the molars [159]. The breakage of food is one of the most important events in terms of perceiving texture. The sensation of texture and the process of perception is usually done within the first few bites by the incisors [158].

The process of texture perception has also been conceptualized into two steps [157]. The first is the active breaking of food. This is important because the rate, amount and force required to break food can lead to textural sensation physiologically and physically. The second is that the perception of texture is a sum of activities of the tactile as well as kinesthetic receptors in dermal, muscle and connective tissue. Another important concept is the chewing rate and the frequency at which food is broken down. This rate depends on the hardness of the food material being chewed [160]. Therefore, the material properties of the food along with the parts of the mandible (nerves, muscles etc.) contribute to the entire process of mastication.

Head and neck cancer patients have multiple complications relating to mastication following surgery leading to a decreased quality of life [161]. The way that food is ingested after these procedures vary depending on the degree of the procedure. Decline in chewing efficacy has also been seen in head and neck cancer patients [162]. These patients suffer from loss in body mass

index due to improper chewing and nutrition [161]. It has also been observed that since they are not able to process food efficiently and break it down, they also suffer from swallowing disorders [163]. This is due to the several drawbacks such as change in anatomy due to reconstructive surgery and a decreased sensation and judgement of events happening during chewing. The ability to identify food textures is also impaired due to the loss of surrounding parts of the mouth [157].

These patients usually have oral implants in order to assist them with day-to-day chewing [164]. The maximum bite force can decrease or increase due to patients being cautious, having a lower pain threshold and loss of sensation of force. It has also been seen that the chewing pattern in humans with full dentures is very different from that of people with teeth [159]. In this case, the food bolus makes more contact with the incisors during multiple chewing cycles. These patients also show a decrease in masticatory efficiency [165]. This means that they are unable to break down food into smaller particle sizes which then leads to troubles in chewing. These individuals also break down food into smaller particles non-selectively whereas for individuals with normal dentition large particles are broken down much faster than smaller ones. The need for a device that integrates with the oral implants and provides biofeedback about the amount of force and the texture of food being masticated is immense and has to be addressed.

5.1.2 Psychophysics and perception

Psychophysics is the area of study that mathematically describes the relationship between the body and the mind, the conscious experience of sensation resulting from an external stimulus [166]. This was originally coined by Fechner who said that if one knows that mathematical form of the psychophysical relation between a physical variable (stimulus) and its corresponding sensation, they can measure mental attributes by measuring their physical correlates. This has been

used to define variables and study vibrotactile perception. The perception of the magnitude of tactile sensations is related to the physical amplitude of vibration of the stimulus that is applied on the skin. The relationship between them was studied by Ernst Weber. His observations led to the "Weber's law", that there is a linear relationship between the intensity of the stimulus and the increase of a stimulus from a particular level to obtain a "just noticeable difference".

Researchers also did a study to observe cutaneous perception on small areas of the palm [167]. The weber fractions from the study were for a larger range of stimulus intensities but were seen to be consistent except the two intense extremities. More studies done estimated the values to be 0.05. For the just noticeable difference in terms of frequency, it was observed that the ability of humans to discriminate between two frequencies through the fingertip was seen to be 3% for the range of 1-256 Hz to 38% at a frequency of 200 Hz. Researchers have also reported higher tactile sensitivity for increasing stimulus frequencies. Some of them have also found that there is no relationship between the JND and stimulus frequency.

Texture perception has been studied as a part of perception as well. Bergen et al constructed textures using micropatterns of alphabets in random orientation [168]. Morton et al studied the perception of texture among 48 participants with aluminum papers with different grit values [169]. The smaller the grit value, the rougher the paper feels. They did experiments with both visual and haptic information and only haptic information to compare the results. They observed no significant difference in results for both methods concluding that visual information doesn't affect tactual perception in terms of texture.

Spatial distribution of stimuli and its perception is important to give multipixel information. Two-point threshold have been done by Stevens et al and many other researchers [170]. They found that the density of the tactile displays must be related to the spatial resolution of the skin. It

also has to be noted that there are differences amongst patterns of spatial resolution depending on the location of the body sites. Dellon et al studied a moving two-point discrimination test in which a paper clip is made into a testing instrument [171]. They placed a paper clip with both ends separated by 5 to 8 mm and moved along the surface of the fingertip. The participant was then asked questions about if they felt two moving parts or one. The test was randomized between one and two points. The two-point discrimination was found to be 3mm for nine participants.

Signal detection theory is applied in psychology when analyzing how to different signals can be discriminated [172]. In a forced choice task, which represents the tests performed in Section 5.2, each trial presents one or more signals. Depending on the number of stimuli, the task is defined. For tasks with two signals, the method is called two alternative forced choice (2AFC). Signal detection theory states that if the user does not favor any of the presented signals, the proportion of correct responses on the task is a measure of sensitivity and is not affected by response bias. For example, in a 2AFC this measure of sensitivity ranges from ½ to a maximum of 1. Values less than ½ may result from response confusion or sampling error.

5.2 Experimental section

5.2.1 Perception study

The smart headband was tested among the author and the supervisors for the ability to send signals with precise control. The reporting of the development and pilot phase data was approved by the Health Research Ethics Board of University of Alberta, Pro00114366. During the development and piloting phase, the research team members including the thesis committee and the candidate tested the suitability of the device for delivering meaningful vibrotactile texture signals. The piezoelectric discs embedded in the smart headband are powered by the Boreas technologies board

(BOS-1901). Different types of food representing a variety of textures namely cranberry, cookie, banana and toast were chosen. A load cell was used to break them, and data was collected from the experiment as a representation of chewing in the mouth. These signals were then processed in the MATLAB platform using amplitude modulation method and resampled to the sampling rate of the load cell. The final signals were then used for the perception tests.

The location of placement of the smart textile was also an important factor to consider since some areas of the body are less sensitive when compared to other areas [173]. This test included passing several sinusoidal signals of different input intensities to different part of the body for example the neck, the palms, the fingers, the upper arm, the lower back, the forehead as well as the feet. The fingers, forehead and the toes were quite sensitive to the signals. However, the toes were not considered as a good location since the time required for the signal to be processed by the human brain and then sent to the user would be long for providing chewing related feedback [174].

The perception tests involved three different methods: a) ability of the authors to distinguish between different input intensities of vibration, b) understanding the spatial differentiation for the placement of actuators, c) ability to distinguish different textures and d) determination of the sensory threshold. A schematic representation is shown in Figure 5.1.

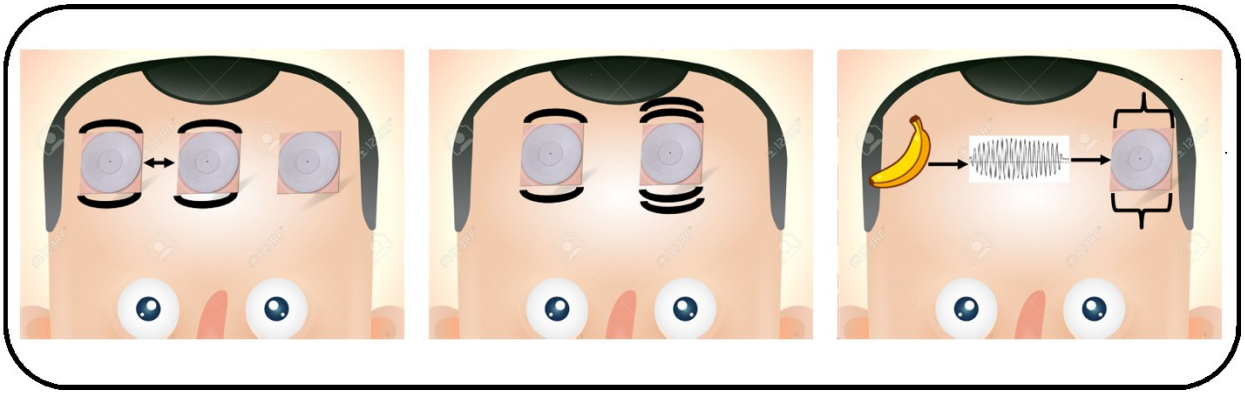

Figure 5.1: Schematic representation of the spatial differentiation, just noticeable difference and texture discrimination tests.

5.2.2 Sensation of vibration from piezo actuator on different parts of the body

Two-point discrimination test was used to determine the location of the actuators on the body. This determines how sensitive the particular location is to the vibrational signals from the actuator. It will also help in determining the type of smart textile structure that would be ideal depending on the location of the body. It needs to be noted that the location of the placement of actuators is also significant from the perception point of view. This is because a delay in signal transmission of more than 1 s is not ideal when transmitting real time food signals. For the experiments, Figure 5.2 was taken as reference and all locations were tested and tabulated as seen in Table 5. The locations with higher sensitivity were seen to be the toes, forehead, sole and the fingers. Since the fingers would be used for eating, it was decided that the location would not be ideal and could interfere with the act of holding cutlery. The toes and sole are far away from the mouth and hence a time delay in the signal transmission would occur. The location of the forehead was seen to be most favorable since it is closer to the mouth and the brain for interpretation.

Table 5: Sensation of vibration felt in different body parts

Body part	Sensation
Fingers	Yes
Thumb	Yes
Palm	Yes

Forearm	No
Forehead	Yes
Cheek	Yes
Upper arm	No
Shoulder	No
Back	No
Belly	Slight sensation of vibration
Thigh	No
Calf	No
Sole	Yes
Toe	Yes

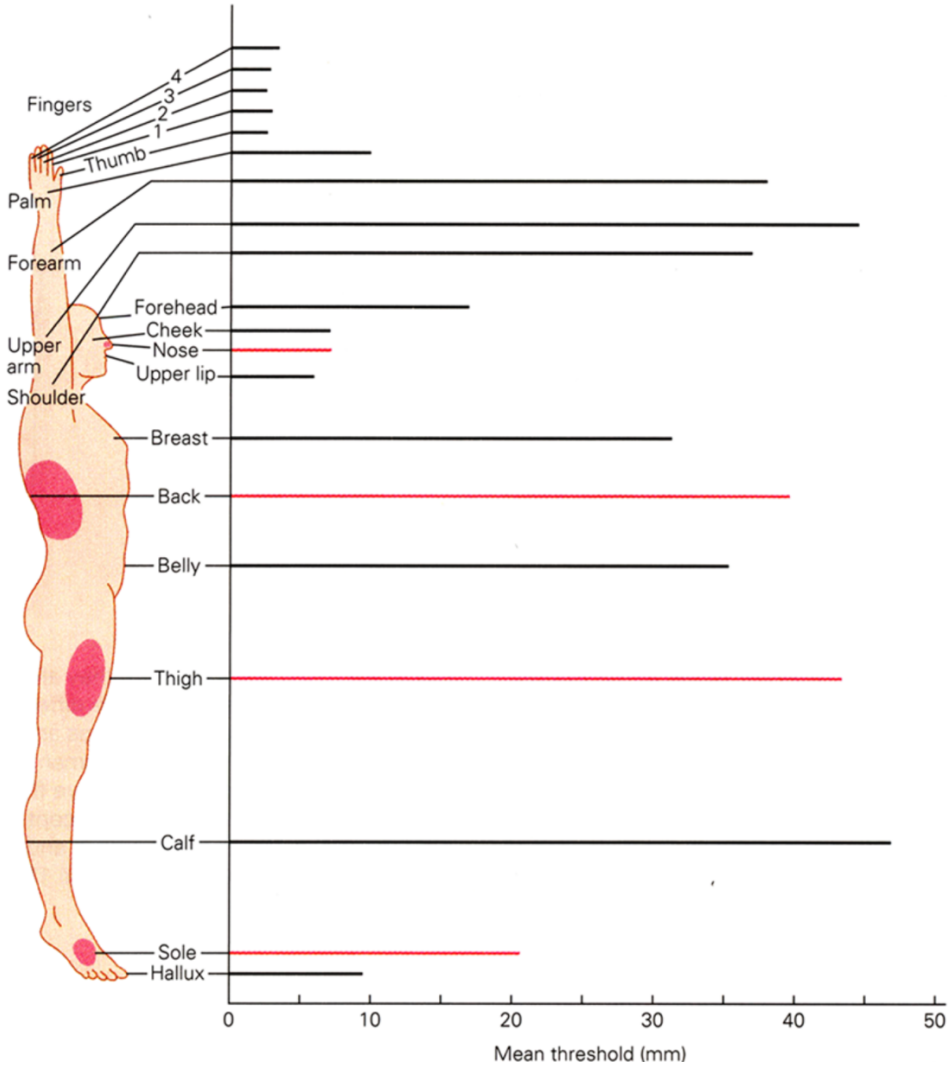

Figure 5.2: Two-point discrimination on different parts of the body [175].

5.2.3 Just noticeable difference in input intensity test

For the ability of the author and supervisors to distinguish between different input intensity of vibration, the Kaernbach method was used [176]. They were presented with two sinusoidal signals of the format:

$$s(t) = \sin(2 * \pi * a * f * t) \quad \text{....(iv)}$$

where a is the amplitude and the factor that keeps changing during the experiment, f is the frequency and is set between 100-300 Hz and t is the duration of the signal and is set to 0.5 seconds.

Both signals have two different input intensities of vibration. The duration between two signals was 1 s. The user is then asked to provide a response according to which signal was stronger. The algorithm used was an adaptive one proposed by Kaernbach [176]. If the response from the user is "correct", the difference between the two input intensities decreases by a factor of a $2^{(-1/3)}$ and if the response is "wrong", the difference is increased by a factor of two. This method is also called the weight up-down method. The advantage of this method is that it can be used in cases where the chance of answering correct are high. The convergence for this method occurs at X_{75}.

A total of 150 trials were performed for finding the just noticeable difference. The answers were recorded and analyzed for the just noticeable difference of input intensity. Logistic regression was performed using R programming language to find the just noticeable difference and the value of X_{75}.

5.2.4 Tactile spatial resolution test

Two-point discrimination is very widely used in tactile spatial resolution. It helps in providing basic knowledge about how far apart two different actuators should be, for them to be considered as two different stimuli [177]. It can be considered a starting point for comprehending sensory discrimination. The forehead is a very sensitive part of the body because of the high number of neurons per square area that are present. The two-point discrimination test was performed using actuators at 3 cm apart in the forehead. Two of these actuators are placed near the temples and one of them is on the center of the forehead. The user is asked to answer whether they can feel one or two of the actuators and the results are recorded.

Two cases are presented to them randomly. The first case involved two of the three actuators vibrating and the second case involves one of the three actuators vibrating. The user is then asked

to answer if they can feel one or two actuators vibrating. The answers were recorded and analyzed for spatial differentiation. This helps in determining how spatially different these actuators need to be, to be recognized as different vibrating components.

5.2.5 Texture differentiation test

For the third test, the author and her supervisors are presented with the four different texture signals in an ABX method of testing. MATLAB was used to process the signals using the method of amplitude modulation, save them as .wav files and used in the program for the test. The steps involved in the processing of the signals are shown in Figure 5.3. The author and supervisors are presented with two different texture signals (A and B signal) followed by a third signal (X signal) that is either A or B [178]. The answers were recorded, and all the different pairs of food textures were analyzed. The texture signals were also normalized for their energy. This was done so by finding the root mean square average (RMS) of the amplitudes of the signals after amplitude modulation. Each value was then divided by the RMS average and the signals were then used in the ABX test. The method was used to eliminate the influence of energy on the ability to distinguish texture. These results were then analyzed to form a confusion matrix and a binomial distribution plot.

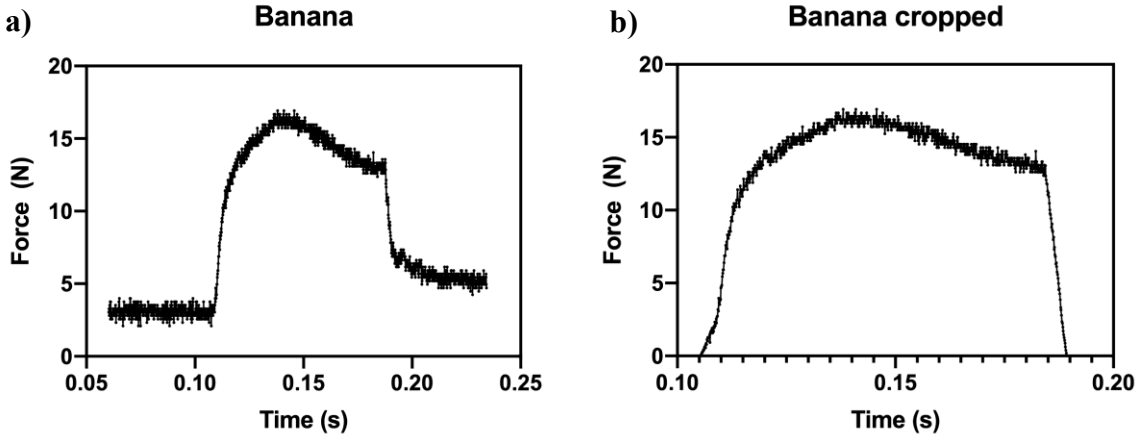

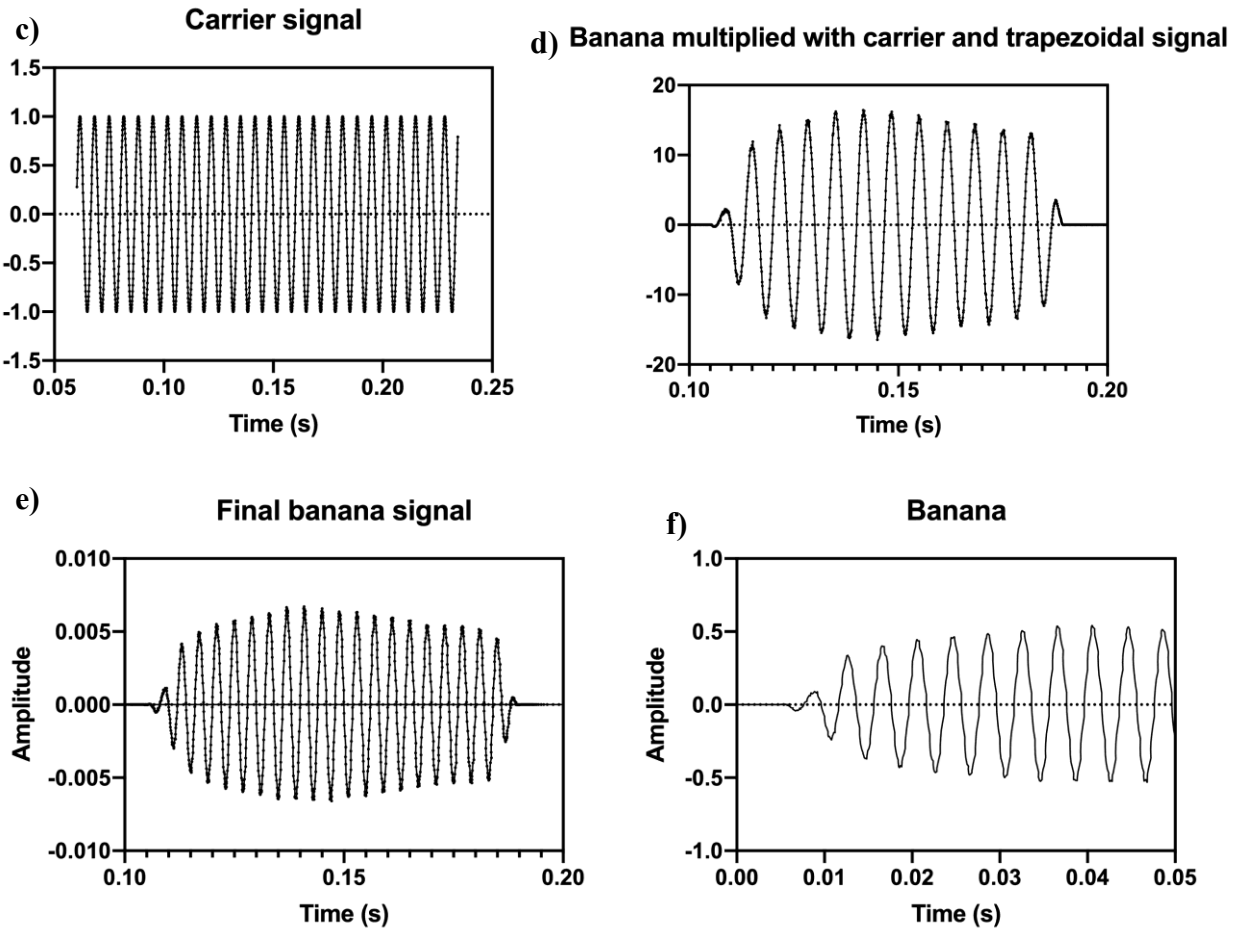

Figure 5.3: a) Raw signal of breaking banana with the load cell b) Cropped banana signal c) Carrier signal d) Banana signal multiplied with a trapezoidal function and the carrier signal e) Banana signal after resampling (used for texture perception analysis) f) Banana signal after normalization (used for normalized texture perception analysis)

5.2.6 Determination of the sensory threshold

Understanding the sensory threshold of the author and supervisors gives a good understanding of the threshold among humans. This is important in order to know the range of input intensity that the actuator needs to be operated in, so its perceivable by the human skin. The test involves measuring the time required by the user to respond to a particular signal. Signals with varying

input intensities are presented to the user and they are asked to press a key and the time taken to respond is recorded and analyzed. Typically, a response time of less than 1 s is considered ideal for haptic applications.

5.3 Results and discussion

5.3.1 Just noticeable difference in input intensities test

The perception tests were carried out with the smart headband. The aim of this study is to determine the just noticeable difference between the author and the supervisors. This will give a good understanding of the range of input intensities that can be used in the feedback system and how different their intensities must be. This test is important because different food textures are masticated with different forces and to distinguish different food textures, signals with different intensities need to be provided. The user was provided with two simultaneous signals of two different intensities and is asked to provide input regarding which one is more intense.

The data was then analyzed by the method of logistic regression and the estimate for just noticeable difference was found to be -0.141. This means that when the difference in intensities increases, the chances for the user to right correctly also increases. The p value in the null hypothesis testing showed a value of 0.003 and that the data was significant. X_{75} was calculated in order to determine the amount of difference in intensities there needs to be, for the probability to be 75%. The value was calculated to be an average of 0.23 using equation 4:

$$X_{75} = \frac{\ln(3)}{b} \qquad \ldots.(v)$$

where a represents the estimate for the intercept and b is the estimate for the difference in intensities. It also needs to be noted that the sign of the estimate for difference in intensities depends on the question being asked to the user. If the question asked is which signal has a higher

intensity, the sign is negative, and it would be reversed when the opposite is asked. From the observed results, we can see that the difference in intensities of two signals needs to be an average of 0.23 for them to be perceived as two different signals. This also allows for a wider range of intensities to be used in the biofeedback system.

5.3.2 Tactile spatial resolution test

Spatial resolution is significant in tactile stimulation because every region in the body has receptors that are two dimensional. An understanding of how the body discriminates between them when a stimulus is presented has a major role to play when correlating mastication events to a vibrotactile feedback system [179]. Understanding the representation of spatial variables of a tactile stimulus and then correlating that with a neural response is one of the underlying factors of tactile neuroscience. Studying the neural coding is investigating the detailed discrimination pattern across a wide range of tactile stimulation parameters and the way the body responds to these stimuli.

From Table 6, we can see that the user was able to distinguish between the stimuli provided by both the actuators. The user is also able to distinguish when the skin is being stimulated by one actuator and by two actuators most of the time. This confirms that the distance between actuators can be set at 3 cm for providing spatial feedback. It is interesting to correspond spatial feedback with textural tactile feedback in order to understand how food enters the mouth, is being broken down depending on the food characteristics and tooth shape. It is then processed by the jaw muscle activity to form a bolus and then swallowed. These events can be processed into tactile signals and be provided to the user for continuous timely spatial feedback.

Also, since we have three different actuators representing three different areas of the mouth, we want to be able to space them apart so there is no cross talk between them during high

intensity signals. The shape of the head contours almost the same way the parts of the jaw do, which make it much easier to correspond events in the mouth to the tactile stimulations three dimensionally.

Table 6: Results for the tactile spatial resolution test

Case type	Percentage of correct answers
One actuator vibrating	100%
Two actuators vibrating	90%

5.3.3 Texture differentiation test

The aim of this test is to examine if the piezoelectric disc is able to provide different types of food textures as a vibrotactile signal. The importance of the piezoelectric actuator behaving as a sensory substitute and being able to deliver signals are vibration is huge. This test was conducted to see if the author and the supervisors are able to differentiate between four different textures namely banana, cookie, toast and cranberry. These signals were procured and processed. The processing is necessary because the frequency at which the load cell (representative of the human mouth) breaks food is low when compared to the frequency sensitivity of the skin [180]. It is important to note that frequency sensitivity also depends on the location of the body, the actuator stimulating the skin and the output displacement being provided [173]. The food textures were also tested using the ABX method without processing. The signals could not be felt without the amplitude modulation and the addition of the carrier signal. This confirms the notion of the need for processing them. It also needs to be noted that the essential information about the textures is not lost during the processing, they are rather enhanced.

The food textures were amplitude modulated and presented to the author and supervisors in a random manner. The method used was ABX and the results were collected, and the matrix of food textures and the percentages are shown in Table 7. A picture of one of the supervisors doing the trial is shown in Figure 5.4.

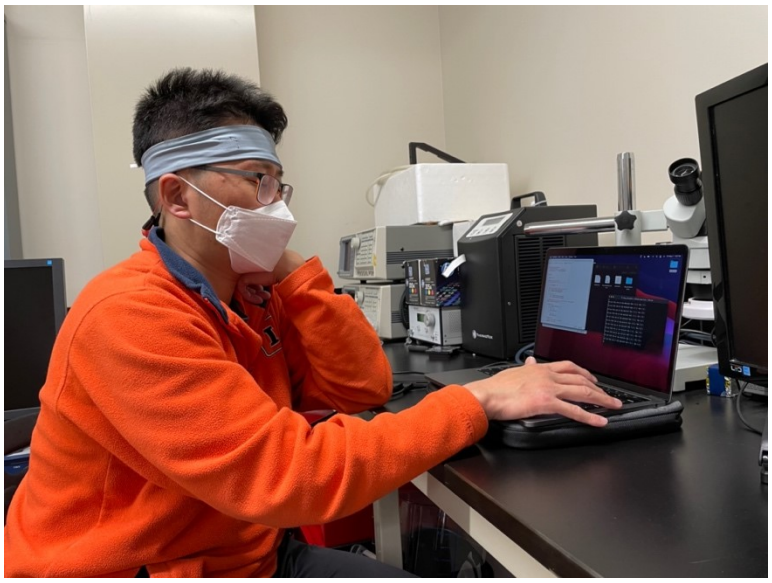

Figure 5.4: Supervisor doing a trial of the test

The overall percentage for correct answers was seen to always be greater than 70%. This indicates that the piezoelectric actuator is able to provide signals that help the author and supervisors to differentiate between them. The method when two options are provided to the users and they are forced to answer one is called the two alternative force choice. In psychophysics, a correct answer percentage above 50% is indicative of the case when the test participant is not guessing the answers and can meaningfully differentiate between the signals accurately. Since the correct answer percentage is above 50%, we are able to conclude that the actuator is able to provide distinct vibrotactile signals to the skin [181]. The binomial distribution for the test is shown in Figure 5.5.

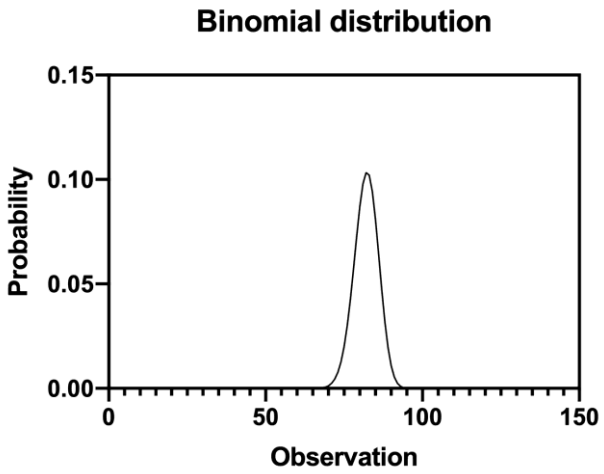

Figure 5.5: Binomial distribution

Table 7. Confusion matrix for the texture perception analysis

Pairs	Fraction of correct answers	1-P
Banana and cookie	18/20	0.0002
Banana and cranberry	18/20	0.0002
Banana and toast	20/20	9.536743e-07
Cookie and cranberry	14/20	0.0570
Cookie and toast	13/20	0.1310
Cranberry and toast	17/20	0.0012

From the non-normalized food texture test, it was found that cookie and toast were very similar in texture signals which led to confusion as seen in Table 7. The reliability of distinguishing these textures is low from the 1-P value. Hence it was decided to eliminate cookie in this normalized texture perception test. For the ABX test with normalized food texture signals, the signals were normalized for their energy before their use in the test. The method used for normalizing them is called Root mean square average. This was done in order to eliminate the

effect of energy in the process of differentiating between two different food texture signals. This makes it harder for the test participant to distinguish between them and also helps in confirming that the user is indeed answering the questions based on the difference in textures. It is a good way to eliminate other factors and only look into the differentiation of textures. The confusion matrix for this is seen in Table 8. The percentage for correct answers was seen to be greater than 60%. This can also be explained by the fact that each food texture is a complex signal that contains different energies, amplitudes and patterns that depends on the material properties of the food being broken down. The ability of the actuator to provide feedback only related to texture is remarkable in this study. It can be very telling of the fact that the vibrotactile piezoelectric disc is a fitting device for providing feedback related to chewing.

Table 8. Confusion matrix for normalized texture perception test

Pairs	Fraction of correct answers	1-P
Banana and cranberry	17/20	0.0013
Banana and toast	18/20	0.0002
Cranberry and banana	11/20	0.4110
Toast and banana	13/20	0.1310
Cranberry and toast	16/20	0.0059

5.3.4 Determination of the sensory threshold

Determining the sensory threshold of the helps in understanding the lower limit of the sensory stimulus that can be provided to the skin [182]. It is advantageous to know because the lower the threshold the more sensitive the skin is to these vibrotactile signals. It helps in understanding the

lower threshold so as to amplify signals that have a lower intensity than the sensory threshold. This is significant in terms of signals processing as well as signal delivery for the biofeedback system. It also helps in providing a range of input intensities to work around while processing and delivery signals. An experiment was conducted to study the range of displacement that needs to be provided to the human skin, to make the signals perceivable. The author and supervisors were presented with signals of different input intensities in a random fashion and were asked to provide answers. The response time vs input intensity is significant during the rehabilitation of the subject since a response time lower than 1 s is the duration of one chewing cycle. The time taken to respond was recorded and as seen from Figure 5.6, it is apparent that there is a decreasing trend in the response time as the input intensity decreases.

The results also show that after 0.3 intensity, the response time doesn't decrease too much and remains rather constant. This is because signals with input intensities 0.4 (~370 μm) and above have enough displacement to stimulate the skin around the 100-300 Hz [183]. The response time vs input intensity graphs with the headband also compare well with that of the fingertips because the pressure being applied to the forehead by the headband remains constant throughout the study. This data would also help with processing food texture signals that typically take lower forces (example banana) to be chewed. Since the lower force would correspond to a lower input intensity, for an effective texture feedback, the intensity of the signal would have to be scaled up in order to be perceived.

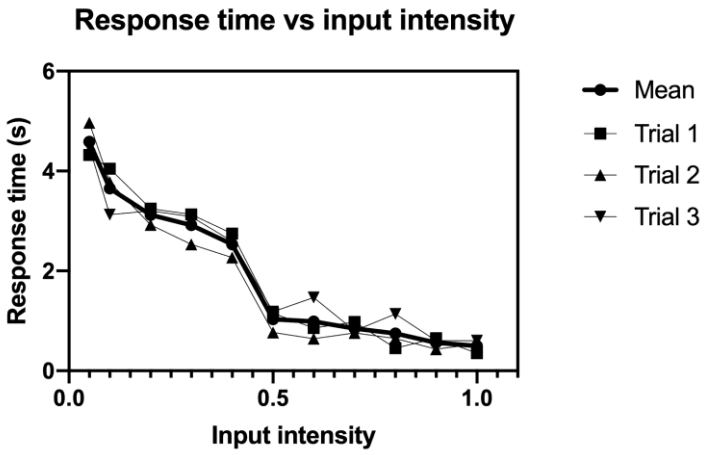

Figure 5.6: Sensory threshold measured with the smart headband

5.4 Conclusion

The human skin is so versatile and has multiple functions like maintaining the temperature of the body, receptors for touch, for electrical pulses, and is a social interactive tool. One of the aspects of the skin is to provide a direct connection for communicating with the nervous system because of the high number of innervations present. This aspect has been manipulated and used in the technology of vibro-tactile stimulations. The skin plays the role of a sensory substitute here since there is a loss of sensation after procedures involving head and neck cancer patients. The smart garment was able to provide the stimulations to the skin. It was seen to provide different food texture signals in the form of vibrotactile stimulations. It was also able to stimulate the skin with different intensities to use as alarm signals. The testing was also seen to have potential to provide spatial data based on events happening in different parts of the mouth during chewing. It appears based on the initial testing that the device has the potential to deliver vibrotactile signals that allow differentiation of food textures.

Chapter 6- Conclusion and future work

6.1 Conclusion

This work attempts to develop a smart garment for patients undergoing jaw rehabilitation. We studied different methods of biofeedback and principles and narrow down on piezoelectric actuators. The vibrational behavior and characteristics of the piezoelectric actuator used was studied with a laser Doppler vibrometer. We then used the actuators to develop a smart textile design that is washable. Further, this smart headband was used to design and perform psychophysical perception tests on the author and supervisors.

In chapter 1, we talk about head and neck cancer and the difficulties faced by patients from complications of cancer. The need for a rehabilitation device that can provide feedback during chewing is very crucial to post cancer care. The role of smart textiles in rehabilitation was studied and is seen as a solution for providing feedback to patients.

Chapter 2 includes a review of sensory substitution as a method of providing stimuli at a different part of the body than originally intended. It was found that feedback can be provided in different sites for rehabilitation due to the neuroplasticity of the brain. Vibrotactile perception was discussed in further detail as a method of biofeedback due to the ease of providing stimuli to the skin. The role of providing vibrotactile perception by using smart textiles was looked into for closer contact to the skin. For this, piezoelectricity was studied for its role in providing feedback in rehabilitation. The different piezoelectric materials in biomedicine were reviewed. PZT actuator is seen as a relevant solution because of its many advantages like ability to control frequency and output displacement of vibration.

Chapter 3 starts with describing piezoelectric actuators. Different configurations of PZT actuators were reviewed and cymbal actuators were explored in more details. The analysis of PZT

cymbal actuators helped in understanding how to control it. The PZT actuator was studied using a laser Doppler vibrometer for further analysis of its vibration functioning. It was observed that the actuator's displacement increased with the applied voltage. The vibrational characteristics also differ when we go from the center to the edge. During the analysis with food texture signals, it was seen that the actuator's vibrational characteristics match those of the input food texture signals. The results obtained with the piezoelectric actuator were compared with the characteristics of linear resonating actuators. It showed that that linear resonating actuators are not suitable for the particular application targeted here. These results were further used in designing the perception tests done on the author and the supervisors.

Chapter 4 involves the design of the smart headband. In this chapter we looked into the requirements for the smart headband. Silicone encapsulation was explored as a way to make the actuators washable. However, it was finally decided to build a washable structure using removable actuators secured with velcro. Conductive wires were used for powering the actuators since conductive yarns had an electrical resistance that was too high to effectively power the actuators or a structure that was too fragile to sustain the textile manufacturing process. It is able to provide enough pressure for stimulation of the skin.

In chapter 5, perception tests were performed by the author and supervisors to determine the best location for the actuation, to see if the actuator is able to deliver varying signals and characterize their ability to differentiate between food textures using the biofeedback smart textile. The forehead was selected as the location of actuation for its sensitivity towards the signals. The food texture differentiation tests showed a correct answer percentage higher than 50%, which is more than chance. The authors and supervisors were also able to differentiate between signals of

different input intensities. Finally, the actuators are able to allow distinguishing between one and two vibrating actuators according to the results of the spatial differentiation data.

Ultimately, this research opens interesting perspectives to provide jaw rehabilitation patients with biofeedback about chewing force and food textures using a smart headband, which can be used in social settings, is comfortable and washable.

6.2 Future work

The proof of concept was established for the biofeedback smart headband. However, some modifications can be made to make it more user-friendly.

In the current design of the smart headband, one control board is used for each piezoelectric actuator. This makes the structure a little cumbersome. This can however be solved by programming the board, so it drives all the three actuators. This would also require more than one voltage amplifier to be combined into one board.

Further, the role of the pressure sensor can be integrated into the piezoelectric actuators. This is advantageous in order to avoid a cumbersome design of the smart textile. This can be done by programming the function of the sensor using the source code of the Boreas Technologies board.

The range of operation of the actuators can also be increased and provide a wider range of amplitudes. This is important to make sure that some of the information regarding the food texture and the force required to chew it isn't lost. It can be done by changing how the piezoelectric actuator is controlled.

Lastly, the structure could also become more mobile by using a Bluetooth and Wi-Fi connection between the oral implants and the headband to provide vibrotactile feedback corresponding to the chewing events without the need for cables.

References

[1] K. Guru, U. K. Manoor, and S. S. Supe, "A comprehensive review of head and neck cancer rehabilitation: Physical therapy perspectives," *Indian Journal of Palliative Care*, vol. 18, no. 2. pp. 87–97, 2012, doi: 10.4103/0973-1075.100820.

[2] S. B. Movsas, V. T. Chang, R. S. Tunkel, V. V. Shah, L. S. Ryan, and S. R. Millis, "Rehabilitation Needs of an Inpatient Medical Oncology Unit," *Arch. Phys. Med. Rehabil.*, vol. 84, no. 11, pp. 1642–1646, 2003, doi: 10.1053/S0003-9993(03)00345-9.

[3] S. Maltser, A. Cristian, J. K. Silver, G. S. Morris, and N. L. Stout, "A Focused Review of Safety Considerations in Cancer Rehabilitation," *PM and R*, vol. 9, no. 9. pp. S415–S428, 2017, doi: 10.1016/j.pmrj.2017.08.403.

[4] N. E. Adler and A. E. K. Page, *Cancer care for the whole patient: Meeting psychosocial health needs*. 2008.

[5] A. L. Cheville, "Cancer rehabilitation," *Semin. Oncol.*, vol. 32, no. 2, pp. 219–224, 2005, doi: 10.1053/j.seminoncol.2004.11.009.

[6] B. R. Pauloski, "Rehabilitation of Dysphagia Following Head and Neck Cancer," *Physical Medicine and Rehabilitation Clinics of North America*, vol. 19, no. 4. pp. 889–928, 2008, doi: 10.1016/j.pmr.2008.05.010.

[7] R. A. Barrowman, P. R. Wilson, and D. Wiesenfeld, "Oral rehabilitation with dental implants after cancer treatment," *Aust. Dent. J.*, vol. 56, no. 2, pp. 160–165, 2011, doi: 10.1111/j.1834-7819.2011.01318.x.

[8] L. Chen *et al.*, "Textile-Based Capacitive Sensor for Physical Rehabilitation via Surface Topological Modification," *ACS Nano*, vol. 14, no. 7, pp. 8191–8201, 2020, doi: 10.1021/acsnano.0c01643.

[9] V. Koncar, *Smart textiles and their applications*. 2016.

[10] L. Vinet and A. Zhedanov, *A "missing" family of classical orthogonal polynomials*, vol. 44, no. 8. 2011.

[11] F. Axisa, A. Dittmar, and G. Delhomme, "Smart clothes for the monitoring in real time and conditions of physiological, emotional and sensorial reactions of human," in *Annual International Conference of the IEEE Engineering in Medicine and Biology - Proceedings*, 2003, vol. 4, pp. 3744–3747, doi: 10.1109/iembs.2003.1280974.

[12] X. X. Zhang and X. M. Tao, "Smart textiles (2): Active smart," *Text. Asia*, vol. 32, no. 7, pp. 49–52, 2001.

[13] K. Cherenack and L. Van Pieterson, "Smart textiles: Challenges and opportunities," *Journal of Applied Physics*, vol. 112, no. 9. 2012, doi: 10.1063/1.4742728.

[14] Sungmee Park, K. Mackenzie, and S. Jayaraman, "The wearable motherboard: a framework for personalized mobile information processing (PMIP)," 2003, pp. 170–174, doi: 10.1109/dac.2002.1012614.

[15] M. Hamedi, R. Forchheimer, and O. Inganäs, "Towards woven logic from organic electronic fibres," *Nat. Mater.*, vol. 6, no. 5, pp. 357–362, 2007, doi: 10.1038/nmat1884.

[16] J. Decaens and O. Vermeersch, "Wearable technologies for personal protective equipment: Embedded textile monitoring sensors, power and data transmission, end-life indicators," in *Smart Textiles and Their Applications*, 2016, pp. 519–537.

[17] C. Randell, S. Baurley, M. Chalmers, and H. Muller, "Textile Tools for Wearable Computing," *Proc. 1st Int. Forum Appl. Wearable Comput. IFAWC 2004*, pp. 63–74, 2004.

[18] A. Patnaik and S. Patnaik, *Fibres to Smart Textiles: Advances in Manufacturing, Technologies, and Applications*. CRC Press, 2019.
[19] A. Harlin, M. Mäkinen, and A. Vuorivirta, "Development of polymeric optical fibre fabrics as illumination elements and textile displays," *Autex Res. J.*, vol. 3, no. 1, pp. 1–8, 2003.
[20] P. Lemmens, F. Crompvoets, D. Brokken, J. Van Den Eerenbeemd, and G. J. De Vries, "A body-conforming tactile jacket to enrich movie viewing," in *Proceedings - 3rd Joint EuroHaptics Conference and Symposium on Haptic Interfaces for Virtual Environment and Teleoperator Systems, World Haptics 2009*, 2009, pp. 7–12, doi: 10.1109/WHC.2009.4810832.
[21] P. Bach-y-Rita, "Tactile sensory substitution studies," in *Annals of the New York Academy of Sciences*, 2004, vol. 1013, pp. 83–91, doi: 10.1196/annals.1305.006.
[22] P. Bach-y-Rita, K. A. Kaczmarek, M. E. Tyler, and J. Garcia-Lara, "Form perception with a 49-point electrotactile stimulus array on the tongue: A technical note," *J. Rehabil. Res. Dev.*, vol. 35, no. 4, pp. 427–430, 1998.
[23] C. I. Howarth, "Review: Brain Mechanisms in Sensory Substitution," *Perception*, vol. 1, no. 4, pp. 491–492, 1972, doi: 10.1068/p010491.
[24] N. Vuillerme *et al.*, "Pressure sensor-based tongue-placed electrotactile biofeedback for balance improvement--biomedical application to prevent pressure sores formation and falls.," *Conf. Proc. IEEE Eng. Med. Biol. Soc.*, pp. 6114–6117, 2007.
[25] N. Vuillerme, M. Boisgontier, O. Chenu, J. Demongeot, and Y. Payan, "Tongue-placed tactile biofeedback suppresses the deleterious effects of muscle fatigue on joint position sense at the ankle," *Exp. Brain Res.*, vol. 183, no. 2, pp. 235–240, 2007, doi: 10.1007/s00221-007-1039-4.
[26] P. Bach-Y-Rita, C. C. Collins, F. A. Saunders, B. White, and L. Scadden, "Vision substitution by tactile image projection [18]," *Nature*, vol. 221, no. 5184. pp. 963–964, 1969, doi: 10.1038/221963a0.
[27] B. Petry, T. Illandara, D. S. Elvitigala, and S. Nanayakkara, "Supporting rhythm activities of deaf children using music-sensory-substitution systems," in *Conference on Human Factors in Computing Systems - Proceedings*, 2018, vol. 2018-April, doi: 10.1145/3173574.3174060.
[28] K. A. Kaczmarek, J. G. Webster, P. Bach-y-Rita, and W. J. Tompkins, "Electrotactile and Vibrotactile Displays for Sensory Substitution Systems," *IEEE Trans. Biomed. Eng.*, vol. 38, no. 1, pp. 1–16, 1991, doi: 10.1109/10.68204.
[29] F. A. Saunders, W. A. Hill, and B. Franklin, "A wearable tactile sensory aid for profoundly deaf children," *J. Med. Syst.*, vol. 5, no. 4, pp. 265–270, 1981, doi: 10.1007/BF02222144.
[30] C. C. Collins and P. Bach-y-Rita, "Transmission of pictorial information through the skin.," *Advances in biological and medical physics*, vol. 14. pp. 285–315, 1973, doi: 10.1016/b978-0-12-005214-1.50010-8.
[31] J. C. Bliss, M. H. Katcher, C. H. Rogers, and R. P. Shepard, "Optical-to-Tactile Image Conversion for the Blind," *IEEE Trans. Man-Machine Syst.*, vol. 11, no. 1, pp. 58–65, 1970, doi: 10.1109/TMMS.1970.299963.
[32] C. C. Collins and J. M. J. Madey, "Tactile Sensory Replacement.," 1974, pp. 15–26.
[33] D. W. Sparks, L. A. Ardell, M. Bourgeois, B. Wiedmer, and P. K. Kuhl, "Investigating the MESA (Multipoint Electrotactile Speech Aid): The transmission of connected discourse,"

J. Acoust. Soc. Am., vol. 65, no. 3, pp. 810–815, 1979, doi: 10.1121/1.382502.
[34] R. Ackerley, I. Carlsson, H. Wester, H. Olausson, and H. Backlund Wasling, "Touch perceptions across skin sites: Differences between sensitivity, direction discrimination and pleasantness," *Front. Behav. Neurosci.*, vol. 8, no. FEB, 2014, doi: 10.3389/fnbeh.2014.00054.
[35] A. B. Vallbo, H. Olausson, J. Wessberg, and N. Kakuda, "Receptive field characteristics of tactile units with myelinated afferents in hairy skin of human subjects.," *J. Physiol.*, vol. 483, no. 3, pp. 783–795, 1995, doi: 10.1113/jphysiol.1995.sp020622.
[36] H. Pongrac, "Vibrotactile perception: Examining the coding of vibrations and the just noticeable difference under various conditions," *Multimed. Syst.*, vol. 13, no. 4, pp. 297–307, 2008, doi: 10.1007/s00530-007-0105-x.
[37] Y. H. Jung, J. H. Kim, and J. A. Rogers, "Skin-Integrated Vibrohaptic Interfaces for Virtual and Augmented Reality," *Advanced Functional Materials*. 2020, doi: 10.1002/adfm.202008805.
[38] "Human Skin and Sensory Receptors. Stock Vector - Illustration of cross, epithelial: 84441495." https://www.dreamstime.com/stock-illustration-human-skin-sensory-receptors-pressure-vibration-temperature-toutch-transmitted-via-special-receptory-organs-nerves-image84441495 (accessed Sep. 18, 2021).
[39] N. Sadato *et al.*, "Activation of the primary visual cortex by Braille reading in blind subjects," *Nature*, vol. 380, no. 6574, pp. 526–528, 1996, doi: 10.1038/380526a0.
[40] A. Barghout, J. Cha, A. El Saddik, J. Kammerl, and E. Steinbach, "Spatial resolution of vibrotactile perception on the human forearm when exploiting funneling illusion," in *2009 IEEE International Workshop on Haptic Audio Visual Environments and Games, HAVE 2009 - Proceedings*, 2009, pp. 19–23, doi: 10.1109/HAVE.2009.5356122.
[41] S. Weinstein, "Intensive and extensive aspects of tactile sensitivity as a function of body part, sex and laterality," in *First International Symposium on Skin Senses*, 1968, pp. 195–222.
[42] A. Tajadura-Jiménez, A. Väljamäe, and K. Kuusk, "Altering One's Body-Perception Through E-Textiles and Haptic Metaphors," *Front. Robot. AI*, vol. 7, 2020, doi: 10.3389/frobt.2020.00007.
[43] C. Cipriani, M. Dalonzo, and M. C. Carrozza, "A miniature vibrotactile sensory substitution device for multifingered hand prosthetics," *IEEE Trans. Biomed. Eng.*, vol. 59, no. 2, pp. 400–408, 2012, doi: 10.1109/TBME.2011.2173342.
[44] L. Cancar, A. Diaz, A. Barrientos, D. Travieso, and D. M. Jacobs, "Tactile-Sight: A sensory substitution device based on distance-related vibrotactile flow regular paper," *Int. J. Adv. Robot. Syst.*, vol. 10, 2013, doi: 10.5772/56235.
[45] M. Hollins, K. A. Delemos, and A. K. Goble, "Vibrotactile adaptation on the face," *Percept. Psychophys.*, vol. 49, no. 1, pp. 21–30, 1991, doi: 10.3758/BF03211612.
[46] C. H. Wedell and S. B. Cummings, "Fatigue of the vibratory sense," *J. Exp. Psychol.*, vol. 22, no. 5, pp. 429–438, 1938, doi: 10.1037/h0059105.
[47] G. von Békésy, "Synchronism of Neural Discharges and Their Demultiplication in Pitch Perception on the Skin and in Hearing," *J. Acoust. Soc. Am.*, vol. 31, no. 3, pp. 338–349, 1959, doi: 10.1121/1.1907722.
[48] R. T. Verrillo, "Comparison of vibrotactile threshold and suprathreshold responses in men and women," *Percept. Psychophys.*, vol. 26, no. 1, pp. 20–24, 1979, doi: 10.3758/BF03199857.

[49] G. D. Goff, B. S. Rosner, T. Detre, and D. Kennard, “Vibration perception in normal man and medical patients.,” *J. Neurol. Neurosurg. Psychiatry*, vol. 28, no. 6, pp. 503–509, 1965, doi: 10.1136/jnnp.28.6.503.
[50] R. T. Verrillo and S. J. Bolanowski, “Effects of temperature on the subjective magnitude of vibration,” *Somatosens. Mot. Res.*, vol. 20, no. 2, pp. 133–137, 2003, doi: 10.1080/089902203100105163.
[51] A. Fleury, M. Sugar, and T. Chau, “E-textiles in clinical rehabilitation: A scoping review,” *Electron.* , vol. 4, no. 1, pp. 173–203, 2015, doi: 10.3390/electronics4010173.
[52] A. Pantelopoulos and N. G. Bourbakis, “A survey on wearable sensor-based systems for health monitoring and prognosis,” *IEEE Transactions on Systems, Man and Cybernetics Part C: Applications and Reviews*, vol. 40, no. 1. pp. 1–12, 2010, doi: 10.1109/TSMCC.2009.2032660.
[53] G. López, V. Custodio, and J. I. Moreno, “LOBIN: E-textile and wireless-sensor-network-based platform for healthcare monitoring in future hospital environments,” *IEEE Trans. Inf. Technol. Biomed.*, vol. 14, no. 6, pp. 1446–1458, 2010, doi: 10.1109/TITB.2010.2058812.
[54] M. Coyle, “Ambulatory cardiopulmonary data capture,” in *2nd Annual International IEEE-EMBS Special Topic Conference on Microtechnologies in Medicine and Biology - Proceedings*, 2002, pp. 297–300, doi: 10.1109/MMB.2002.1002333.
[55] J. Coosemans, B. Hermans, and R. Puers, “Integrating wireless ECG monitoring in textiles,” *Sensors Actuators, A Phys.*, vol. 130–131, no. SPEC. ISS., pp. 48–53, 2006, doi: 10.1016/j.sna.2005.10.052.
[56] A. Angelucci *et al.*, “Smart textiles and sensorized garments for physiological monitoring: A review of available solutions and techniques,” *Sensors (Switzerland)*, vol. 21, no. 3. pp. 1–23, 2021, doi: 10.3390/s21030814.
[57] L. Van Langenhove, *Smart textiles for medicine and healthcare: Materials, systems and applications*. 2007.
[58] J. McCann, “Smart protective textiles for older people,” in *Smart Textiles for Protection*, 2013, pp. 244–275.
[59] M. Adnane, Z. Jiang, S. Choi, and H. Jang, “Detecting specific health-related events using an integrated sensor system for vital sign monitoring,” *Sensors*, vol. 9, no. 9, pp. 6897–6912, 2009, doi: 10.3390/s90906897.
[60] Y. G. Lim, K. K. Kim, and K. S. Park, “ECG recording on a bed during sleep without direct skin-contact,” *IEEE Trans. Biomed. Eng.*, vol. 54, no. 4, pp. 718–725, 2007, doi: 10.1109/TBME.2006.889194.
[61] A. M. Bianchi, M. O. Mendez, and S. Cerutti, “Processing of signals recorded through smart devices: Sleep-quality assessment,” *IEEE Trans. Inf. Technol. Biomed.*, vol. 14, no. 3, pp. 741–747, 2010, doi: 10.1109/TITB.2010.2049025.
[62] J. Hännikäinen, T. Vuorela, and J. Vanhala, “Physiological measurements in smart clothing: A case study of total body water estimation with bioimpedance,” *Trans. Inst. Meas. Control*, vol. 29, no. 3–4, pp. 337–354, 2007, doi: 10.1177/0142331207073488.
[63] J. C. Márquez, F. Seoane, and K. Lindecrantz, “Textrode functional straps for bioimpedance measurements-experimental results for body composition analysis,” *Eur. J. Clin. Nutr.*, vol. 67, pp. S22–S27, 2013, doi: 10.1038/ejcn.2012.161.
[64] T. Vuorela, V. P. Seppä, J. Vanhala, and J. Hyttinen, “Design and implementation of a portable long-term physiological signal recorder,” *IEEE Trans. Inf. Technol. Biomed.*, vol.

14, no. 3, pp. 718–725, 2010, doi: 10.1109/TITB.2010.2042606.
[65] R. McLaren, F. Joseph, C. Baguley, and D. Taylor, “A review of e-textiles in neurological rehabilitation: How close are we?,” *Journal of NeuroEngineering and Rehabilitation*, vol. 13, no. 1. 2016, doi: 10.1186/s12984-016-0167-0.
[66] P. Tormene *et al.*, “Estimation of human trunk movements by wearable strain sensors and improvement of sensor’s placement on intelligent biomedical clothes,” *Biomed. Eng. Online*, vol. 11, 2012, doi: 10.1186/1475-925X-11-95.
[67] F. Lorussi, S. Galatolo, and D. E. De Rossi, “Textile-based electrogoniometers for wearable posture and gesture capture systems,” *IEEE Sens. J.*, vol. 9, no. 9, pp. 1014–1024, 2009, doi: 10.1109/JSEN.2009.2024867.
[68] A. Tognetti *et al.*, “Wearable kinesthetic system for capturing and classifying upper limb gesture in post-stroke rehabilitation,” *J. Neuroeng. Rehabil.*, vol. 2, 2005, doi: 10.1186/1743-0003-2-8.
[69] V. E. Kuzmichev, I. V. Tislenko, and D. C. Adolphe, “Virtual design of knitted compression garments based on bodyscanning technology and the three-dimensional-to-two-dimensional approach,” *Text. Res. J.*, vol. 89, no. 12, pp. 2456–2475, 2019, doi: 10.1177/0040517518792722.
[70] D. Farina, T. Lorrain, F. Negro, and N. Jiang, “High-density EMG E-textile systems for the control of active prostheses,” in *2010 Annual International Conference of the IEEE Engineering in Medicine and Biology Society, EMBC’10*, 2010, pp. 3591–3593, doi: 10.1109/IEMBS.2010.5627455.
[71] C. M. Yang, Z. S. Lin, C. L. Hu, Y. S. Chen, L. Y. Ke, and Y. R. Chen, “A novel dynamic sensing of wearable digital textile sensor with body motion analysis,” in *2010 Annual International Conference of the IEEE Engineering in Medicine and Biology Society, EMBC’10*, 2010, pp. 4898–4901, doi: 10.1109/IEMBS.2010.5627270.
[72] C. Cochrane, C. Hertleer, and A. Schwarz-Pfeiffer, “Smart textiles in health: An overview,” in *Smart Textiles and Their Applications*, 2016, pp. 9–32.
[73] K. Bjerså and T. Andersson, “High frequency TENS as a complement for pain relief in postoperative transition from epidural to general analgesia after pancreatic resection,” *Complement. Ther. Clin. Pract.*, vol. 20, no. 1, pp. 5–10, 2014, doi: 10.1016/j.ctcp.2013.11.004.
[74] J. Mccann, “Smart medical textiles in rehabilitation,” in *Smart textiles for medicine and healthcare: Materials, systems and applications*, 2007, pp. 166–182.
[75] E. Korzeniewska, A. Krawczyk, J. Mróz, E. Wyszyńska, and R. Zawiślak, “Applications of smart textiles in post-stroke rehabilitation,” *Sensors (Switzerland)*, vol. 20, no. 8, 2020, doi: 10.3390/s20082370.
[76] P. Zhang, *Chapter 3 - Sensors and actuators*. 2010.
[77] J. L. Pons, E. Rocon, A. Forner-Cordero, and J. Moreno, “Biomedical instrumentation based on piezoelectric ceramics,” *J. Eur. Ceram. Soc.*, vol. 27, no. 13–15, pp. 4191–4194, 2007, doi: 10.1016/j.jeurceramsoc.2007.02.126.
[78] P. K. Panda and B. Sahoo, “PZT to lead free piezo ceramics: A review,” *Ferroelectrics*, vol. 474, no. 1, pp. 128–143, 2015, doi: 10.1080/00150193.2015.997146.
[79] W. G. Cady and J. Valasek, “BOOK REVIEWS: Piezoelectricity: An Introduction to the Theory and Applications of Electro-mechanical Phenomena in Crystals,” *Phys. Teach.*, vol. 3, no. 3, pp. 130–130, 1965, doi: 10.1119/1.2349067.
[80] I. A. Parinov, *Piezoelectric materials and devices*. 2011.

[81] M. Henini, “Principles of Electronic Materials and Devices (Second Edition),” *Microelectronics J.*, vol. 33, no. 8, p. 681, 2002, doi: 10.1016/s0026-2692(02)00042-3.
[82] M. T. Chorsi *et al.*, “Piezoelectric Biomaterials for Sensors and Actuators,” *Advanced Materials*, vol. 31, no. 1. 2019, doi: 10.1002/adma.201802084.
[83] K. Asaka and H. Okuzaki, *Soft actuators: Materials, modeling, applications, and future perspectives*, vol. 9784431547. 2014.
[84] K. S. Ramadan, D. Sameoto, and S. Evoy, “A review of piezoelectric polymers as functional materials for electromechanical transducers,” *Smart Materials and Structures*, vol. 23, no. 3. 2014, doi: 10.1088/0964-1726/23/3/033001.
[85] K. Ohnuma, “Method for producing an organic piezoelectric material shaped in a film.” Google Patents, Sep. 19, 2013.
[86] Y. Q. Fu *et al.*, “Advances in piezoelectric thin films for acoustic biosensors, acoustofluidics and lab-on-chip applications,” *Progress in Materials Science*, vol. 89. pp. 31–91, 2017, doi: 10.1016/j.pmatsci.2017.04.006.
[87] S. Zhang *et al.*, “Organic/inorganic superabsorbent hydrogels based on xylan and montmorillonite,” *J. Nanomater.*, vol. 2014, 2014, doi: 10.1155/2014/675035.
[88] B. Tiwari, T. Babu, and R. N. P. Choudhary, “AC Impedance and Modulus Spectroscopic Studies of Pb(Zr0.35-xCexTi0.65)O3 (x = 0.00, 0.05, 0.10, 0.15) Ferroelectric Ceramics,” *Mater. Chem. Phys.*, vol. 256, 2020, doi: 10.1016/j.matchemphys.2020.123655.
[89] T. Someya, *Stretchable Electronics*. John Wiley & Sons, 2012.
[90] L. M. Swallow, J. K. Luo, E. Siores, I. Patel, and D. Dodds, “A piezoelectric fibre composite based energy harvesting device for potential wearable applications,” *Smart Mater. Struct.*, vol. 17, no. 2, 2008, doi: 10.1088/0964-1726/17/2/025017.
[91] D. Paul and A. Roy, “Piezoelectric Effect: Smart roads in green energy harvesting,” *International Journal of Engineering and Technical Research (IJETR)*, vol. 3, no. 2. p. 114, 2015.
[92] K. Cung *et al.*, “Biotemplated synthesis of PZT nanowires,” *Nano Lett.*, vol. 13, no. 12, pp. 6197–6202, 2013, doi: 10.1021/nl4035708.
[93] Q. Wei, “Emerging approaches to the surface modification of textiles,” in *Surface Modification of Textiles*, 2009, pp. 318–323.
[94] A. Janotti and C. G. Van De Walle, “Fundamentals of zinc oxide as a semiconductor,” *Reports Prog. Phys.*, vol. 72, no. 12, 2009, doi: 10.1088/0034-4885/72/12/126501.
[95] Y. Zhang, T. Nayak, H. Hong, and W. Cai, “Biomedical Applications of Zinc Oxide Nanomaterials,” *Curr. Mol. Med.*, vol. 13, no. 10, pp. 1633–1645, 2013, doi: 10.2174/1566524013666131111130058.
[96] Y. Chu *et al.*, “Flexible ZnO nanogenerator for mechanical energy harvesting,” in *Proceedings - 2013 14th International Conference on Electronic Packaging Technology, ICEPT 2013*, 2013, pp. 1292–1295, doi: 10.1109/ICEPT.2013.6756694.
[97] J. Lu, L. Zhang, H. Takagi, T. Itoh, and R. Maeda, “Hybrid piezoelectric mems resonators for application in bio-chemical sensing,” *J. Appl. Sci. Eng.*, vol. 17, no. 1, pp. 17–24, 2014, doi: 10.6180/jase.2014.17.1.03.
[98] A. Dogan, J. F. Fernandez, K. Uchino, and R. E. Newnham, “`Cymbal’ electromechanical actuator,” in *IEEE International Symposium on Applications of Ferroelectrics*, 1996, vol. 1, pp. 213–216.
[99] C. Dagdeviren *et al.*, “Conformal piezoelectric systems for clinical and experimental characterization of soft tissue biomechanics,” *Nat. Mater.*, vol. 14, no. 7, pp. 728–736,

2015, doi: 10.1038/nmat4289.
[100] T. D. Nguyen *et al.*, “Piezoelectric nanoribbons for monitoring cellular deformations,” *Nat. Nanotechnol.*, vol. 7, no. 9, pp. 587–593, 2012, doi: 10.1038/nnano.2012.112.
[101] C. Dagdeviren *et al.*, “Conformal piezoelectric energy harvesting and storage from motions of the heart, lung, and diaphragm,” *Proc. Natl. Acad. Sci. U. S. A.*, vol. 111, no. 5, pp. 1927–1932, 2014, doi: 10.1073/pnas.1317233111.
[102] H. Mirzaei and M. Darroudi, “Zinc oxide nanoparticles: Biological synthesis and biomedical applications,” *Ceramics International*, vol. 43, no. 1. pp. 907–914, 2017, doi: 10.1016/j.ceramint.2016.10.051.
[103] Y. Li, L. Sun, and T. J. Webster, “The investigation of ZnO/poly(vinylidene fluoride) nanocomposites with improved mechanical, piezoelectric, and antimicrobial properties for orthopedic applications,” *J. Biomed. Nanotechnol.*, vol. 14, no. 3, pp. 536–545, 2018, doi: 10.1166/jbn.2018.2519.
[104] K. Kapat, Q. T. H. Shubhra, M. Zhou, and S. Leeuwenburgh, “Piezoelectric Nano-Biomaterials for Biomedicine and Tissue Regeneration,” *Advanced Functional Materials*, vol. 30, no. 44. 2020, doi: 10.1002/adfm.201909045.
[105] N. Puvvada *et al.*, “Novel ZnO hollow-nanocarriers containing paclitaxel targeting folate-receptors in a malignant pH-microenvironment for effective monitoring and promoting breast tumor regression,” *Sci. Rep.*, vol. 5, 2015, doi: 10.1038/srep11760.
[106] A. Zaszczyńska, A. Gradys, and P. Sajkiewicz, “Progress in the applications of smart piezoelectric materials for medical devices,” *Polymers*, vol. 12, no. 11. pp. 1–19, 2020, doi: 10.3390/polym12112754.
[107] A. Kos, V. Milutinović, and A. Umek, “Challenges in wireless communication for connected sensors and wearable devices used in sport biofeedback applications,” *Futur. Gener. Comput. Syst.*, vol. 92, pp. 582–592, 2019, doi: 10.1016/j.future.2018.03.032.
[108] J. Dargahi and S. Najarian, “Human tactile perception as a standard for artificial tactile sensing--a review.,” *The international journal of medical robotics + computer assisted surgery : MRCAS*, vol. 1, no. 1. pp. 23–35, 2004, doi: 10.1002/rcs.3.
[109] Y. Lee, J. Park, A. Choe, S. Cho, J. Kim, and H. Ko, “Mimicking Human and Biological Skins for Multifunctional Skin Electronics,” *Advanced Functional Materials*, vol. 30, no. 20. 2020, doi: 10.1002/adfm.201904523.
[110] K. Kim *et al.*, “Tactile Avatar: Tactile Sensing System Mimicking Human Tactile Cognition,” *Adv. Sci.*, vol. 8, no. 7, 2021, doi: 10.1002/advs.202002362.
[111] J. Rantala *et al.*, “Gaze Interaction With Vibrotactile Feedback: Review and Design Guidelines,” *Human-Computer Interact.*, vol. 35, no. 1, pp. 1–39, 2020, doi: 10.1080/07370024.2017.1306444.
[112] A. T. Maereg, A. Nagar, D. Reid, and E. L. Secco, “Wearable Vibrotactile Haptic Device for Stiffness Discrimination during Virtual Interactions,” *Front. Robot. AI*, vol. 4, no. SEP, 2017, doi: 10.3389/frobt.2017.00042.
[113] T. N. Do, H. Phan, T. Q. Nguyen, and Y. Visell, “Miniature Soft Electromagnetic Actuators for Robotic Applications,” *Adv. Funct. Mater.*, vol. 28, no. 18, 2018, doi: 10.1002/adfm.201800244.
[114] G. Song, V. Sethi, and H. N. Li, “Vibration control of civil structures using piezoceramic smart materials: A review,” *Eng. Struct.*, vol. 28, no. 11, pp. 1513–1524, 2006, doi: 10.1016/j.engstruct.2006.02.002.
[115] K. H. Lam, X. X. Wang, and H. L. W. Chan, “Lead-free piezoceramic cymbal actuator,”

Sensors Actuators, A Phys., vol. 125, no. 2, pp. 393–397, 2006, doi: 10.1016/j.sna.2005.08.028.
[116] W. Gao, Y. Zhu, Y. Wang, G. Yuan, and J. M. Liu, "A review of flexible perovskite oxide ferroelectric films and their application," *Journal of Materiomics*, vol. 6, no. 1. pp. 1–16, 2020, doi: 10.1016/j.jmat.2019.11.001.
[117] K. Uchino, "The Development of Piezoelectric Materials and the New Perspective," in *Advanced Piezoelectric Materials*, 2017, pp. 1–92.
[118] P. Ochoa, J. L. Pons, M. Villegas, and J. F. Fernandez, "Advantages and limitations of cymbals for sensor and actuator applications," *Sensors Actuators, A Phys.*, vol. 132, no. 1 SPEC. ISS., pp. 63–69, 2006, doi: 10.1016/j.sna.2006.05.031.
[119] K. H. Lam, H. L. W. Chan, H. S. Luo, Q. R. Yin, Z. W. Yin, and C. L. Choy, "Cymbal actuators fabricated using PMN-PT single crystal," in *Ferroelectrics*, 2001, vol. 263, no. 1, pp. 235–240, doi: 10.1080/00150190108225205.
[120] S. J. Rothberg *et al.*, "An international review of laser Doppler vibrometry: Making light work of vibration measurement," *Opt. Lasers Eng.*, vol. 99, pp. 11–22, 2017, doi: 10.1016/j.optlaseng.2016.10.023.
[121] L. E. Drain, "The laser-Doppler technique.," 1980, doi: 10.1088/0031-9112/31/9/045.
[122] J. Oldengarm, A. H. van Krieken, and H. J. Raterink, "Laser Doppler velocimeter with optical frequency shifting," *Opt. Laser Technol.*, vol. 5, no. 6, pp. 249–252, 1973, doi: 10.1016/0030-3992(73)90050-9.
[123] G. Bank and G. T. Harthaway, "Revolutionary 3-D Interferometric Vibrational Mode Display.," *Audio Eng. Soc. Prepr.*, 1980.
[124] B. Junge, "<title>Experiences with scanning laser vibrometry in automotive industries</title>," in *First International Conference on Vibration Measurements by Laser Techniques: Advances and Applications*, 1994, vol. 2358, pp. 377–385, doi: 10.1117/12.185348.
[125] J. Hancox, B. C. Staples, and R. J. Parker, "The application of scanning laser Doppler vibrometry in aero-engine development," *Proceedings of the Institution of Mechanical Engineers, Part G: Journal of Aerospace Engineering*, vol. 209, no. 1. pp. 35–42, 1995, doi: 10.1243/PIME_PROC_1995_209_268_02.
[126] C. Rembe and A. Dräbenstedt, "Laser-scanning confocal vibrometer microscope: Theory and experiments," *Rev. Sci. Instrum.*, vol. 77, no. 8, 2006, doi: 10.1063/1.2336103.
[127] Q. V. Davis and W. K. Kulczyk, "Vibrations of turbine blades measured by means of a laser [14]," *Nature*, vol. 222, no. 5192. pp. 475–476, 1969, doi: 10.1038/222475a0.
[128] C. Rembe and R. S. Muller, "Measurement system for full three-dimensional motion characterization of MEMS," *J. Microelectromechanical Syst.*, vol. 11, no. 5, pp. 479–488, 2002, doi: 10.1109/JMEMS.2002.803285.
[129] J. F. Vignola *et al.*, "Characterization of silicon micro-oscillators by scanning laser vibrometry," *Rev. Sci. Instrum.*, vol. 73, no. 10, p. 3584, 2002, doi: 10.1063/1.1502014.
[130] C. Rembe, R. Kowarsch, W. Ochs, A. Dräbenstedt, M. Giesen, and M. Winter, "Optical three-dimensional vibrometer microscope with picometer-resolution in x, y, and z," *Opt. Eng.*, vol. 53, no. 3, p. 034108, 2014, doi: 10.1117/1.oe.53.3.034108.
[131] T. J. F. Buunen and M. S. Vlaming, "Laser-doppler velocity meter applied to tympanic membrane vibrations in cat," *J. Acoust. Soc. Am.*, vol. 69, no. 3, pp. 744–750, 1981, doi: 10.1121/1.385574.
[132] J. F. Willemin, R. Dändliker, and S. M. Khanna, "Heterodyne interferometer for

submicroscopic vibration measurements in the inner ear," *J. Acoust. Soc. Am.*, vol. 83, no. 2, pp. 787–795, 1988, doi: 10.1121/1.396122.
[133] A. M. Huber, G. R. Ball, D. Veraguth, N. Dillier, D. Bodmer, and D. Sequeira, "A new implantable middle ear hearing device for mixed hearing loss: A feasibility study in human temporal bones," *Otol. Neurotol.*, vol. 27, no. 8, pp. 1104–1109, 2006, doi: 10.1097/01.mao.0000244352.49824.e6.
[134] H. Tabatabai, D. E. Oliver, J. W. Rohrbaugh, and C. Papadopoulos, "Novel applications of laser doppler vibration measurements to medical imaging," *Sensing and Imaging*, vol. 14, no. 1–2. pp. 13–28, 2013, doi: 10.1007/s11220-013-0077-1.
[135] L. Mioche, "Mastication and food texture perception: Variation with age," in *Journal of Texture Studies*, 2004, vol. 35, no. 2, pp. 145–158, doi: 10.1111/j.1745-4603.2004.tb00830.x.
[136] Q.-M. Wang and L. E. Cross, "Performance analysis of piezoelectric cantilever bending actuators," *Ferroelectrics*, vol. 215, no. 1, pp. 187–213, 1998, doi: 10.1080/00150199808229562.
[137] D. WANG, Y. GUO, S. LIU, Y. ZHANG, W. XU, and J. XIAO, "Haptic display for virtual reality: progress and challenges," *Virtual Real. Intell. Hardw.*, vol. 1, no. 2, pp. 136–162, 2019, doi: 10.3724/sp.j.2096-5796.2019.0008.
[138] A. Taguchi *et al.*, "A New Device for Fine-Needle Aspiration Cytology Consisting of a Vibrating Linear Resonant Actuator," *Laryngoscope*, vol. 131, no. 4, pp. E1393–E1399, 2021, doi: 10.1002/lary.29143.
[139] S. Liu, J. Tong, C. Yang, and L. Li, "Smart E-textile: Resistance properties of conductive knitted fabric – Single pique," *Text. Res. J.*, vol. 87, no. 14, pp. 1669–1684, 2017, doi: 10.1177/0040517516658509.
[140] S. Dong, F. Xu, Y. Sheng, Z. Guo, X. Pu, and Y. Liu, "Seamlessly knitted stretchable comfortable textile triboelectric nanogenerators for E-textile power sources," *Nano Energy*, vol. 78, 2020, doi: 10.1016/j.nanoen.2020.105327.
[141] F. Abtahi, G. Ji, K. Lu, K. Rodby, and F. Seoane, "A knitted garment using intarsia technique for Heart Rate Variability biofeedback: Evaluation of initial prototype," in *Proceedings of the Annual International Conference of the IEEE Engineering in Medicine and Biology Society, EMBS*, 2015, vol. 2015-Novem, pp. 3121–3124, doi: 10.1109/EMBC.2015.7319053.
[142] M. Penciuc, M. Blaga, and R. Ciobanu, "Principle of creating 3d effects on knitted fabrics developed on electronic flat knitting machines," *Bul. Institutului Politeh. Din IASI*, no. January 2010, pp. 15–21, 2010.
[143] L. Li, Wai Man au, Y. Li, K. M. Wan, Sai ho Wan, and K. S. Wong, "Design of Intelligent Garment with Transcutaneous Electrical Nerve Stimulation Function Based on the Intarsia Knitting Technique," *Text. Res. J.*, vol. 80, no. 3, pp. 279–286, 2010, doi: 10.1177/0040517509105276.
[144] K. Jost *et al.*, "Knitted and screen printed carbon-fiber supercapacitors for applications in wearable electronics," *Energy Environ. Sci.*, vol. 6, no. 9, pp. 2698–2705, 2013, doi: 10.1039/c3ee40515j.
[145] S. Lee, M. O. Kim, T. Kang, J. Park, and Y. Choi, "Knit Band Sensor for Myoelectric Control of Surface EMG-Based Prosthetic Hand," *IEEE Sens. J.*, vol. 18, no. 20, pp. 8578–8586, 2018, doi: 10.1109/JSEN.2018.2865623.
[146] V. Mecnika, M. Hoerr, I. Krievins, S. Jockenhoevel, and T. Gries, "Technical Embroidery

for Smart Textiles: Review," *Mater. Sci. Text. Cloth. Technol.*, vol. 9, p. 56, 2015, doi: 10.7250/mstct.2014.009.
[147] C. Zeagler, S. Gilliland, H. Profita, and T. Starner, "Textile interfaces: Embroidered jog-wheel, beaded tilt sensor, twisted pair ribbon, and sound sequins," in *Proceedings - International Symposium on Wearable Computers, ISWC*, 2012, pp. 60–63, doi: 10.1109/ISWC.2012.29.
[148] A. R. Köhler, "Challenges for eco-design of emerging technologies: The case of electronic textiles," *Mater. Des.*, vol. 51, pp. 51–60, 2013, doi: 10.1016/j.matdes.2013.04.012.
[149] S. U. Zaman, X. Tao, C. Cochrane, and V. Koncar, "Market readiness of smart textile structures - Reliability and washability," in *IOP Conference Series: Materials Science and Engineering*, 2018, vol. 459, no. 1, doi: 10.1088/1757-899X/459/1/012071.
[150] M. S. Sarif Ullah Patwary, "Smart Textiles and Nano-Technology: A General Overview," *J. Text. Sci. Eng.*, vol. 05, no. 01, 2015, doi: 10.4172/2165-8064.1000181.
[151] B. Ju *et al.*, "Inkjet Printed Textile Force Sensitive Resistors for Wearable and Healthcare Devices," *Adv. Healthc. Mater.*, p. 2100893, 2021, doi: 10.1002/adhm.202100893.
[152] Y. Cao, T. Li, Y. Gu, H. Luo, S. Wang, and T. Zhang, "Fingerprint-Inspired Flexible Tactile Sensor for Accurately Discerning Surface Texture," *Small*, vol. 14, no. 16, 2018, doi: 10.1002/smll.201703902.
[153] B. Zhu *et al.*, "Hierarchically Structured Vertical Gold Nanowire Array-Based Wearable Pressure Sensors for Wireless Health Monitoring," *ACS Appl. Mater. Interfaces*, vol. 11, no. 32, pp. 29014–29021, 2019, doi: 10.1021/acsami.9b06260.
[154] L. Bi, Z. Yang, L. Chen, Z. Wu, and C. Ye, "Compressible AgNWs/Ti3C2TxMXene aerogel-based highly sensitive piezoresistive pressure sensor as versatile electronic skins," *J. Mater. Chem. A*, vol. 8, no. 38, pp. 20030–20036, 2020, doi: 10.1039/d0ta07044k.
[155] B. de Bakker, "Force Sensing Resistor (FSR) with Arduino Tutorial," *Verfügbar unter https//www. makerguides. com/fsr-arduino-tutorial/(Zugriff am 26*, vol. 15, no. 09, 2020.
[156] R. J. de Groot, A. J. W. P. Rosenberg, A. van der Bilt, D. Aalto, M. A. W. Merkx, and C. M. Speksnijder, "The association between a mixing ability test and patient reported chewing ability in patients treated for oral malignancies," *J. Oral Rehabil.*, vol. 46, no. 2, pp. 140–150, 2019, doi: 10.1111/joor.12734.
[157] C. M. Christensen, "Food Texture Perception," *Adv. Food Res.*, vol. 29, no. C, pp. 159–199, 1984, doi: 10.1016/S0065-2628(08)60057-9.
[158] "Mechanism of mastication; a quantitative cinematographic and electromyographic study of masticatory movements in children, with special reference to occlusion of the teeth," *Am. J. Orthod.*, vol. 53, no. 3, pp. 225–228, 1967, doi: 10.1016/0002-9416(67)90156-x.
[159] L. WICTORIN, "Masticatory Function in Cases With Denture, in Cases With Natural Teeth and the Importance To Digestion," in *Oral Physiology*, 1972, pp. 223–226.
[160] J. E. Steiner, J. Michman, and A. Litman, "Time sequence of the activity of the temporal and masseter muscles in healthy young human adults during habitual chewing of different test foods," *Arch. Oral Biol.*, vol. 19, no. 1, pp. 29–34, 1974, doi: 10.1016/0003-9969(74)90221-0.
[161] A. Ohkoshi *et al.*, "Predictors of chewing and swallowing disorders after surgery for locally advanced oral cancer with free flap reconstruction: A prospective, observational study," *Surg. Oncol.*, vol. 27, no. 3, pp. 490–494, 2018, doi: 10.1016/j.suronc.2018.05.029.
[162] C. M. Speksnijder, H. W. van der Glas, A. van der Bilt, R. J. J. van Es, E. van der Rijt,

and R. Koole, “Oral Function After Oncological Intervention in the Oral Cavity: A Retrospective Study,” *J. Oral Maxillofac. Surg.*, vol. 68, no. 6, pp. 1231–1237, 2010, doi: 10.1016/j.joms.2009.09.016.
[163] M. B. Kronenberger and A. D. Meyers, “Dysphagia following head and neck cancer surgery,” *Dysphagia*, vol. 9, no. 4, pp. 236–244, 1994, doi: 10.1007/BF00301917.
[164] F. M. C. Van Kampen, A. Van Der Bilt, M. S. Cune, F. A. Fontijn-Tekamp, and F. Bosman, “Masticatory function with implant-supported overdentures,” *J. Dent. Res.*, vol. 83, no. 9, pp. 708–711, 2004, doi: 10.1177/154405910408300910.
[165] A. A. Yurkstas, “The masticatory act. A review,” *J. Prosthet. Dent.*, vol. 15, no. 2, pp. 248–260, 1965, doi: 10.1016/0022-3913(65)90094-6.
[166] J. D. Greenspan and S. J. Bolanowski, “The Psychophysics of Tactile Perception and its Peripheral Physiological Basis,” in *Pain and Touch*, 1996, pp. 25–103.
[167] K. M. Dallenbach, “Pain: History and Present Status,” *Am. J. Psychol.*, vol. 52, no. 3, p. 331, 1939, doi: 10.2307/1416740.
[168] J. R. Bergen and E. H. Adelson, “Early vision and texture perception,” *Nature*, vol. 333, no. 6171, pp. 363–364, 1988, doi: 10.1038/333363a0.
[169] M. A. Heller, “Visual and tactual texture perception: Intersensory cooperation,” *Percept. Psychophys.*, vol. 31, no. 4, pp. 339–344, 1982, doi: 10.3758/BF03202657.
[170] R. W. Cholewiak and A. A. Collins, “The generation of vibrotactile patterns on a linear array: Influences of body site, time, and presentation mode,” *Percept. Psychophys.*, vol. 62, no. 6, pp. 1220–1235, 2000, doi: 10.3758/BF03212124.
[171] A. L. Dellon, “The moving two-point discrimination test: Clinical evaluation of the quickly adapting fiber/receptor system,” *J. Hand Surg. Am.*, vol. 3, no. 5, pp. 474–481, 1978, doi: 10.1016/S0363-5023(78)80143-9.
[172] H. Stanislaw and N. Todorov, “Calculation of signal detection theory measures,” *Behav. Res. Methods, Instruments, Comput.*, 1999, doi: 10.3758/BF03207704.
[173] A. WILSKA, “On the Vibrational Sensitivity in Different Regions of the Body Surface,” *Acta Physiol. Scand.*, vol. 31, no. 2–3, pp. 285–289, 1954, doi: 10.1111/j.1748-1716.1954.tb01139.x.
[174] K. K. Stover and S. H. Williams, “Intraspecific scaling of chewing cycle duration in three species of domestic ungulates,” *J. Exp. Biol.*, 2011, doi: 10.1242/jeb.043646.
[175] “Notes on Medicine/Surgery: Image.” https://dundeemedstudentnotes.files.wordpress.com/2012/04/untitled-picfewture14.png (accessed Sep. 24, 2021).
[176] C. Kaernbach, “Simple adaptive testing with the weighted up-down method,” *Percept. Psychophys.*, vol. 49, no. 3, pp. 227–229, 1991, doi: 10.3758/BF03214307.
[177] R. L. Ringel and S. J. Ewanowski, “Oral perception: 1. Two-point discrimination,” *J. Speech Hear. Res.*, vol. 8, no. 4, pp. 389–398, 1965.
[178] M. J. Hautus and X. Meng, “Decision strategies in the ABX (matching-to-sample) psychophysical task,” *Percept. Psychophys.*, vol. 64, no. 1, pp. 89–106, 2002, doi: 10.3758/bf03194559.
[179] K. O. Johnson and J. R. Phillips, “Tactile spatial resolution. I. Two-point discrimination, gap detection, grating resolution, and letter recognition,” *J. Neurophysiol.*, vol. 46, no. 6, pp. 1177–1191, 1981, doi: 10.1152/jn.1981.46.6.1177.
[180] N. D. J. Strzalkowski, J. J. Triano, C. K. Lam, C. A. Templeton, and L. R. Bent, “Thresholds of skin sensitivity are partially influenced by mechanical properties of the

skin on the foot sole," *Physiol. Rep.*, vol. 3, no. 6, 2015, doi: 10.14814/phy2.12425.
[181] F. A. A. Kingdom and N. Prins, "Classifying Psychophysical Experiments∗," in *Psychophysics*, 2016, pp. 11–35.
[182] H. R. BLACKWELL, "Studies of psychophysical methods for measuring visual thresholds.," *J. Opt. Soc. Am.*, vol. 42, no. 9, pp. 606–616, 1952, doi: 10.1364/JOSA.42.000606.
[183] C. E. Sherrick, R. W. Cholewiak, and A. A. Collins, "The localization of low- and high-frequency vibrotactile stimuli," *J. Acoust. Soc. Am.*, vol. 88, no. 1, pp. 169–179, 1990, doi: 10.1121/1.399937.

Appendix

MATLAB code for amplitude modulating the textures

```
[v,T,vT]=xlsread('17.0psi giant cranberry 5 breaks.xlsx');
t=v(:,1);y=v(:,2);

fsActuator = 8000;
carrierFrequency = 250;

fs=10000; %The sampling frequency of the measurement device; a piston is
        %driven at 1Hz frequency to create chewing motions

        %baseline offset and amplitude of the noise are approximately
gain=0.007;
mean(y<5)

std(y<5)

find(y>5,1) %gives t0 = 0.1196s
%t1 should be around the peak value of y
find(y>151,1)

%gives t1 = 0.1928s
%
%we add a buffer

%temporal points of interest
t0 = .0502;
t1 = .5076+0.05;

%Buffers before and after by 0.05s

tCropped = [round((t0-0.05)*fs):round((t1+0.05)*fs)]'/fs;
yCropped = y(round((t0-0.05)*fs):round((t1+0.05)*fs));

%windowing
w=trapmf(tCropped,[(t0-.005) (t0) (t1) (t1+.005)]);
yW = w.*yCropped;

subplot(2,3,1)
plot(tCropped, yCropped,'r');
ylabel('Force (N)')
xlabel('Time (s)')
title('Cranberry')
hold on;
plot(tCropped, 40*w,'b')
```

```
subplot(2,3,2)
plot(tCropped,yW)

subplot(2,3,3)
carrier = sin(carrierFrequency*2*pi*tCropped);
plot(tCropped, carrier)

subplot(2,3,4)
plot(tCropped, carrier.*yW)

%downsampling the signal
%
%the new sampling rate


x0=resample(tCropped,fs,fsActuator);
y0=resample(carrier.*yW*gain,fs,fsActuator);
subplot(2,3,5)
plot(x0,y0);
audiowrite('cranberry.wav',y0,8000)
```

MATLAB code for just noticeable difference test

```
f = 250;
fs=8000;

% min_A = 0.5;
% max_A = 10;
a_A = 10;
a_X = 5;
a_X_min=1;

% while (a_A < min_A)
%     a_A = rand(1,1) * max_A;
% end
%
% while (a_X < min_A)
%     a_X = rand(1,1) * max_A;
% end

ts = 1/8000;
T = 0.5;
t = 0:ts:T;

% How many times to run this?
```

```
j = 100;

random_order=round(rand(j,1))
result_arr = {};
result = 0;

for i = 1:j
   disp(i);


y_A = a_A * sin(2*pi*f*t);
y_X = a_X * sin(2*pi*f*t);

   % Give y_A and y_X
%    play_audio(y_A, fs, 1);
%    pause (0.8);
%    play_audio(y_X, fs, 1);
if random_order(i)==0
   y_output = [y_A(:);0*y_A(:);y_X(:)];
else
   y_output=  [y_X(:);0*y_A(:);y_A(:)];
end
%y_output
play_audio(y_output/10,fs,1);

   response = ask();
   pause(1)
   while (response ~= 'l' && response ~= 'm')
      disp("Invalid respose, try again.");
      response = ask();
   end

   temp_arr = {a_A, a_X};

   a_X
   a_A
   if (((random_order(i)==0)==(response=='l'))|((random_order(i)==1)==(response=='m')))
      diff = (a_A - a_X) *2^(-1/3);
      a_X=a_A-diff;
      result=1;
   else
      diff = (a_A - a_X) *2^(1);
      a_X=max(a_A-diff,a_X_min);
      result=0;
   end
```

```
%     if (a_A > a_X)
%         if (response == 'l')
%             diff = (a_A - a_X) *2^(-1/3);
%             [a_A, a_X] = find_diff(diff, max_A);
%             result = 1;
%         else
%             diff = (a_X - a_A) * 2;
%             [a_A, a_X] = find_diff(diff, max_A);
%             result = 0;
%         end
%     else
%         if (response == 'm')
%             diff = (a_A - a_X) *2^(-1/3);
%             [a_A, a_X] = find_diff(diff, max_A);
%             result = 1;
%         else
%             diff = (a_X - a_A) * 2;
%             [a_A, a_X] = find_diff(diff, max_A);
%             result = 0;
%         end
%     end

    % Vertically concatenate new data in required format
    order=random_order(i)
    temp_arr = horzcat(temp_arr, response, result, order);

    % Reset Result
    result_arr = vertcat(result_arr, temp_arr);
end

t = array2table(result_arr);
t.Properties.VariableNames(1:5) = {'amp_A', 'amp_X', 'response', 'result', 'order'};
writetable(t, 'part1JND_Jul9.csv');
disp(result_arr);

function response = ask()
    response = input("Which signal is more intense? ('l') or ('m')\n", 's')
    response = lower(response)
end
```

MATLAB code for food texture differentiation test

```
fsActuator=8000;
file_arr = ["cranberryrms1.wav", "toastrms21.wav", "bananarms.wav"]
[audio_1, fsActuator] = audioread(file_arr(1));
[audio_2, fsActuator] = audioread(file_arr(2));
```

```
[audio_3, fsActuator] = audioread(file_arr(3));

audio_arr = {audio_1, audio_2, audio_3};

permutations = perms(audio_arr);
possible_pairs = permutations(:, 1:2);
n_pair_times = 20;
pair_counter = ones(size(possible_pairs,1),1) * n_pair_times;

% Names of possible possible_pairs
permutations_names = perms(file_arr);
possible_pairs_names = permutations_names(:, 1:2);

audioid=2;

%prompt = 'How many runs? : ';
%j = input(prompt)

result_arr = []

total_rounds = n_pair_times * size(possible_pairs,1);

for i = 1:total_rounds

   rand_pair = randi(size(possible_pairs,1), 1);

   % Get audio from said pair
   audio_a = cell2mat(possible_pairs(rand_pair, 1));
   audio_b = cell2mat(possible_pairs(rand_pair, 2));
   rand_x = randi(2,1);
   audio_x = cell2mat(possible_pairs(rand_pair, rand_x));

   % Decrement the pair counter
   pair_counter(rand_pair) = pair_counter(rand_pair) - 1;

   % If count is 0, remove pair, eliminate from selection
   if pair_counter(rand_pair) == 0;
      possible_pairs(rand_pair, :) = [];
      pair_counter(rand_pair, :) = [];
   end

   ISI=0.8;

   outputsignal=zeros(fsActuator*3*ISI,1);
   outputsignal(1:length(audio_a))=audio_a;
   outputsignal(ISI*fsActuator+[1:length(audio_b)]-1)=audio_b;
```

```
    outputsignal(2*ISI*fsActuator+[1:length(audio_x)]-1)=audio_x;

%     disp("Playing audio l\n")
%     play_audio(audio_a,fsActuator,audioid);
%     pause(0.8)
%     disp("Playing audio m\n")
%     play_audio(audio_b,fsActuator,audioid);
%     pause(0.8)
%     disp("Playing audio x\n")
%     play_audio(audio_x,fsActuator,audioid);
%     pause(0.8)
    play_audio(outputsignal,fsActuator,audioid);

    x = input("Which sound was played? First ('l'); Second ('m')\n", 's');
    pause(1);
    temp_arr = [possible_pairs_names(rand_pair, 1), possible_pairs_names(rand_pair, 2),
possible_pairs_names(rand_pair, rand_x), x];
    result_arr = vertcat(result_arr, temp_arr);
end

t = array2table(result_arr)
t.Properties.VariableNames(1:4) = {'l', 'm', 'x', 'response'}
writetable(t, 'participant1_Jul9.csv')
```

MATLAB code for analysing food texture data

```
A = readtable('participant1_Jul9.csv');
C = table2cell(A);
[n_rows, n_cols] = size(C);

% Creating a new column for storing binary result
b_col = nan(n_rows, 1);

% Creating a new cell for storing pairs
pair_table = {};

% Variables for storing percentages
total_correct_percentage = 0;
total_incorrect_percentage = 0;

% Trying to find all pairs
% ========================
% First we create a table with only the first two columns
% Conversion to char to enable use of unique()
A = char(C(:, 1));
B = char(C(:, 2));
```

```
AB = [A B];

% Then we get the indexes of all unique pairs
[X, ia, ib] = unique(AB, 'rows'); % X is all unique pairs
ia = sort(ia); % index of unique pairs
sib = sort(ib); % Where they occur
ib_count = groupcounts(sib); % count how many times they each occur
[xRows, xCols] = size(X)

% Populate cells table
for n = 1 : xRows
   row = [C(ia(n), 1), C(ia(n), 2), ib_count(n)];
   pair_table = vertcat(pair_table, row);
end

% Creating a new column for storing pair correct results
pair_correct_col = zeros(xRows, 1);
pair_incorrect_col = zeros(xRows, 1);

% Loop through every row of the table
% ====================================
for n = 1 : n_rows
   % Get a single row
   row = C(n, :);

   % Figure out if l or m
   % Then get respective value
   if strcmp(row(4), 'l')
     t = row(1);
   elseif strcmp(row(4), 'm')
     t = row(2);
   end

   % Compare t with correct output
   % Write to binary column
   p_row = ib(n, 1);
   if strcmp(t, row(3))
      b_col(n, 1) = 1;
      pair_correct_col(p_row) = pair_correct_col(p_row) + 1;
   else
      b_col(n, 1) = 0;
      pair_incorrect_col(p_row) = pair_incorrect_col(p_row) + 1;
   end

end
```

```
% At the end of this loop we should have enough data
% For percentage calculation
total_correct_percentage = sum(b_col) / n_rows * 100;
total_incorrect_percentage = 100 - total_correct_percentage;

% Original table with appended b_Col
res_C = horzcat(C, num2cell(b_col));

% Write original table to file
t = array2table(res_C);
t.Properties.VariableNames(1:5) = {'l', 'm', 'x', 'response', 'result'};
writetable(t, 'result_all.csv');

% Original table with appended pair_results
res_pair = horzcat(pair_table, num2cell(pair_correct_col));
res_pair = horzcat(res_pair, num2cell(pair_incorrect_col));

% Write pair table to file
tt = array2table(res_pair);
tt.Properties.VariableNames(1:5) = {'l', 'm', 'total', 'correct', 'incorrect'};
writetable(tt, 'result_pairs.csv');
```

Python code for spatial differentiation test

```
import sounddevice as sd
import soundfile as sf
import random
import threading
import csv
import time

# Setting some default values
sd.default.samplerate = 8000

# List of Audio IDs
audioIds = [0, 1, 2]
numAudioIds = len(audioIds)

# Reading the audio file
data, fs = sf.read('sine2.wav', dtype='float32')


def play_audio(audioId):
    # print("Playing on ", audioId)
    sd.play(data, fs, device=audioId)
```

```
def main():

    resArr = []

    # Start the actual tests
    n = int(input("How many runs? : "))

    for i in range(0, n):

        # Get two random numbers between 0-3
        r1 = random.choice(audioIds)
        r2 = random.choice(audioIds)

        while r1 == r2:
            r1 = random.choice(audioIds)
            r2 = random.choice(audioIds)

        # Randomly decide whether to play one or two signals
        mode = random.randint(1, 2)

        if mode == 1:
            rS = random.randint(1, 3)
            if rS == 1:
                r2 = "NA"
                play_audio(r1)
            else:
                r1 = "NA"
                play_audio(r2)

        elif mode == 2:
            # Play two signals in parallel
            inputs = [r1, r2]
            threads = [threading.Thread(target=play_audio, args=(i, )) for i in inputs]
            [t.start() for t in threads]
            [t.join() for t in threads]

        # Wait for audio to complete playing
        sd.wait()

        # Ask for response
        resp = int(
            input("Did you feel one or two devices? One ('1'); Two ('2'); 's'\n"))

        while resp != 1 and resp != 2:
            print("Invalid respose, try again.")
```

```
            resp = int(
                input("Did you feel one or two devices? One ('1'); Two ('2'); 's'\n"))

            # Create the run result
            rRes = [r1, r2, resp]
            resArr.append(rRes)

        # Write the result to a file
        with open("draaltoseq_Jul27.csv", "w+") as my_csv:
            csvWriter = csv.writer(my_csv, delimiter=',')
            headers = ['device_a', 'device_b', 'response']
            csvWriter.writerow(headers)
            csvWriter.writerows(resArr)


if __name__ == "__main__":
    main()
```